

JOURNAL OF CAVE AND KARST STUDIES

August 1998
Volume 60 Number 2
ISSN 1090-6924



Journal of Cave and Karst Studies

Volume 60 Number 2 August 1998

CONTENTS

Editorial

- Conservation and protection of the biota of karst:
Assimilation of scientific ideas through artistic perception
Dan L. Danielopol 67

Articles - Isla de Mona Special Issue

- Introduction to the Isla de Mona special issue
Carol M. Wicks - Guest Editor 68
- Geology of Isla de Mona, Puerto Rico
*Edward F. Frank, Carol Wicks, John Mylroie, Joseph Troester,
E. Calvin Alexander, Jr., and James Carew* 69
- Karst development and speleogenesis, Isla de Mona, Puerto Rico
*Edward F. Frank, John Mylroie, Joseph Troester,
E. Calvin Alexander, Jr., and James Carew* 73
- Condensation corrosion in caves on Cayman Brac and Isla de Mona
Rozemarijn F.A. Tarhule-Lips and Derek C. Ford 84
- Magnetostratigraphy of Cueva del Aleman, Isla de Mona, Puerto Rico
and the species duration of Audubon's shearwater
*Bruce C. Panuska, John M. Mylroie, Darrell Armentrout,
and Donald McFarlane* 96
- A radiocarbon date of 380 ± 60 BP for a Taino site, Cueva Negra,
Isla de Mona, Puerto Rico
Edward F. Frank 101
- Vertebrate paleontology of Isla de Mona, Puerto Rico
Edward F. Frank and Richard Benson 103
- Groundwater geochemistry of Isla de Mona, Puerto Rico
Carol M. Wicks and Joseph W. Troester 107
- An electromagnetic geophysical survey of the freshwater lens of
Isla de Mona, Puerto Rico
Ronald T. Richard, Joseph W. Troester, and Myrna I. Martínez 115
- History of the guano mining industry, Isla de Mona, Puerto Rico
Edward F. Frank 121
- Cave Science News** 126
- Authors** 127

The *Journal of Cave and Karst Studies* (ISSN 1090-6924) is a multi-disciplinary, refereed journal published three times a year by the National Speleological Society, 2813 Cave Avenue, Huntsville, Alabama 35810-4431; (256) 852-1300; FAX (256) 851-9241, e-mail: nss@caves.org; World Wide Web: <http://www.caves.org/~nss/>. The annual subscription fee, worldwide, by surface mail, is \$18 US. Airmail delivery outside the United States of both the *NSS News* and the *Journal of Cave and Karst Studies* is available for an additional fee of \$40 (total \$58); The *Journal of Cave and Karst Studies* is not available alone by airmail. Back issues and cumulative indices are available from the NSS office. POSTMASTER: send address changes to the *Journal of Cave and Karst Studies*, 2813 Cave Avenue, Huntsville, Alabama 35810-4431.

Copyright © 1998 by the National Speleological Society, Inc. Printed on recycled paper by American Web, 4040 Dahlia Street, Denver, Colorado 80216

Cover: Cueva de Frío, Isla de Mona, view of east side by Marc J. Ohms.

Editor

Louise D. Hose
Environmental Studies Program
Westminster College
Fulton, MO 65251-1299
(573) 573-5303 Voice
(573) 592-2217 FAX
HoseL@jaynet.wcmo.edu

Production Editor

James A. Pisarowicz
Wind Cave National Park
Hot Springs, SD 57747
(605) 673-5582
pisarowi@gwtc.net

BOARD OF EDITORS Earth Sciences-Journal Index

Ira D. Sasowsky
Department of Geology
University of Akron
Akron, OH 44325-4101
(330) 972-5389
ids@uakron.edu

Conservation George Huppert

Department of Geography
University of Wisconsin, LaCrosse
LaCrosse, WI 54601
Huppert@uwlax.edu

Life Sciences David Ashley

Department of Biology
Missouri Western State College
St. Joseph, MO 64507
(816) 271-4334
ashley@griffon.mwsc.edu

Social Sciences Marion O. Smith

P.O. Box 8276
University of Tennessee Station
Knoxville, TN 37996

Anthropology Patty Jo Watson

Department of Anthropology
Washington University
St. Louis, MO 63130

Exploration Douglas Medville

11762 Indian Ridge Road
Reston, VA 22091
medville@patriot.net

Book Reviews Betty Wheeler

1830 Green Bay Street
LaCrosse, WI 54601

Proofreader Donald G. Davis

JOURNAL ADVISORY BOARD

| | |
|-----------------|-----------------|
| Penelope Boston | Rane Curl |
| Andy Flurkey | Horton Hobbs |
| David Jagnow | Jim Mead |
| Jim Nepstad | Margaret Palmer |
| Will White | |

CONSERVATION AND PROTECTION OF THE BIOTA OF KARST: ASSIMILATION OF SCIENTIFIC IDEAS THROUGH ARTISTIC PERCEPTION

DAN L. DANIELOPOL

Limnological Institute, Austrian Academy of Sciences, A-5310 Mondsee, AUSTRIA

At the symposium, "Conservation and Protection of the Biota of Karst," organized by the Karst Waters Institute (Nashville, Tennessee, February 13-16, 1997), Dr. Stuart Pimm, one of the leading authorities in nature conservation, proposed that besides the maintenance of pristine groundwater as the rationale for conservation and protection of karstic ecosystems, one should use artistic arguments, too. He had in mind the idea to protect the karstic environment and their unique organisms because they are beautiful! I shall here develop further this argument and give a practical example that should emphasize the importance of metaphorical language using the artistic perception of the layman in order to better assimilate scientific ideas.

Naturalists, when dealing with organisms and their ecology, are often impressed by the pleasant, aesthetic appearance of their object of study. Take, as example, the appearance of the delicate cave shrimp moving in search of its food through the clear water of a subterranean lake. A sense of wonder and ecstasy permeates the study of such organisms and a deep desire exists in the scientist to communicate these aspects to a larger public in a similar way to what artists do. What Dobzhansky and Boesiger (1983: 135) wrote about the cultural mission of artists "...one of the great humanistic roles of the artist is to make natural beauty visible to those who either cannot see it or can see it only poorly..." equally applies to scientists and their research achievements.

As our knowledge and perception are organized into integrative frameworks, creative ideas are often activated through metaphorical language. Paton (1992) mentions that we often describe what is unknown in terms of what is familiar, and artistic images allow a better grasp of complex scientific ideas. As an example, we can mention the possibility of communicating to the layman how and why to conserve or to protect the unique cave dwelling animals, i.e. in order to appreciate their unusual habitat and strange habits, as evolutionary products of a long, adaptive history. Such animals are now in various locations under a strong threat of extinction through anthropogenic pollution. In this case, therefore, such an environment and its inhabitants deserve better attention and protection from

humans. Because the artistic education of people is, in many cases, better developed than their grasp of science, it would appear more useful to employ a metaphorical description of the cave dwelling animals in their home as a museum of marvellous images. Emil Racovitza, years ago (1926), pointed out that caves in Europe are filled with "living fossils" and they could be compared to common museums.

The analogy between caves with their visually attractive creatures and an Art Museum, with its unique paintings and sculptures for which our human culture tells us that the exposed artistic objects are beautiful and have to be conserved and protected, can help the layman to grasp the biological interest and importance of the former. Hence, in order to widen the cultural education of the layman, the combination of artistic perception with scientific facts can be one of the best techniques to convey a meaningful idea: the unique organisms living in karstified areas represent public goods with amenity value (Morowitz 1991) and, therefore, they have to be integrated in our cultural heritage.

ACKNOWLEDGMENTS

I am grateful to the following colleagues who commented and/or encouraged the submission for publication on this note. They are: D. Culver (Washington, D.C.), W. Humphreys (Perth), P. Pospisil (Vienna), R. Rouch (Fronton). This contribution is an output of the FWF Project Nr.11149 BIO, dealing with the ecology of groundwater fauna in the Danube wetlands at Vienna.

REFERENCES

- Dobzhansky, T. & Boesiger, E. (1983). *Human culture, a moment in evolution*. Columbia University Press, New York: 175 p.
- Morowitz, H.J. (1991). Balancing species preservation and economic considerations. *Science* 253: 752-754.
- Paton, R.C. (1992). Towards a metaphorical biology. *Biology and Philosophy* 7: 279-294.
- Racovitza, E.G. (1926). Speologia. *Academia Româna, Discursuri de Receptie* 61: 1-64.

INTRODUCTION TO THE ISLA DE MONA SPECIAL ISSUE

CAROL M. WICKS

Guest Editor

Department of Geological Sciences, University of Missouri, Columbia, Missouri 65211 USA

Isla de Mona is an isolated uplifted carbonate island that offers a unique laboratory in which to study the development of karst landscapes and groundwater flow. The remote island is home to sea turtles, iguanas, and a variety of other rare species in an exotic setting. The Isla de Mona Project began in May of 1992 when Joe Troester led a trip of five other scientists to the island for 10 days, to analyze the groundwater, study the bedrock characteristics, begin paleomagnetic studies, and examine the caves. Return trips in 1993 and 1994 brought more scientists to the island, where research projects of the preceding year continued and new studies, such as condensation corrosion research, cave morphology analysis, and geophysical investigation of the groundwater, were initiated. Since that time, trips have been conducted under the direction of Dr. John Mylroie. At the 1993 and 1994 Geological Society of America Annual Meetings, the newly proclaimed "Friends of Mona" gathered. At those meetings, preliminary research findings were presented and many voiced the need to find a place to present the findings of the various research projects. After the 1995 GSA meeting, I requested that they submit the results of their work to a special issue of the *Journal of Cave and Karst Studies*. The papers presented in this issue represent the culmination of the cave and karst work that was done through the Mona Project. As a group of cave scientists who also love caving, we hope that the *Journal of Cave and*

Karst Studies readership enjoys the articles, which represent a variety of techniques utilized to increase our understanding of caves, karst, and karst waters.

The researchers acknowledge the financial and logistical support provided by the U.S. Geological Survey, Reston, Virginia and San Juan, Puerto Rico Offices, and the logistical support provided by the Puerto Rico Department of Natural Resources during several field sessions on Isla de Mona. In addition, we thank the Cave Research Foundation and the Department of Geological Sciences at the University of Missouri for assistance in conducting field work on Isla de Mona, for processing of samples collected from the island, and for help with the Special Issue. We thank Robert Matos, Director of the Puerto Rico Natural Reserves and Wildlife Refuges Division, and Department of Natural Environmental Resources personnel Angel Nieves Rivera, José Jiménez, and Eduardo Ciutrón for their aid in arranging trips to Isla de Mona and their help while conducting field work.

Please remember that all visitors to Isla de Mona need permits from the Puerto Rico Department of Natural Resources. In addition, scientists need scientific permits to sample on the island as there are federally endangered species and archaeological materials that deserve and require our utmost respect. Take care, and cave and study softly.



GEOLOGY OF ISLA DE MONA, PUERTO RICO

EDWARD F. FRANK

Department of Geology and Geophysics, University of Minnesota, Minneapolis, MN 55455 USA

CAROL WICKS

Department of Geological Sciences, University of Missouri-Columbia, Columbia, MO 65211 USA

JOHN MYLROIE

Department of Geosciences, Mississippi State University, Mississippi State, MS 39762 USA

JOSEPH TROESTER

U.S. Geological Survey, GSA Center, 651 Federal Drive, Suite 400-15, Guaynabo, PR 00965-5703

E. CALVIN ALEXANDER, JR.

Department of Geology and Geophysics, University of Minnesota, Minneapolis, MN 55455 USA

JAMES L. CAREW

Department of Geology, University of Charleston, Charleston, SC 29424 USA

Isla de Mona is a carbonate island located in the Mona Passage 68 km west of Puerto Rico. The tectonically uplifted island is 12 km by 5 km, with an area of 55 km², and forms a raised flat-topped platform or meseta. The meseta tilts gently to the south and is bounded by near vertical cliffs on all sides. These cliffs rise from 80 m above sea level on the north to 20 m above the sea on the southern coast. Along the southwestern and western side of the island a three- to six-meter-high Pleistocene fossil reef abuts the base of the cliff to form a narrow coastal plain. The meseta itself consists of two Mio-Pliocene carbonate units, the lower Isla de Mona Dolomite and the upper Lirio Limestone. Numerous karst features, including a series of flank margin caves primarily developed at the Lirio Limestone/Isla de Mona Dolomite contact, literally ring the periphery of the island.

Isla de Mona is a tectonically uplifted Mio-Pliocene carbonate island in the Mona Passage approximately half way between Puerto Rico and Hispanola. The kidney-shaped island is 12 km long and 5 km wide and covers 55 km² (Peck *et al.* 1981). The bulk of the island forms a flat-topped, raised platform, or meseta, that dips gently to the south (Fig. 1). This meseta is bounded on all sides by vertical to near-vertical cliffs. (The Puerto Ricans refer to the flat-topped, raised platform of Isla de Mona as a meseta. For consistency, the authors



Figure 1. North shore of Isla de Mona showing 70 m high cliffs and flat surface of the meseta or raised platform surface.

of papers in this volume will also use meseta, however, it should not be confused with the geographic definition of the term). Along the north coast the cliff drops vertically from a maximum elevation of 80 m to a depth of at least 30 m below sea level. Along the southern and western margins of the island a Pleistocene fossil reef abuts the base of the 20 to 30 m high cliffs to form a 3 to 6 m high coastal flat. This reef flat is generally narrow with a maximum width of 1 kilometer in the Piedra del Carabinero area of the southern coast. Offshore a modern coral reef parallels the shore from Punta Este, around the southern coast, and northward almost to Punta el Capitan along the western coast of the island. This reef is separated from shore by a shallow lagoon that ranges from a few meters to a few hundred meters wide. A small sister island, Monito, is located 5 km northwest. It is similar in description but occupies only 0.17 km² of area (Peck *et al.* 1981) (Fig. 2).

TECTONICS

The major tectonic features of the region are the Puerto Rico Trench to the north, the Muertos Trough to the south and southwest, the Anegada Passage to the southeast, and the Mona Canyon trending north-south between Puerto Rico and Hispaniola (Fig. 3). The Puerto Rico Trench marks the boundary between the Caribbean and North American plates. Because it is not completely linear, portions of the boundary of the Caribbean plate are undergoing subduction, while in other areas the relative motion results in strike-slip faults.

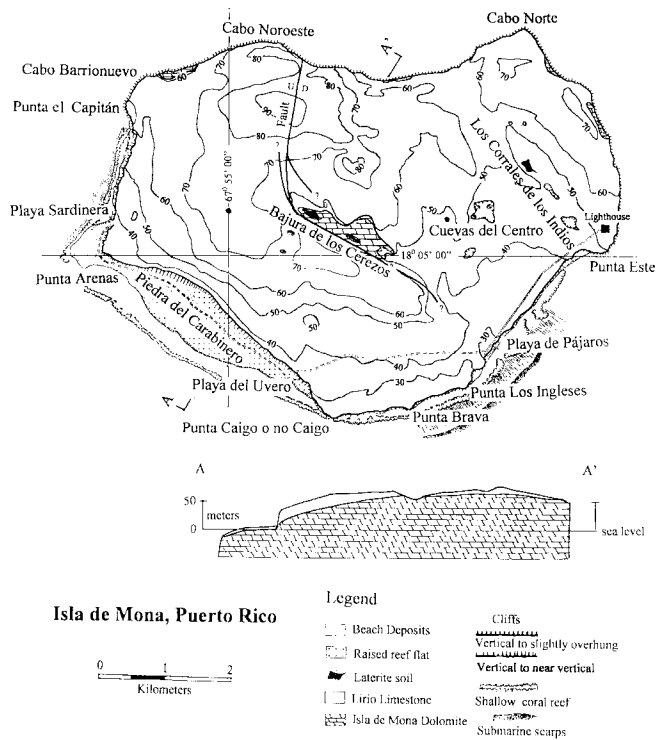


Figure 2. General geologic map and cross section of Isla de Mona, Puerto Rico. Major topographic features are marked. Adapted from Kaye (1959) and Briggs and Seiders (1972).

Compression along the Muertos Trough decreases gradually eastward, ultimately to be replaced by extension in Aneгада Passage. Northwest of Puerto Rico, an obvious structural break occurs along Mona Canyon. However, no obvious structural or seismic continuity links Mona Canyon to the Muertos Trough to the south. One possibility is that Puerto Rico and eastern Hispaniola are both undergoing counterclockwise movement as independent or semi-independent blocks. The extensional forces that produced Mona Canyon are a result of the relative movement between them (Masson & Scanlon 1991).

Isla de Mona itself expresses a number of tectonic features. A series of low amplitude, southward plunging anticlines/synclines cross the island. The island has undergone tectonic uplift since deposition and is generally tilted to the south at five to ten meters per kilometer (0.3° to 0.6° dip). A large fault (Fig. 2) extends inward from the north shore through the Bajura de los Cerezos and terminates in the south central portion of the meseta (Briggs & Seiders 1973).

STRATIGRAPHY

Isla de Mona is dominated by a carbonate meseta consisting of two units, the Isla de Mona Dolomite and the Lirio Limestone (Fig. 2). Kaye (1959) placed the age of the Lirio

Limestone as Middle Miocene based upon a limited foraminifera assemblage identified in samples. More recent work by Gonzales et al. (1997) suggests a younger date of late Miocene to early Pliocene age for the major carbonate units of the island based upon overall coral assemblages.

The Isla de Mona Dolomite is a pale tan, very finely crystalline, calcitic dolostone. It is thick to massively bedded, and locally cross bedded (Quinlan 1974). The maximum exposure above sea level is 80 m near Cabo Noroeste (Briggs 1974). The dolostone has a limited surface area of outcrop. Volumetrically, however, it makes up the largest portion of the island, extensively cropping along the near vertical cliff faces surrounding the island and in the Bajura los Cerezos area in the central portion of the island.

The Lirio Limestone overlies the Mona Dolomite and forms the cap on the island. It is a pale tan, finely crystalline limestone. The maximum exposed thickness is 40 m near Playa Sardinera, but averages only 10 to 15 m thick along the cliff tops. The limestone bedding ranges from 2 to 5 meters in thickness, with cross beds locally up to 2 to 3 cm thick. The Lirio Limestone is moderately fossiliferous, with accumulations of large coral heads and patch reefs near Cueva del Capitan and Cuevas del Centro (Briggs 1974). This unit is extensively karstified with caves, karren, sinkholes, pits, and enlarged joints across the plateau surface.

Ruiz (1993) did detailed petrographic work on rock samples collected from the island. He provides a description of the origin of the carbonate units as follows: "The carbonate build-up of Isla de Mona is the result of the development of a barrier reef of middle Miocene to earliest Pliocene age. Four reef facies have been identified in the Tertiary deposits of the island. Fore-reef deposits characterized by muds, pelagic foraminifera, and steeply dipping strata are present on the

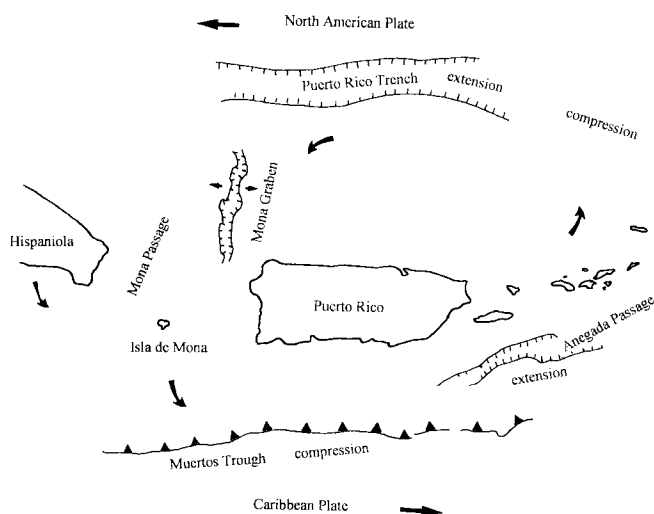


Figure 3. Regional tectonics of the Isla de Mona area showing major structural features and relative plate motions. Adapted from Mason and Scanlon (1991).

southwestern cliffs. A reef is exposed along the southeastern coast as well as in the western tip of the island. A transition between reef-flat and back-reef deposits is present to the north of the reef. Lagoon deposits composed of pelleted muds, benthic foraminifera, and coralline algae, makes up the bulk of the island's carbonates. Scattered patch-reefs are locally developed in the lagoon facies" (p. 70-71). Ruiz treats both units as part of a single reef complex.

The nature of the contact between the Lirio Limestone and the Isla de Mona Dolomite has been the subject of much speculation. In the cliffs along the eastern and northern shores of the island, there is a marked difference in the coloration of the rock units above and below the major band of cave development. Kaye (1959) found that the unit above the band was darker and a relatively pure limestone while the unit below the cave band was a lighter color and dolomitic limestone or dolomite. An apparent angular unconformity was also noted at the contact between the upper darker-colored rocks and the lower lighter-colored rocks in the cliffs around Punta Este. Kaye (1959) defined the upper unit, which forms a thin cap over much of the island, as the Lirio Limestone and the lower unit, which makes up the bulk of the island, as the Isla Mona Limestone.

Briggs and Seiders (1972) redefined these units so that the entire exposed cliff near Punta Arenas was reassigned to the Lirio Limestone and the Isla Mona Limestone was renamed the Isla de Mona Dolomite. Briggs (1974) suggested, as an alternative interpretation, that the contacts between the two units might be essentially conformable with the apparent angular unconformity simply being large scale crossbeds. He also notes that where the contact is exposed in the cliffs along the western and southeastern shores of the island, examination from a distance gives the impression that the lower few meters of the Lirio Limestone grade laterally into the upper Isla de Mona Dolomite. Ruiz (1993) does not directly address the question of the nature of the contact between the Lirio Limestone and the Isla de Mona Dolomite. Gonzales *et al.* (1997) found the Lirio Limestone/Isla de Mona Dolomite contact to be conformable. The lithology at the base of the Lirio Limestone is dolomitic limestone and gradually changes upward into almost pure limestone at the top of the unit. The dolomitized section extends several meters above the unit contacts.

The Pleistocene-aged reef tracts, composed primarily of a mixed head-coral facies overlain by an extensive *Acropora*

palmata reef-crest facies, extend along 14 km of the southern and western coasts of the island (Fig. 2). These deposits are found at elevations of up to 5 m msl, and at distances of several hundred meters from the present day shoreline (Taggart 1993).

Radiometric dating using the $^{230}\text{Th}/^{234}\text{U}$ method have shown these reefs to have been active from 128-107 Ka (Taggart 1993). The presence of these last interglacial deposits at positions between sea level and 6 m msl indicate there has been no tectonic movement of the Mona platform for over 100,000 years.

Locally, these reef tracts are capped by beach sands. Boulders of Isla de Mona Dolomite and Lirio Limestone fell from the cliffs and are sporadically located at the base of the cliffs surrounding the island. Large coral boulders up to 5 m across have been torn from the Holocene reefs and deposited on top of the late Pleistocene coastal flats in the southwestern portion of the island within the last 3,000 years (Taggart *et al.* 1993).

KARST DEVELOPMENT

A variety of karst features are found on the island. The most prominent of these are a series of caves that ring the periphery of the island. The majority of these caves are developed at the Lirio Limestone/Isla de Mona Dolomite contact, whereas others are independent of this formational boundary. The caves are flank margin caves and range in size from a meter or less across to caves containing series of large interconnected rooms that extend more than one kilometer. Floor areas of some individual caves and cave systems are in excess of 150,000 m². The caves are all restricted to the edge of the island with a maximum inward penetration of 240 m from the cliff face (Frank 1993; Mylroie *et al.* 1995, Frank *et al.* 1998).

Another significant karst feature is Bajura de los Cerezos, a closed, internally drained, depression in the center of the island, developed along a fault line. Other important karst features include: (1) Cuevas del Centro, a series of large nested sinkholes; (2) Los Corrales de los Indios, a dissolutional valley formed along a fracture; (3) Camino de los Cerezos pit area, an area containing a large number of vertical shafts; and (4) the surface of the meseta has been etched by dissolution into small-scale pits.

REFERENCES

- Briggs, R.P. (1974). Economic geology of the Isla de Mona quadrangle, Puerto Rico. *U. S. Geological Survey, Open File Report 74-226*: 116 p.
- Briggs, R.P. and Seiders, V.M. (1972). Geologic map of the Isla de Mona quadrangle, Puerto Rico. *U. S. Geological Survey Miscellaneous Geological Investigations*, Map I-718, 1:20,000.
- Cintron, B. & Rogers, L. (1991). Plant communities of Mona Island. *Acta Científica; Asociación de Maestros de Ciencia de Puerto Rico 5*: 10-64.
- Frank, E.F. (1993). *Aspects of karst development and speleogenesis, Isla de Mona, Puerto Rico: An analogue for Pleistocene speleogenesis in the Bahamas*. MS Thesis, Mississippi State University: 288 p.
- Frank, E.F., Mylroie, J.M., Troester, J.W., Alexander, Jr., E.C. & Carew, J.L. (1998). Karst development and speleogenesis, Isla de Mona, Puerto Rico. *Journal of Cave and Karst Studies 60(2)*: 73-83.
- Gonzalez, L.A., Ruiz, H. & Monell, V. (1990). Diagenesis of Isla Mona, Puerto Rico [abs]. *American Association of Petroleum Geologists Bulletin 74*: 663-664.
- Gonzales, L.A., Ruiz, H.A., Taggart, B.E., Budd, A.F., & Monell, V. (1997). Geology of Isla de Mona, Puerto Rico. In Vacher, H.L. & Wuinn, T. (eds.). *Geology and Hydrogeology of Carbonate Islands. Developments in Sedimentology 54*. Elsevier, New York: 327-358.
- Kaye, C.A. (1959). Geology of Isla Mona, Puerto Rico, and notes on the age of the Mona Passage. *U.S. Geological Survey, Professional Paper 317C*: 141-178.
- Martinez, M.I., Troester, J.W. & Richards, R.T. (1995). Surface electromagnetic geophysical exploration of the ground-water resources of Isla de Mona, Puerto Rico, a Caribbean carbonate island. *Carbonates and Evaporites 10*: 184-192.
- Masson, D.G. & Scanlon, K.M. (1991). The neotectonic setting of Puerto Rico. *Geological Society of America Bulletin 103*: 144-154.
- Mylroie, J.E., Panuska, B.C., Carew, J.L., Frank, E.F., Taggart, B.E., Troester, J.W. & Carrasquillo, R. (1995). Development of flank margin caves on San Salvador Island, Bahamas and Isla de Mona, Puerto Rico. In Boardman, M. (ed.). *Proceedings of the seventh symposium on the geology of the Bahamas: June 16-20, 1994*, Bahamian Field Station, San Salvador, Bahamas: 49-81.
- Peck, S.B. & Kukulova-Peck, J. (1981). The subterranean fauna and conservation of Mona Island, Puerto Rico. *National Speleological Society Bulletin 43*: 59-68.
- Quinlan, J.F. (1974). *Preliminary exploration and evaluation of the caves of Mona Island, including a description of origin*. U.S. National Park Service, unpublished administrative report, on file with U.S. Geological Survey, GSA Center, Guaynabo, PR: 33 p.
- Richards, R.T., Troester, J.W., and Martínez, M.I. (1995). A comparison of electromagnetic techniques used in a reconnaissance of ground-water resources under the coastal plain of Isla de Mona, Puerto Rico. *The symposium on the applications of geophysics to environmental and engineering problems (SAGEEP'95) proceedings*, Orlando, Florida: 251-260.
- Ruiz, H.M. (1993). *Sedimentology and diagenesis of Isla de Mona, Puerto Rico*. MS Thesis, University of Iowa, Iowa City: 86 p.
- Ruiz, H., Gonzalez, L.A. & Budd, A.F. (1991). Sedimentology and diagenesis of Miocene Lirio Limestone, Isla de Mona, Puerto Rico [abs]. *American Association of Petroleum Geologists Bulletin 75*: 664-665.
- Taggart, B.E. (1993). *Tectonic and eustatic correlations of radiometrically dated marine terraces in northwest Puerto Rico and Isla de Mona, Puerto Rico*. PhD dissertation, University of Puerto Rico, Mayaguez: 252 p.
- Taggart, B.E., Lundberg, J.I., Carew, J.L. & Mylroie, J.E. (1993). Holocene reef-rock boulders on Isla de Mona, Puerto Rico: Transported by a hurricane or seismic sea wave. *Geological Society of America Annual Meeting Abstracts with Program 25*: 61.

KARST DEVELOPMENT AND SPELEOGENESIS, ISLA DE MONA, PUERTO RICO

EDWARD F. FRANK

Department of Geology and Geophysics, University of Minnesota, Minneapolis, MN 55455 USA

JOHN MYLROIE

Department of Geosciences, Mississippi State University, Mississippi State, MS 39762 USA

JOSEPH TROESTER

U.S. Geological Survey, GSA Center, 651 Federal Drive, Suite 400-15, Guaynabo, PR 00965-5703

E. CALVIN ALEXANDER, JR.

Department of Geology and Geophysics, University of Minnesota, Minneapolis, MN 55455 USA

JAMES L. CAREW

Department of Geology, University of Charleston, Charleston, SC 29424 USA

Isla de Mona consists of a raised table-top Miocene-Pliocene reef platform bounded on three sides by vertical cliffs, up to 80 m high. Hundreds of caves ring the periphery of the island and are preferentially developed in, but not limited to, the Lirio Limestone/Isla de Mona Dolomite contact. These flank margin caves originally formed at sea level and are now exposed at various levels by tectonic uplift of the island (Frank 1983; Mylroie et al. 1995b).

Wall cusps, a characteristic feature of flank margin caves, are ubiquitous features. Comparisons among similar caves formed in the Bahamas and Isla de Mona reveal the same overall morphology throughout the entire range of sizes and complexities.

The coincidence of the primary cave development zone with the Lirio Limestone/Isla de Mona Dolomite contact may result from syngenetic speleogenesis and dolomitization rather than preferential dissolution along a lithologic boundary. Tectonic uplift and glacioeustatic sea level fluctuations produced caves at a variety of elevations. Speleothem dissolution took place in many caves under phreatic conditions, evidence these caves were flooded after an initial period of subaerial exposure and speleothem growth. Several features around the perimeter of the island are interpreted to be caves whose roofs were removed by surficial denudation processes. Several large closed depressions and dense pit cave fields are further evidence of surficial karst features. The cliff retreat around the island perimeter since the speleogenesis of the major cave systems is small based upon the distribution of the remnant cave sections.

Isla de Mona is remarkable for the large number of caves that open onto its carbonate cliffs (Fig. 1). James Quinlan (1974) used the term "phantasmagorical" to describe the immensity and grandeur of these caves. Based on the then current understanding of cave formation, he called the voids "sea caves", but it is clear from his writing that he was not fully satisfied with that explanation. The majority of the caves on Isla de Mona are located at or near the Mona Dolomite/Lirio Limestone contact. However, there are some caves that do not seem to be related to this formation boundary. The numerous caves seen in the cliffs of Isla de Mona are now known to be flank margin caves (Frank 1993; Mylroie *et al.* 1995b). Other karst features on Isla de Mona include: several extensive closed depressions, a dissolutional valley formed along a frac-

ture, and an area containing a dense concentration of vertical shafts or pit caves (Fig. 2). An overview of the geology of Isla de Mona is provided by Frank *et al.* (1998).

Figure 1. Vertical cliffs 40 m high on the east side of Isla de Mona, Puerto Rico. Cave openings are present near the top of the cliff at the Lirio Limestone/Isla de Mona Dolomite contact.

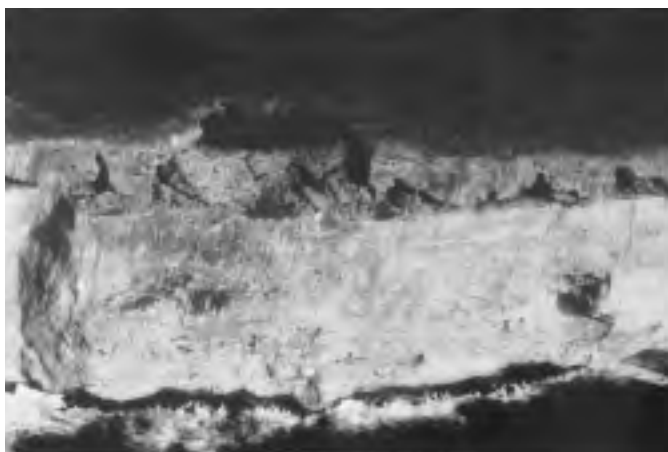
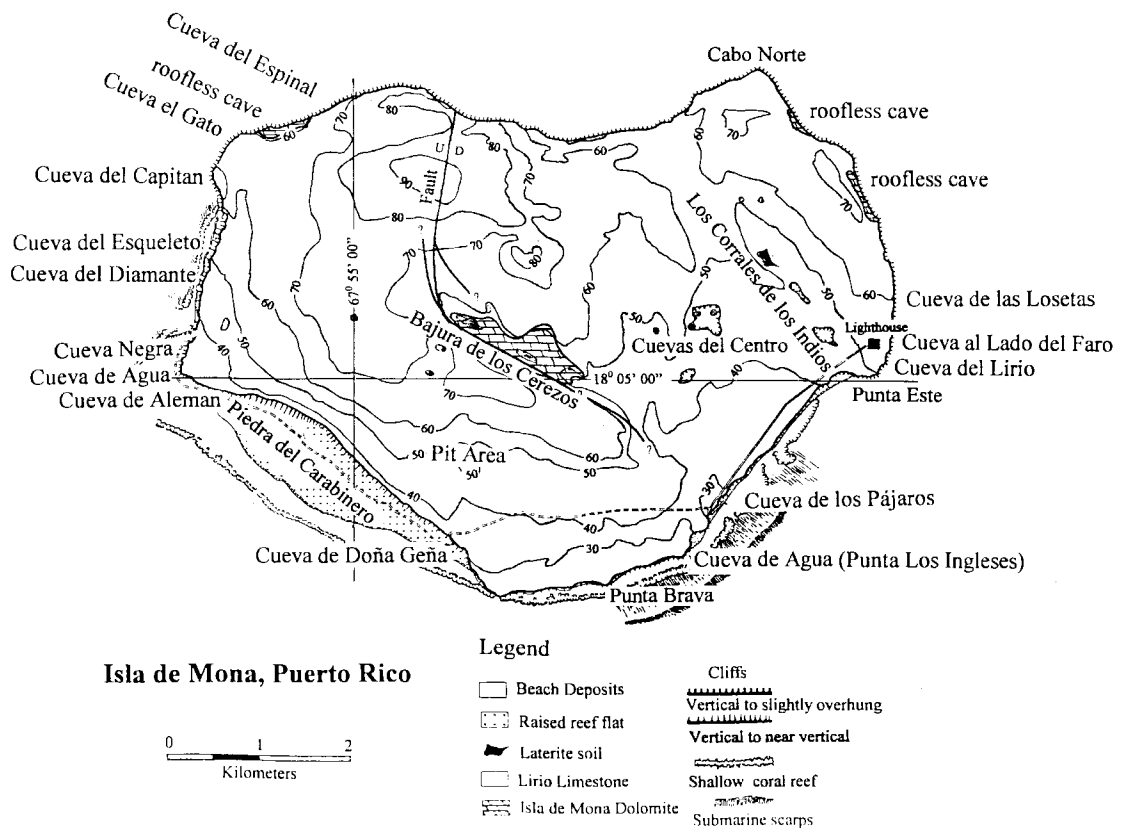


Figure 2.
Major cave and karst features of Isla de Mona, Puerto Rico.



FLANK MARGIN CAVE MODEL

Carbonic acid, formed by the dissolution and ionization of carbon dioxide in water, is capable of dissolving limestone and forming caves. Infiltrating water in limestone areas quickly approaches calcite saturation. Bogli (1980) described a process for enhancing calcite dissolution termed *mischungskorrosion*, or mixing corrosion. Because the saturation curve for calcite is not linear, mixing of two solutions saturated at different partial pressures of CO₂ yield a third solution that is undersaturated with respect to calcite. This phenomenon allows additional dissolution at the mixing zone between infiltrating vadose water and phreatic water at the water table.

Plummer (1975) showed that fresh water saturated, or even slightly supersaturated, with respect to calcite, became undersaturated when mixed with up to 70% sea water that is also saturated. These calculations indicated dissolution can take place at the halocline, or mixing zone, at the base of the fresh-water lens within carbonate coasts and islands. This principle, explaining the origin of many caves in Bermuda (Palmer *et al.* 1977; Mylroie *et al.* 1995a), along the Yucatan coast (Back *et al.* 1979), and in the Bahamas (Mylroie & Carew 1990), is now a well accepted phenomenon.

The flank margin model for the genesis of caves was first proposed for the caves of the Bahamas (Mylroie & Carew 1990). It suggests that the margin of the fresh-water lens is an area of intense dissolution driven both by the mixing of vadose

and phreatic water at the top of the fresh-water lens, and by mixing of fresh water and sea water at the halocline. Those two mixing zones merge at the lens margin. Flank margin caves have a distinctive morphology. "They consist of oval or linear chambers that are oriented parallel to the trend of, and just under the flank of, the ridge in which they have formed. Small radiating tubes extend from these large chambers into the ridge interior where they end abruptly or pinch out. Many cave passages loop back into one another or the main chamber, and isolated bedrock pillars and thin wall-partitions are common." (Mylroie & Carew 1991: 140).

A variety of other chemical processes may also play a role in the rapid development of flank margin caves. The top and bottom of the freshwater lens are density interfaces where organic material may collect. After the initial dissolution cavities form, bacterial decomposition of the organic matter depletes the available oxygen and increases the partial pressure of dissolved CO₂. Anaerobic bacteria then use more organic matter to reduce the sulfate to form H₂S. If oxidizing conditions return, oxidation of the H₂S can produce H₂SO₄ which reacts to dissolve the limestone and produces gypsum (Bottrell *et al.* 1993). These processes may be taking place simultaneously in different parts of the system.

Flank margin caves receive and discharge their water by diffuse flow through the carbonate aquifer. The caves form as mixing chambers and, over time, they tend to develop headward into the fresh-water lens. Salt Pond Cave on Long Island,



Figure 3. Punta Esta, Isla de Mona, Puerto Rico, showing many entrances leading into Cueva del Lirio and Cueva el Lado del Faro at the Lirio Limestone/Isla de Mona Dolomite contact near the top of these 40 m high cliffs.

Bahamas (Mylroie *et al.* 1991), includes a chamber with a volume in excess of 14,000 m³ that formed in a maximum time period of 12 Ka, representing a dissolution rate of over 1 cm³/year. As the fresh-water lens thins at the lens margin, the water discharges through an ever decreasing cross-sectional area. As a result, flow velocities are high, allowing the rapid removal of dissolutional products (Reisi & Mylroie 1995).

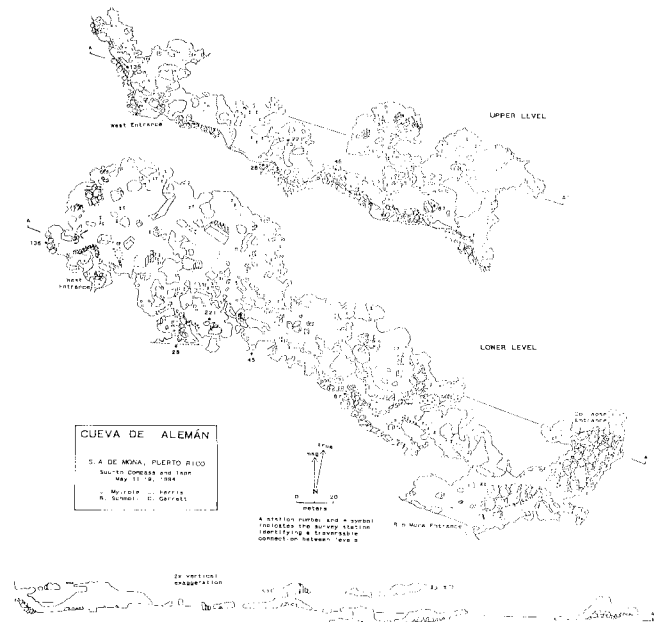


Figure 4. Map of Cueva de Aleman, Isla de Mona, Puerto Rico, an example of a typical plan for a large flank margin cave.

Flank margin caves fit the hypogenic model of Palmer (1991), in that these caves develop through mixing of waters in the subsurface, and are not directly coupled to the surface hydrology.

CAVES OF ISLA DE MONA

Caves literally ring the perimeter of Isla de Mona, preferentially developed at the Lirio Limestone/Isla de Mona Dolomite contact. A geologic map of the island (Briggs & Seiders 1972) depicts the entrances of 25 large caves, and outlines the extent of the largest caves. On the southeast corner of the island Cueva de los Losetsa, Cueva el Lado del Faro, and Cueva del Lirio extend continuously for over 2 km along the coast (Fig. 3). Other significant caves include Cueva de los Pájaros on the southeast coast, Cueva de Aleman (Fig. 4) and

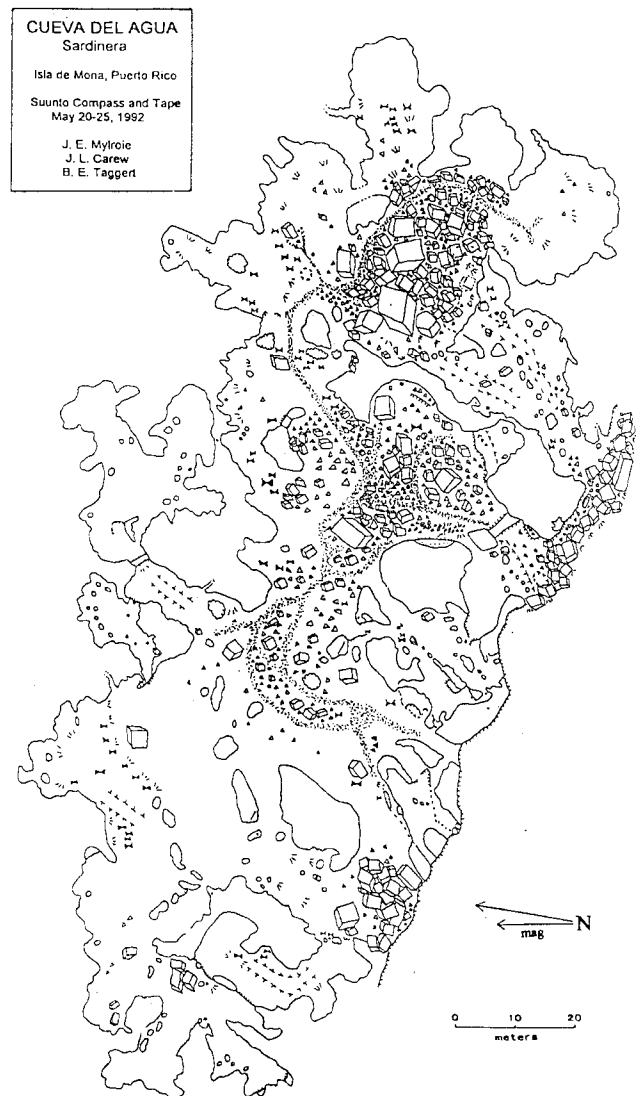


Figure 5. Map of Cueva de Agua, Isla de Mona, Puerto Rico, an example of a typical plan for a large flank margin cave.



Figure 6. Wall cusps found in Cueva de Agua, Isla de Mona, Puerto Rico.

Cueva de Agua (Fig. 5) on the southwest, Cueva del Diamante/Cueva de Esqueleto and Cueva Capitan along the west, and Cueva de Esperanza, Cueva del Gato, and Cueva de Espinal along the northwest coast of the island (Fig. 2). The combined floor areas of the twelve major caves, as explored by Briggs and Seiders in the 1960s, totaled 444,000 m² (Briggs 1974). Frank (1993) and Mylroie *et al.* (1995b) contain descriptions and maps of many of these caves.

ORIGIN OF WALL CUSPS

An important unresolved question in the flank margin model is the origin of the ubiquitous meter-scale curvilinear dissolution features that cover the walls, floors, and ceilings of the cave chambers (Fig. 6). These features are called “cusps” to differentiate them from scallops found in stream passage caves. In places, these cusps cut through a joint-filling breccia made of light-colored carbonate clasts in a reddish matrix. This breccia is interpreted to have originated as a soil that slumped into fractures, lithified, and was subsequently cut by dissolution. Cusps cut through both the wall rock and the breccia material as smooth dissolutional surfaces.

Several lines of evidence indicate these cusps are primary dissolution features. Hundreds of large cave chambers on Isla de Mona have been enlarged by upward stoping of their ceilings. Cusps are present on all original dissolutional cave walls, but are absent on broken rock surfaces produced by stoping between cave levels (Fig. 7). No exceptions were found to this observation. Panuska *et al.* (1998) conclude from paleomagnetic data that portions of these caves are at least 1.8 to 2.0 Ma old. Collapse features formed by stoping are also very old as shown by the large masses of stalagmites and flowstone that have overgrown portions of the breakdown debris. Cusps are also known to exist on comparatively young cave walls. Cueva de Agua (Punta los Ingleses) is developed in a 125 Ka coral rubble facies (Mylroie *et al.* 1997) at a level corresponding to the oxygen isotope 5e sea-level highstand occurring during the



Figure 7. Cave wall section in the lower entrance to Cueva de Aleman, Isla de Mona, Puerto Rico. The upper portion is a relatively smooth breakdown face. The lower portion, containing wall cusps, is from the part of the cave formed by bedrock dissolution.

same period. These 125 Ka old cave wall surfaces are marked by cusps, yet cusps are absent on stoping wall surfaces in many upper-level caves which may be sixteen times older. The ubiquitous distribution of the cusps on cave dissolutional surfaces and their absence on stoping surfaces are evidence that the cusps are primary features formed during the primary speleogenesis process. Another argument is that the basic shapes of the large cave chambers themselves appear to be part of the same progression of curved features that include the cusps (Rice-Snow *et al.* 1997). This suggests that the same primary dissolution process that produced the cave chambers also produced the cusps.

Lips (1993) and Tarhule-Lips and Ford (1995, 1996, 1998) propose that condensation corrosion associated with air currents could have formed the wall cusps after the caves were subaerially exposed. If cusps are formed by condensation corrosion, then they should be equally likely to form, given sufficient time, on breakdown surfaces as on dissolutional surfaces within the caves. Some of the breakdown surfaces are many times older than the ages of the dissolutional surfaces in Cueva de Agua (Punta los Ingleses) marked by cusps. The absence of cusps on old breakdown surfaces is evidence that condensation corrosion is not responsible for cusp formation.

Other arguments against condensation corrosion and air current eddies as the mechanism of cusp formation include the following: (1) cusps are universally present on dissolution surfaces in the caves. Secondary overprinting of the cave surfaces is unlikely to produce as pervasive a cusp distribution as is observed; (2) if air circulation is the driving mechanism of the condensation corrosion process there should be a progressive change in the cusp pattern moving away from a cave entrance as air circulation characteristics change. No such pattern is observed on Isla de Mona; however, such a pattern has been suggested for caves on Cayman Brac (Tarhule-Lips & Ford

1998); (3) no mechanism has been suggested to remove the material stripped from the walls by the condensation corrosion process, and there is no evidence of accumulated residue; (4) even if condensation corrosion were affecting the morphology of the cave walls, it is not clear that the dissolution pattern would reflect the circular pattern of the hypothesized wind eddy currents, so there is no reason to believe that curvilinear cusps would result. We recognize that condensation corrosion does occur, but it plays a minor role in the alteration of specific features within caves. For example, some speleothems that have been eroded by condensation corrosion can be seen at a few localities, such as near the lower entrance to Cueva de Aleman.

Water enters and leaves the developing cave chamber by diffuse flow rather than turbulent flow through open conduits. Therefore another mechanism must generate the currents necessary to produce the cusps. At the large scale, these circulation phenomena could serve to maintain the overall circular to oval shape of the chambers and on a smaller scale to form the cusps that cut across the lithologic variations. Several mechanisms might be responsible. Tidal fluctuations could provide a pumping mechanism that affects circulation, particularly if there is some hysteresis between different portions of the system. Thermally driven convective flow, solute-density driven convective flow, or flow from vadose input could also generate such circulation.

CAVE MORPHOLOGY

Isla de Mona caves have the same overall morphology as flank margin caves previously described from the Bahamas; however, on Isla de Mona many caves are larger and better integrated. This difference can be attributed to differences in fresh-water lens size, stability of lens position, and time available for speleogenesis between the two localities. The flank margin caves exposed in the Bahamas formed in small fresh-water lenses within partially flooded dune ridges over a period of 12 Ka (Carew & Mylroie 1987; Mylroie *et al.* 1991). On Isla de Mona, a larger freshwater lens, possibly a single freshwater lens occupying the entire 55 km² mass of the island, drove the dissolution process. The 1.8 to 2.0 Ma age (Panuska *et al.* 1998) for some cave segments place the genesis of these segments prior to the onset of Quaternary glacioeustasy and its rapid, large sea level fluctuations. Several periods of relative lens position stability, allowing extended periods of speleogenesis, have also likely occurred during the last 2.0 Ma.

Isla de Mona caves are found in a variety of scales and degrees of complexity. The simplest caves consists of single disk-shaped chambers. These chambers enlarge laterally and deeper into the hillside. Eventually adjacent caves may link to form a cave complex consisting of a series of linked chambers than run parallel to the margin of the lens. Several such bands may develop at the same horizon at progressively farther inland positions within the cave. The central portion of Cueva del Diamante (Fig. 8) consists of an outer band of large cham-

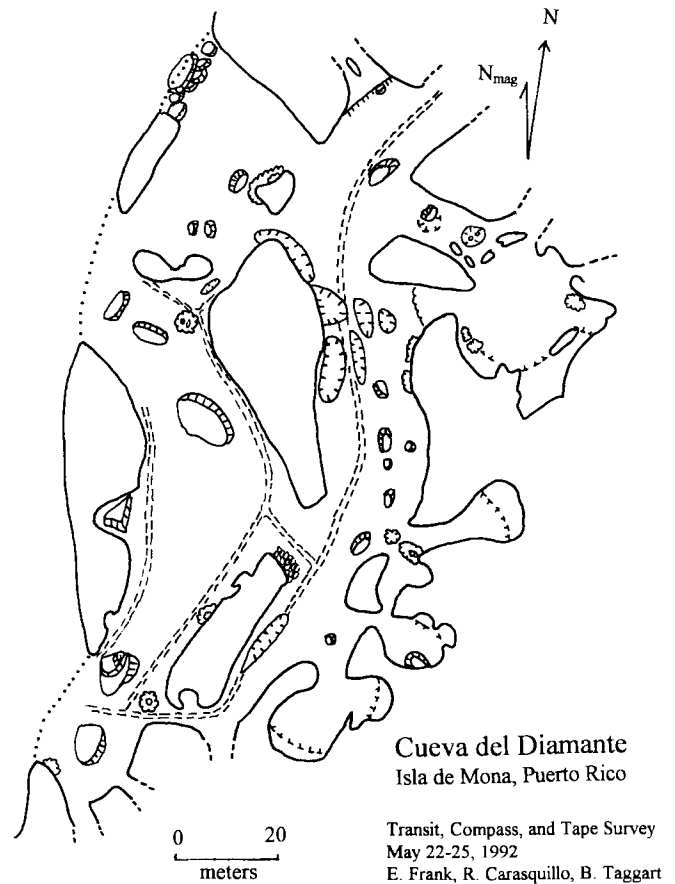


Figure 8. Map of Cueva del Diamante, Isla de Mona, Puerto Rico. Cave map symbols used generally conform to standard symbols by Sprouse and Russell (1980). Parallel lines have been used on selected maps to represent rail beds for mine carts during guano mining operations within the caves.

bers linked laterally by small passages and archways. Off the back of this first band of chambers is a second band of laterally linked chambers. This second band is similarly interconnected laterally and to the chambers in the outer band by smaller passages and archways. Further back in the cave is a third band of chambers which, while linked to the second band, are laterally discontinuous. A similar scaling of size and complexity eventually can produce the complex mazes found in Cueva de los Pájaros and Cueva del Lirio.

A few isolated caves on Isla de Mona exhibit a limited degree of structural control on passage morphology. Cueva Negra, for example, contains several passages oriented along steeply dipping foreset beds. Upward stoping cave ceilings are in many cave chambers with large roof spans. Since Isla de Mona is tectonically active, caves have developed at a variety of levels and on occasion these levels are interconnected by ceiling stoping. In other cases, an extensive horizontal cave may be separated by a meter or less thickness of rock from another extensive, overlying cave.

A fractal analysis of wall cusps and chamber shape in Cueva de Agua (Sardinero) on Isla de Mona by Rice-Snow *et al.* (1997) indicated that these features seem to be morphologically the same and that the process of cusp formation and cave chamber formation scales across at least two orders of magnitude. Based upon maps and observations of these caves, we suggest the gross morphology similarly scales across alcove, single-chamber cave, and multi-chamber cave complexes.

CAVE DEVELOPMENT AND THE LIRIO LIMESTONE/ISLA DE MONA DOLomite CONTACT

Given that the primary zone of cave development is at the base of the Lirio Limestone, at the contact with the underlying Isla de Mona Dolomite, the question arises as to whether the caves formed at that location because of preferential dissolution associated with the difference in composition between the two rock units, or whether the caves are one manifestation of the processes that created the compositional differences between the two units. Kaye (1959) reported that there were two lesser zones of cavern development at stratigraphic positions 15 and 50 m below the Lirio Limestone/Isla de Mona Dolomite (Isla Mona Limestone of Kaye) contact. Briggs (1974) also reported the lesser zones of cave development, and he speculated that because those zones were less dolomitic, the caves formed there because those horizons were more soluble than the surrounding dolomite. Structurally a low amplitude, southwest plunging syncline-anticline-syncline fold sequence is in the island. Overall, the island itself is slightly tilted to the south with the Lirio Limestone/Isla de Mona Dolomite contact at an elevation of 80 m msl along portions of the north coast and absent or below sea level along much of the south and southwestern coast.

Gonzales *et al.* (1990) suggest that dolomitization of the Isla de Mona Dolomite took place in a fresh-water/salt-water mixing zone. Ruiz *et al.* (1991) further suggest that dolomitization of the unit was simultaneous with cave development. Schmoll *et al.* (1997) found, in thin sections of wall rock from Cueva de Aleman, that a significant proportion of the dissolutional porosity in the samples was from diagenesis of high-Mg-calcite red algae, whereas Ruiz (1993) reported that the red algae were not significantly altered in his surface samples. This disparity may represent a difference in dissolutional processes between the carbonic acid systems in the epikarst vadose zone and the mixing-zone chemistry associated with flank margin cave development. These results raise the possibility that Mg-calcite was selectively dissolved in the mixing zone during cave formation and redeposited as part of a concurrent dolomitization of the underlying units. The presence of less dolomitic zones and minor cave development at 15 m and 50 m below the Lirio/Mona contact is interpreted here to be a different stage of this magnesium redistribution process related to a different sea level position, at a different time.

Flank margin caves are in the island at a variety of elevations. Because these caves form at or near sea level, these cave

positions represent the position of relative sea level at the time of their formation. Changes in relative sea level on the island have occurred because of both tectonic activity and glacioeustatic sea level fluctuations. The effects of tectonic uplift are obvious, because there are caves along the northern coast that are now 80 m msl, which is much higher than any glacioeustatic sea level maximum since the deposition of the carbonate units. The effects of glacioeustatic fluctuation can also clearly be seen in some caves. For example Cueva de Agua (Punta los Ingleses) has a passage containing subaerial speleothems that is now below sea level.

SPELEOTHEM MODIFICATION

The caves of Isla de Mona contain abundant subaerial calcite speleothems such as stalactites, stalagmites, columns, flowstone, and rimstone pools. The majority of these speleothems usually appear dry and dead, but a small number are wet and active. However, after 23 cm of rain in 3 days (May 1992), the caves all had large amounts of drip water. Rimstone pools, which had been dry, were then full and flowing. Almost all stalactites and stalagmites were actively dripping water. These chance observations following the biggest storm over a 3-year period indicate that speleothem growth and subsequent modification may be tied to the infrequent precipitation events or to periods of wetter climatic conditions.

The caves of Isla de Mona also contain a wide variety of modified speleothems with pockets, scars, and holes that cut through the primary layering of the speleothems. In certain environments, such as in the twilight of entrance areas, the secondary dissolution of the speleothems is clearly associated with algal and moss growth on the speleothems. However, deep in the caves, where sunlight never reaches, large stalagmites, stalactites, columns and flowstone masses are etched into complex forms. In other places, large dissolution cusps are cut through both the bedrock and adjacent flowstone masses. Like the cusps that cut through the cave wall rock and breccia material, these dissolutional cusps cut through the wall and flowstone mass as a single smooth surface (Fig. 9). Similar features have been reported from Hunts Cave on New Providence Island, Bahamas (Mylroie *et al.* 1991)

While the wall cusps that cut smoothly across rock, breccia, and flowstone clearly seem to be phreatically formed in the fresh-water lens, the complex etching of the stalagmites, stalactites and columns within cave chambers may be more problematic. In a limited number of cases, it is possible that condensation corrosion is at work on these speleothems (Lips 1993; Tarhule-Lips & Ford 1995, 1996, 1998), because many of the caves are very well ventilated through numerous openings on to the cliff face and up to the surface. Such ventilation is uncommon in most other cave settings, so it is possible that minor condensation corrosion effects may be better expressed in the Isla de Mona cave environment.

Another possible explanation for some speleothem etching is the potential for vadose drip water to enter the cave in the

aggressive state, and dissolve calcite in places where drip water had previously precipitated it. The chemistry of the drip water could change as a result of seasonal variations, land use variations, or longer term climatic variations. We believe, however, these highly etched speleothems are mainly the result of phreatic dissolution (Mylroie *et al.* 1995b).

The flank margin caves of Isla de Mona show evidence of: (1) original formation within a fresh-water lens; (2) draining of the lens by a drop in sea level (tectonic or glacio eustatic); (3) abundant growth of subaerial speleothems; (4) partial infill by surface soil to form a breccia; (5) re-occupation of the caves by a fresh-water lens with further dissolution of all components to form cusps and etched speleothems; and (6) tectonic uplift of the island to drain the caves.

SURFICIAL KARST FEATURES

There is some evidence for lowering of the meseta surface by dissolutional removal of bedrock. This includes several small areas (averaging 100 m by 400 m) around the periphery of the island's meseta where the Isla de Mona dolomite is



Figure 9. A pocket of flowstone and wall rock cut smoothly by a wall cusp in Cueva del Lirio, Isla de Mona, Puerto Rico.



Figure 10. Cliff 70 m high along the north coast of Isla de Mona. Foreground area on cliff top is an Isla de Mona Dolomite exposure where a former cave has lost its roof through denudation. The cave entrances in the background are to Cueva de Espinal developed at the Lirio Limestone/ Isla de Mona Dolomite contact. Sections of cave are still present in the upper parts of the blocks that have fallen from the cliff.

exposed at the surface (Fig. 10). These areas are thought to represent caves whose roofs have been removed. They have the following characteristics: (1) they are observably lower in elevation than the adjacent Lirio Limestone areas; (2) the size, shape, and distribution of these dolomite exposures are comparable to adjacent large caves developed at the Lirio Limestone/Isla de Mona contact; (3) the elevations of these surface exposures are approximately the same as the floor elevations in adjacent caves; (4) flowstone is commonly present on the meseta surface within these areas; (5) remains of large stalagmites are occasionally present in these areas; and (6) in some cases, the outline of cave rooms can be distinguished. All of these characteristics support the conclusion that these are caves that have been de-roofed by denudation of the meseta surface.

LARGE SCALE DEPRESSIONS

There are three major internally drained features in the interior of the island: Bajura de los Cerezos, Cuevas del Centro, and Los Corrales de los Indios (Fig. 2). Bajura de los Cerezos consists of a large closed depression and associated valley along a southwest-trending fault in the central part of the island. The edge of the depression is developed in the Lirio Limestone, but the lower part penetrates into the Isla de Mona Dolomite. During heavy rains a small stream forms and sinks in the bottom of the depression.

Cuevas del Centro consists of a multiple sink feature. The largest closed depression consists of a 550 m diameter sinkhole that drops 20 m below the surrounding countryside. From the side of the largest of several small sinks in the basin, a cave extends downward as a wide, short, low crawlway before becoming blocked with rock debris and rubble (M. Morales, personal communications 1992).

Los Corrales de los Indios is a series of shallow sinks aligned in a southeastern trending valley in the eastern portion of the island. Briggs (1974) reported that no caves are known to have developed off any of these sinks. The linear nature of this feature suggests that it may be developed along a dissolutionally enlarged joint swarm or fault.

A question about these internally drained features concerns the distribution of the water they capture. The possibilities include: (1) water is drained and stored in a diffuse aquifer within the Isla de Mona Dolomite; (2) water is discharged along the periphery of the island at current sea level, and (3) water is discharged from subsurface springs around the edge of the island. Work on Guam (Barner 1997) has shown that such internal depressions in Miocene carbonates there drain by both diffuse and fracture flow with different flow rates and destinations. Subsea-level springs have been reported by divers (R. Van Damm, written communication 1995) along the northern coast of the island near Cabo Noroeste. It is not clear what proportion of the water is being distributed by fracture flow or diffuse flow. Some water may also be discharging via sub-sea level conduits that developed during relative sea-level lowstands during the Pleistocene. However, there are no known conduits (as opposed to flank margin caves, which are not conduits) that relate to the +6 m sea-level highstand of the last interglacial that could have drained these internal depressions.

CAMINO DE LOS CEREZOS PIT COMPLEX

The Camino los Cerezos Pits are a dense concentration of vertical shafts and pits located in the south-central portion of the island approximately 1 km north of Playa del Uvero. These are marked as area "N" on the geologic map of the island (Briggs & Seiders 1972). The locations of the pits in a small part of the area were mapped to document their density (Fig. 11). There are hundreds of additional pits and many large sinkholes in the interior of the island (Frank 1993; Mylroie *et al.* 1995).

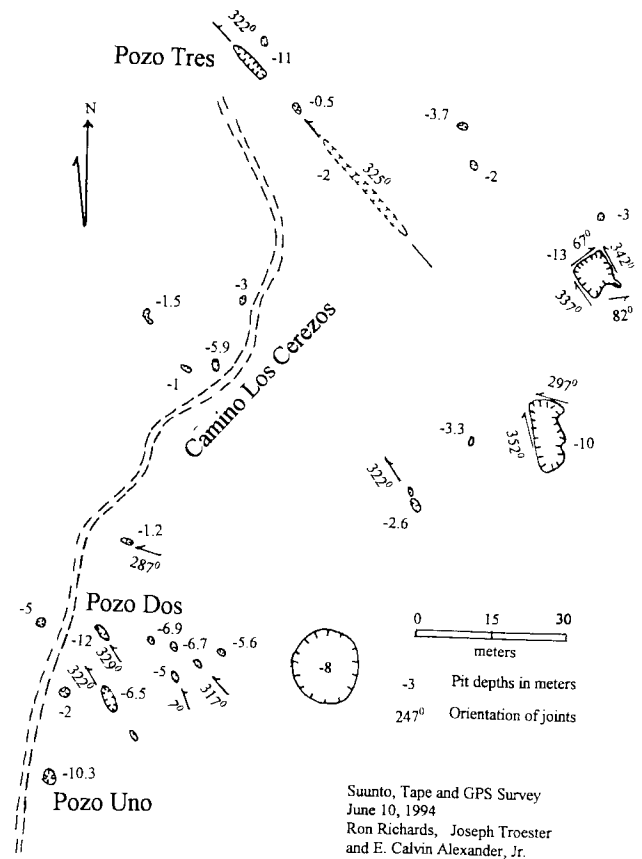
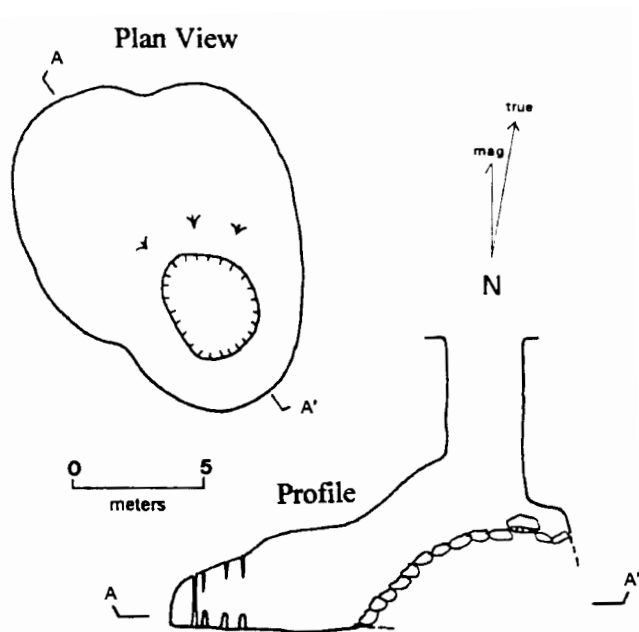


Figure 11. Map of pit locations along a survey loop in the Camino de los Cerezos Pit Complex, Isla de Mona, Puerto Rico.

Quinlan (1974) entered and examined 30 pit caves in this vicinity. In one small area he reported that four cylindrical pits, each 8 m deep, are located within 3 m of each other, yet do not connect, do not have enlarged bottoms, and do not have any passages leading away from their bottoms. Investigations by the authors confirm these observations. On Isla de Mona the pits are typically vertical shafts whose bottoms bell-out into small chambers (Fig. 12). Many pits seem to end at about the same elevation, possibly indicating stratigraphic or past fresh-water lens control.

In December 1996, a deep pit named Quinlan Pit, was discovered and explored (Fig. 13). A 4- to 5-m-wide entrance shaft drops vertically 19 m to a flat floor, with a 5-m-wide-balcony extended off the side of the pit 10 m below the surface. The top of the pit begins in limestone, the floor of the balcony is developed on dolomitic limestone, and the base of the shaft extends into dolomite. The balcony may mark the transition from the Lirio Limestone to the Isla de Mona Dolomite. A similar pit was described by Quinlan (1974) with the same interpretation.

Pace *et al.* (1993) discussed the origin of similar pit complexes found on San Salvador, Bahamas. They proposed that the pits on San Salvador were fed by subterranean flow as well



Pozo Uno
Camino Los Cerezos
Isla de Mona, Puerto Rico

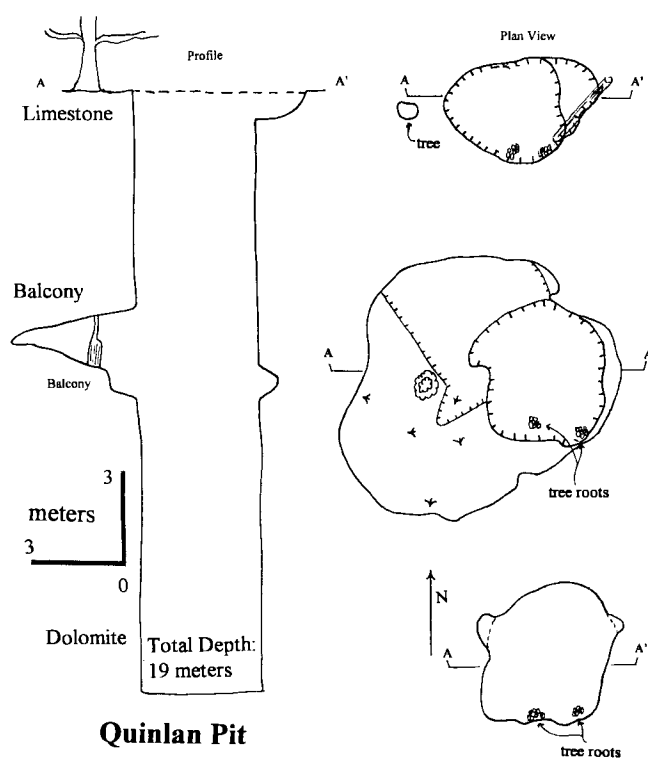
Suuto and Tape Survey
May 26, 1992
E. Frank and J. Mylroie

Figure 12. Map of Pozo Uno in the Camino de los Cerezos Pit Complex. The profile is typical of many of the larger pits in the area.

as surface runoff. Pits develop when a fracture, or other path, to the subsurface was encountered by flow in the epikarst. As new paths to the subsurface develop, pre-existing pits are abandoned. New pits form in a growing ring out from the center of the complex. The presence of subterranean tubes and the similarity of the general plan of the pit field to that found on San Salvador Island support this mode origin for the pit complex at Camino los Cerezos on Isla de Mona.

CLIFF RETREAT

Flank margin caves form without natural entrances, so caves on Isla de Mona that open to the cliff face are evidence that cliff retreat has taken place. Also, many of these cliff-face entrances contain large, hard, massive speleothems, which do not form in open environments. Speleothems formed in the light zone tend to be porous, soft, and contain inclusions of algae.



Quinlan Pit

Isla de Mona, Puerto Rico
Suunto and Tape Survey
December 1996
Edward Frank and Robert Frank

Figure 13. Map of Quinlan Pit in the Camino de los Cerezos Pit area, Isla de Mona, Puerto Rico.

Jennings (1985) describes vertical cliffs in limestone coastal settings in a variety of rocks. Limestone cliffs are typically undercut by bioerosion notches, flank margin caves, and sea cave. These features promote the mechanical collapse of the cliff from the cliff base upward and help maintain the vertical profile. Isolated fallen slabs of rock from the vertical cliff face and cliff parallel fractures along the coast of Isla de Mona are consistent with this base-upward collapse model (Fig. 10). Massive rock boulders can be seen at the base of the cliffs in many places, some with segments of cave still contained within the blocks.

The amount of cliff retreat cannot be determined precisely, but there are several general indications. If the original cave population, formed almost continuously around the island, included tiny, small, medium, and large caves as in the Bahamas, then different amounts of cliff retreat would result in different patterns of cave remnant distribution. A small amount of retreat would remove the tiny caves, leaving a gap between the remaining caves. A large amount of retreat would remove the tiny, small, medium, and much of the large size caves leaving bigger gaps between the remaining segments of the large caves and the scattered original caves. The continuity of caves around much of the island perimeter is best explained by a

small amount of cliff retreat. As flank margin caves do not develop deep into the fresh-water lens, the amount of cliff retreat has likely been a few tens of meters to a maximum of around 100 m since these caves formed over 1 Ma.

Bioerosion notches +6 m above the base of the vertical cliffs at many localities are associated with fossil coral reefs radiometrically dated to 125 Ka and correspond to sea level during that time. If the cliffs formed by this base upward collapse process, then the presence of the bioerosion notches near the base of these cliffs indicate that the cliff profile in these areas has not changed significantly in the last 125 Ka.

CONCLUSIONS

The caves of Isla de Mona are flank margin caves that represent development in a past fresh-water lens. These caves resulted from the exceptional dissolutional potential created by the mixing of fresh and marine waters, coupled with possible oxidation/reduction reactions from decomposing organic matter that was concentrated by density contrasts at the top of the lens and at the halocline. These flank margin caves are morphologically similar to those reported in the Bahamas, but they are older and larger.

The caves of Isla de Mona may date to before the start of the Quaternary, about 2 Ma (Panuska *et al.* 1998). They contain a complex history of development and modification by vadose and phreatic processes, coupled with glacioeustasy and tectonics. The caves near the top of the cliffs formed when the carbonate platform was emergent, and they have been modified by collapse, speleothem deposition, re-flooding by sea-level highstands, and segmentation by cliff retreat. On the island surface, pit caves and large closed depressions have developed since emergence of the platform.

As flank margin caves form at sea level, the sequence of events required to explain their distribution is as follows: (1) deposition of the Isla de Mona and the Lirio units as limestones; (2) folding resulting in the southeast-plunging synclines and anticline; (3) faulting that may have been contemporaneous with folding; (4) subaerial exposure of the carbonate platform; (5) dissolution of the major cave systems; and (6) tilting of the island to the south. The juxtaposition of the major level of cave formation with the top of the dolomitized zone marking the Lirio Limestone/Isla de Mona Dolomite contact can hardly be coincidental.

Isla de Mona is one of the most cavernous localities on Earth. The large size of the caves, the tropical warmth, and the maze-like character of their large rooms and chambers make exploration and cave science unusually enjoyable.

ACKNOWLEDGMENTS

We thank the Cave Research Foundation, the University of Minnesota's Department of Geology and Geophysics, and their George and Orpha Gibson Endowment in hydrogeology for financial assistance in conducting field work on Isla de

Mona and laboratory processing of samples collected from the island.

REFERENCES

- Back, W., Hanshaw, B.B., Pyle, T.E., Plummer, L.N. & Weidie, A.E. (1979). Geotechnical significance of groundwater discharge and carbonate dissolution to the formation of Caleta Xel Ha, Quintana Roo, Mexico. *Water Resources Research* 15: 1521-1535.
- Barner, W. L. (1997). Time of travel in the fresh water lens of northern Guam. In Carew, J.L. (ed.). *Proceedings of the eighth symposium on the geology of the Bahamas*: San Salvador Island, Bahamas, Bahamian Field Station: 1-12.
- Bogli, A. (1980). *Karst hydrology and physical speleology*: New York, Springer-Verlag: 284 p.
- Bottrell, S.H., Carew, J.L. & Mylroie, J.E. (1993). Inorganic and bacteriogenic origins for sulfate crusts in flank margin caves, San Salvador Island, Bahamas. In White, B. (ed.). *Proceedings of the sixth symposium on the geology of the Bahamas*. Port Charlotte, Florida, Bahamian Field Station: 17-21.
- Briggs, R.P. (1974). Economic geology of the Isla de Mona quadrangle, Puerto Rico. *U.S. Geological Survey, Open File Report* 74-226: 116 p.
- Briggs, R.P. & Seiders, V.M. (1972). Geologic map of the Isla de Mona quadrangle, Puerto Rico. *U.S. Geological Survey Miscellaneous Geological Investigations* Map I-718, 1:20,000.
- Chen, J.H., Curran, H.A., White, B. & Wasserburg, G.J. (1991). Precise chronology of the last interglacial period $^{234}\text{U}/^{230}\text{Th}$ data from coral reefs in the Bahamas. *Geological Society of America Bulletin* 103: 82-97.
- Frank, E.F. (1993). *Aspects of karst development and Puerto Rico: An analogue for Pleistocene speleogenesis in the Bahamas*. MS thesis, Mississippi State University: 288 p.
- Frank, E.F., Wicks, C., Mylroie, J.E., Troester, J.W., Alexander Jr., E.C. & Carew, J.L. (1998). Geology of Isla de Mona, Puerto Rico. *Journal of Cave and Karst Studies* 60(2): 69-72.
- Gonzalez, L.A., Ruiz, H. & Monell, V. (1990). Diagenesis of Isla Mona, Puerto Rico [abs]. *American Association of Petroleum Geologists Bulletin* 74: 663-664.
- Gonzales, L.A., Ruiz, H.A., Taggart, B.E., Budd, A.F., & Monell, V. (1997). Geology of Isla de Mona, Puerto Rico. In Vacher, H.L. & Wuinn, T. (eds.). *Geology and Hydrogeology of Carbonate Islands. Developments in Sedimentology* 54. Elsevier, New York: 327-358.
- Harris, J.G., Mylroie, J.E. & Carew, J.L. (1995). Banana holes: Unique karst features of the Bahamas. *Carbonates and Evaporites* 10: 215-224.
- Jennings, J.N. (1985). *Karst geomorphology*. Basil Blackwell, Inc., New York: 293 p.
- Kaye, C.A. (1959). Geology of Isla Mona, Puerto Rico, and notes on the age of the Mona Passage. *U.S. Geological Survey Professional Paper* 317C: 141-178.
- Lips, R.F.A. (1993). *Speleogenesis on Cayman Brac, Cayman Islands, British West Indies*. MS thesis, McMaster University: 233 p.
- Martinez, M.I., Troester, J.W. & Richards, R.T. (1995). Surface electromagnetic geophysical exploration of the ground-water resources of Isla de Mona, Puerto Rico, a Caribbean carbonate island. *Carbonates and Evaporites*, 10: 184-192.

- Myroie, J. E. (1988a). *Field guide to the karst geology of San Salvador Island, Bahamas*. Bahamian Field Station, Fort Lauderdale: 108 p.
- Myroie, J.E. (1988b). Karst of San Salvador. In Myroie, J. E. (ed.). *Field guide to the karst geology of San Salvador Island, Bahamas*, Bahamian Field Station, Fort Lauderdale: 17-44.
- Myroie, J.E. & Carew, J.L. (1988). Solution conduits as indicators of Late Quaternary sea level position. *Quaternary Science Reviews* 7: 55-64.
- Myroie, J.E. & Carew, J.L. (1990). The flank margin model for dissolution cave development in carbonate platforms. *Earth Surface Processes and Landforms* 15: 413-424.
- Myroie, J. E. & Carew, J. L. (1991). Erosional notches in the Bahamian carbonates: Bioerosion or groundwater dissolution? In Bain, R. J., ed., *Proceedings of the fifth symposium on the geology of the Bahamas*, Bahamian Field Station, San Salvador, Bahamas: 185-191.
- Myroie, J.E. & Carew, J.L. (1995). Karst development on carbonate islands. In Budd, D.A., Saller, A.H. & Harris, P.M. (eds.). *Unconformities in carbonate strata their recognition and the significance of associated porosity*. American Association of Petroleum Geologists Memoir 63: 55-76.
- Myroie, J.E., Carew, J.L. & Vascher, H.L. (1995a). Karst development in the Bahamas and Bermuda. In Curran, H. A. & White, B. (eds.). *Terrestrial and shallow marine geology of the Bahamas and Bermuda*, Geological Society of America Special Paper 300: 251-267.
- Myroie, J.E., Lundberg, J. & Carew, J.L. (1997). Rapid flank margin cave formation in the fresh-water lens: An example from Isla de Mona, Puerto Rico [abs.]. *Geological Society of America Abstracts with Programs* 29: A-39
- Myroie, J.E., Panuska, B.C., Carew, J.L., Frank, E.F., Taggart, B.E., Troester, J.W. & Carrasquillo, R. (1995b). Development of flank margin caves on San Salvador Island, Bahamas and Isla de Mona, Puerto Rico. In Boardman, M. (ed.). *Proceedings of the seventh symposium on the geology of the Bahamas*, Bahamian Field Station, San Salvador, Bahamas: 49-81.
- Pace, M.C., Myroie, J.E. & Carew, J.L. (1993). Investigation and review of dissolutional features on San Salvador Island, Bahamas. In White, B. (ed.). *Proceedings of the sixth symposium on the geology of the Bahamas*, Port Charlotte, Florida, Bahamian Field Station: 109-124.
- Palmer, A.N. (1991). Origin and morphology of limestone caves. *Geological Society of America Bulletin* 103: 1-25.
- Palmer, A.N., Palmer, N.W., and Queen, J.M. (1977). Geology and origin of caves in Bermuda. In Ford, T.D. (ed.). *Proceedings of the Seventh International Speleological Congress*, Sheffield, England: 336-338.
- Panuska, B.C., Myroie, J.E. & McFarlane, D. (1998). Magnetostatigraphy at Cueva de Aleman, Isla de Mona, Puerto Rico. *Journal of Cave and Karst Studies* 60(2): 96-100.
- Peck, S.B. & Kukulova-Peck, J. (1981). The subterranean fauna and conservation of Mona Island, Puerto Rico. *National Speleological Society Bulletin* 43: 59-68.
- Plummer, L.N. (1975). Mixing of sea water with calcium carbonate groundwater. In Whillens, E.H.T. (ed.). *Quantitative studies in the geological sciences*, Geological Society of America Memoir 142: 219-236.
- Quinlan, J.F. (1974). *Preliminary exploration and evaluation of the caves of Mona Island, including a description of origin*. U.S. National Park Service, unpublished administrative report, on file with U.S. Geological Survey, GSA Center, Guaynabo, PR: 33 p.
- Reisi, E. & Myroie, J.E. (1995). Hydrodynamics behavior of caves formed in the fresh-water lens of carbonate islands. *Carbonates and Evaporites* 10: 129-135.
- Rice-Snow, S., Wicks, C.M. & Tarhule-Lips, R.F.A. (1997). Detailed wall morphology of an interior flank margin cave room, Isla de Mona, Puerto Rico. In Carew, J.L. (ed.). *Proceedings of the eighth symposium on the geology of the Bahamas*. San Salvador Island, Bahamas, Bahamian Field Station: 158-165.
- Sprouse, P. & Russell, W. (1980). AMCS cave map symbols. *AMCS Newsletter* 11: 64-67.
- Ruiz, H.M. (1993). *Sedimentology and diagenesis of Isla de Mona, Puerto Rico*. MS thesis, University of Iowa, Iowa City: 86 p.
- Ruiz, H., Gonzalez, L.A. & Budd, A.F. (1991). Sedimentology and diagenesis of Miocene Lirio Limestone, Isla de Mona, Puerto Rico [abs.]. *American Association of Petroleum Geologists Bulletin* 75: 664-665.
- Shackleton, N.J. & Opdyke, N.D. (1973). Oxygen isotope and paleomagnetic stratigraphy of equatorial Pacific core V28-238: Oxygen isotope temperatures and ice volumes on a 105 year and 106 year scale. *Quaternary Research* 3: 39-55.
- Schmoll, B.J., Carew, J.L. & Myroie, J.E. (1997). Petrologic analysis of Cueva de Aleman, Isla de Mona, Puerto Rico. In Carew, J.L. (ed.). *Proceedings of the eighth symposium on the geology of the Bahamas*, San Salvador Island, Bahamas, Bahamian Field Station: 166-173.
- Taggart, B.E. (1993). *Tectonic and eustatic correlations of radiometrically dated marine terraces in northwest Puerto Rico and Isla de Mona, Puerto Rico*. PhD dissertation, University of Puerto Rico, Mayaguez: 252 p.
- Tarhule-Lips, R.F.A. & Ford, D.C. (1995). Speleothem dissolution on Cayman Brac and Isla de Mona. *Geological Society of America Abstracts with Programs* 27: A-346.
- Tarhule-Lips, R.F.A. & Ford, D.C. (1996). Timing and causes of speleothem dissolution on cayman Brac, Cayman Islands, BWI. In *Climate change: The karst record*: Bergen, Norway, Karst Waters Institute Special Publication 2: 165-166.
- Tarhule-Lips, R.F.A. & Ford, D.C. (1998). Condensation corrosion in caves on Cayman Brac and Isla de Mona. *Journal of Cave and Karst Studies* 60(2): 84-95.
- Vogel, P.N., Myroie, J.E. & Carew, J.L. (1990). Limestone petrology and cave morphology on San Salvador Island, Bahamas. *Cave Science, Transactions of the British Cave Research Association* 17: 19-30.

CONDENSATION CORROSION IN CAVES ON CAYMAN BRAC AND ISLA DE MONA

ROZEMARIJN F.A. TARHULE-LIPS AND DEREK C. FORD

School of Geography and Geology, McMaster University, Hamilton, Ontario, L8S 4K1 CANADA

Many speleothems in caves on Cayman Brac and Isla de Mona have suffered considerable dissolution. It is suggested that this is a consequence of condensation corrosion rather than of aqueous flooding of the entire cave. A program of temperature and relative humidity measurements during the rainy seasons showed that the entrance zones are areas of comparatively large diurnal variation where condensation from warm air onto cooler walls may occur. Artificial condensation was induced using ice bottles: chemical analysis of the condensation waters determined that they were generally undersaturated with respect to calcite and/or dolomite but that this changes over space and time. Gypsum tablets were suspended inside three sample caves on Cayman Brac and one on Isla de Mona for 16 and 13 months, respectively. At the end of this period, tablets close to the entrances and to the floor were found to have undergone considerable dissolution; this could only have been the result of condensation corrosion

Where water condensing onto cave walls in soluble rocks is undersaturated with respect to the mineral (calcite, dolomite, gypsum, etc.), the potential exists for dissolution to occur; the process is termed "condensation corrosion" (Ford & Williams 1989: 309). It may create some characteristic speleogen features. The most widespread are "air scallops" (Hill 1987: 89), shallow, rounded recesses on walls and ceilings, with lengths ranging from decimeters to several meters. Less common are corrosion channels in ceilings or furrows in floors where condensation water has dripped from above. "Punk rock" (Hill 1987: 89; cavernous weathering with some decomposition of the inter-cavern partitions) may be seen where particularly corrosive air attacks bedrock of heterogeneous solubility. In hydrothermal caves, such speleogens are often large and easily recognized; this is because of the large temperature differences between the thermal water sources of vapour and the bedrock, and also because of greater CO₂ partial pressure and/or the formation of H₂SO₄ from discharged H₂S, both of which will increase the aggressivity of the condensation water. In other categories of caves condensation water is normally less abundant and probably also less aggressive: the resulting speleogens are readily confused with those caused by other processes, primarily phreatic dissolution (Cigna & Forti 1986). This has led to much misinterpretation in some past cave genetic studies.

Small holokarstic oceanic islands in young rocks are ideal sites to study the development of condensation corrosion features. They constitute closed systems without strong external influences: the only fresh water derives from condensation or infiltrating rain because areas above the caves are too small to support surface streams, and the comparatively high primary porosity of the rock dampens the amplitude of any rain floods underground. As a consequence, prolonged flooding (establishing or re-establishing phreatic hydrodynamic conditions) will only be the result of a relative rise in sea level that is due to eustatic or tectonic effects.

The climate in caves is often described as being constant, but in reality this is found only in deep interiors where there is minimal interaction between the cave and the outside environment. Condensation will occur where the air is cooled below its dew-point temperature by mixing with colder air or through contact with colder walls. Condensation should be negligible in cave interiors that have stable temperatures close to the mean annual exterior temperatures of their region and, in humid regions, relative humidities of ~100%. However, it might be observed in the entrance or transition zones. For nearly horizontal caves with single entrances (broadly, the conditions found on Cayman Brac and Isla de Mona) the climate model available is one developed by Wigley and Brown (1971). They modeled the entrance and transition zone for three seasonal conditions - summer, winter and transitional periods (fall or spring) - in humid temperate and alpine climates (i.e. those with warm summers and cold winters). The longitudinal temperature distribution was calculated by:

$$T_{\text{mean}} = T_a + (T_0 - T_a) e^{-x} + (L/c)(q_0 - q_a) X e^{-x} \quad (1)$$

where T_{mean} is the mean temperature of the air in the cave (°C), T_a is the wall temperature (°C), T_0 is the temperature of the air entering the cave (°C), L is the latent heat of vaporization provided that the thermal diffusivity of the wall is much less than that of the air (J/kg), c is the specific heat (at constant pressure) of the air (J/kg/K), q_0 is the specific humidity of the air entering the cave (g/kg), q_a is the specific humidity at the wall (g/kg) and X is a non-dimensional length defined by

$$X = x/x_0 \quad (2)$$

where x is the distance measured from the entrance (m). In caves external temperature and humidity fluctuations decay with increasing penetration distance into a cave. This decay, or damping of specific humidity/temperature in the absence of

moisture is characterized by a relaxation length (or “e-folding” length), x_0 . The latter is determined by the Prandtl, Reynolds and Nusselt numbers, which are non-dimensional groups frequently used in heat transfer and fluid mechanics. Eventually, x_0 only depends on the radius of the cave and the flow velocity as defined by Wigley & Brown (1971):

$$x_0 = 36.44 a^{1.2} V^{0.2} \quad (3)$$

Accordingly, the longitudinal humidity distribution was calculated by

$$q_{\text{mean}} = q_a + (q_0 - q_a) e^{-x} \quad (4)$$

Wigley and Brown (1971) suggest that equilibrium is reached in about $5 x_0$ to $6 x_0$ from the entrance of the cave. This model is for the most ideally simple case: a pipe of circular cross-section and fixed radius. Where the cross-section is tapered or irregular with many constrictions, the relaxation length remains x_0 but it is no longer a constant. Most coastal caves show either taper or irregularities with constrictions or both, and will thus have a changing x_0 .

During the winter and the transition seasons evaporative cooling will occur for all x where T_a is greater than the outside dew-point temperature. In the summer months the situation is reversed and condensation occurs on the cave walls, increasing the air temperature (Wigley & Brown 1971).

The Caribbean region has a tropical marine climate where seasonal temperature variations are small compared to the diurnal variations that occur. This permits measurement of the Wigley-Brown parameters within a short period of time: daytime corresponds with the summer situation and nighttime with the winter situation. The configuration of the caves on Cayman Brac and Isla de Mona is also relatively simple: large entrances give access to large rooms close to coastal cliff faces, from which smaller passages radiate modest distances into the rock. The caves show many of the types of speleogens associated with condensation corrosion. They are also richly decorated with vadose speleothems, many of which are dry and show signs of dissolution, indicating that they are no longer growing. Often a corrosion pocket will cut across both bedrock and speleothem in a uniform facet. Since many caves are well above sea level at present, flooding is unlikely to have occurred. Condensation corrosion is believed to have been the cause of the later phases of dissolution of the cave walls and speleothems. Analysis of the cave microclimate can help establish whether the present-day conditions are suitable for condensation corrosion and if the process is still continuing.

The objectives of the study reported in this paper were to investigate the microclimatology and water chemistry of selected caves on Cayman Brac and Isla de Mona to determine whether significant condensation corrosion could be occurring there at present.

STUDY AREAS

Cayman Brac ($19^{\circ}43'N$ $79^{\circ}47'W$) and Isla de Mona ($18^{\circ}05'N$ $67^{\circ}55'W$) are very similar in appearance, size and geology (Fig. 1). Both islands have cores of Tertiary (mainly Miocene) carbonates. Their coastlines are vertical cliffs partially fringed by narrow coastal plains of Pleistocene limestones. The bedrocks are very pure because the islands are located far from any mainland or continental shelves where rivers might supply clays or sands. The Tertiary strata are extensively dolomitized and have been tectonically uplifted in the past, tilting the islands. Isla de Mona was uplifted 20 m in the south, increasing to 90 m in the north. Cayman Brac displays zero uplift in the west, rising steadily to 45 m at the east end. The presence of horizontal Pleistocene coastal plains and marine erosional notches in the cliffs above them indicates that both islands have been tectonically stable since at least the last interglacial period (oxygen isotope substage 5e, 125,000 years BP; Woodroffe *et al.* 1983; Taggart & González 1994; Frank *et al.* 1998).

Hydrological conditions on both islands are similar and relatively simple. There are no stream channels. Infiltrating rain water creates shallow freshwater lenses which float on top of denser saline water.

The majority of the cave entrances are in the coastal cliffs. The caves are confined to narrow zones behind them, extending inland no more than 50 m from the cliffs on Cayman Brac

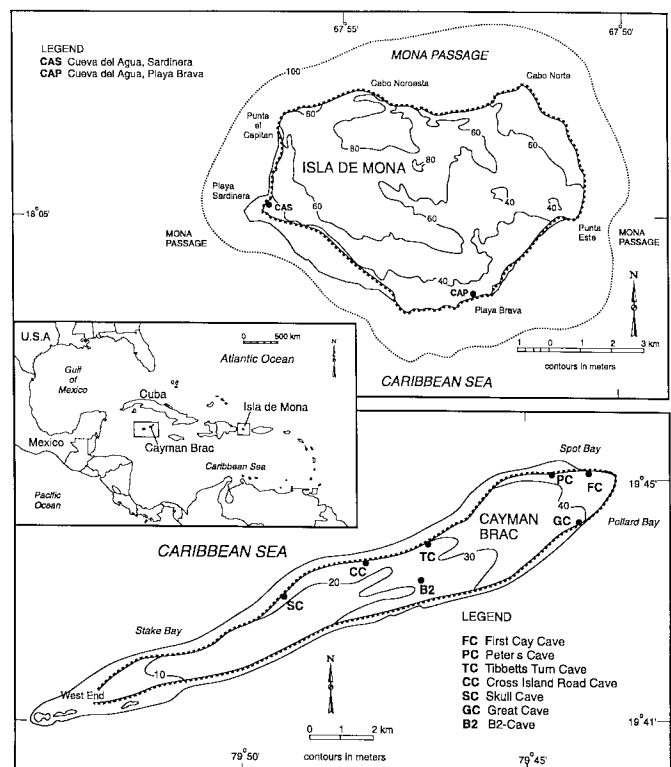


Figure 1. Location of Cayman Brac, Isla de Mona and the caves studied.

and 250 m on Isla de Mona. This suggests that the caves developed around the edges of the islands and were opened up by cliff recession. There are two spatially distinct groups of caves on Cayman Brac: "notch caves" which are located at, or 1 to 2 m above, the +6 m, stage 5e marine notch, and upper caves with entrances at irregular elevations more than 2 m above the notch. The caves of Isla de Mona and the notch caves on Cayman Brac fit the flank margin cave development model, according to which caves form at the discharging margins of the freshwater lens prior to uplift (Myroie *et al.* 1994; Myroie & Carew 1990). The upper caves on Cayman Brac are also interpreted to have formed in the phreatic zone around the margins of the island, but they appear to have been influenced by pre-existing structures in the bedrock to a greater extent. The caves on Isla de Mona are bigger than those of Cayman Brac, which might be partially due to the different configuration of the islands; Isla de Mona is larger in area and quite circular, whereas Cayman Brac is very elongated. Island shape greatly influences the extent and thickness of the freshwater lenses and, thus, the magnitude of the formation of flanking caves. On the plateaus above them, the karst features are limited to dissolution pits, sometimes associated with small cave chambers or shafts.

The sample caves on Cayman Brac include First Cay Cave (FC), Peters Cave (PC), Tibbetts Turn Cave (TC), Cross Island Road Cave (CC) and Skull Cave (SC) located on the north side of the island, Great Cave (GC) on the south side and B2-Cave (B2) on the plateau (Fig. 1). FC and GC are developed in the Brac Formation (late Early Oligocene) - FC being in limestone and GC in dolostone: all other caves in the sample are formed in dolostones of the Cayman Formation (Lower to Middle Miocene; Jones *et al.* 1994). CC, SC and GC are notch caves. They have less speleothem growth than the upper caves. In general, the speleothems far inside the caves are still growing, whereas those closer to the entrances show increasing amounts of corrosion. In FC, speleothem dissolution is very clearly zonal: in the entrance, speleothems have been corroded to the point where their original shape can no longer be recognized; this is succeeded by a zone of corroded speleothems with still recognizable shapes and finally, deep inside the caves, there are actively growing speleothems (Fig. 2). Because of its greater size and this very clear zonation, FC was studied in more detail than the other caves.

On Mona, Cueva de Agua, Sardinera (CAS), is located in the Isla de Mona Dolomite (Late Miocene to Early Pliocene) in the southwest corner of the island (Fig. 1). Cueva de Agua, Playa Brava (CAP) is at the southeast corner (Fig. 1) and has a more complicated geologic history. Initially, a large cave developed in Lirio Limestone (Miocene) which was then filled with reef rubble of Pleistocene age that became lithified. A relative sea level change submerged the site and the present day cave was dissolved in both the Pleistocene rubble and the Miocene limestone (Frank 1993).

The climate on the islands is of the tropical marine type with very small seasonal temperature variations. Annual pre-

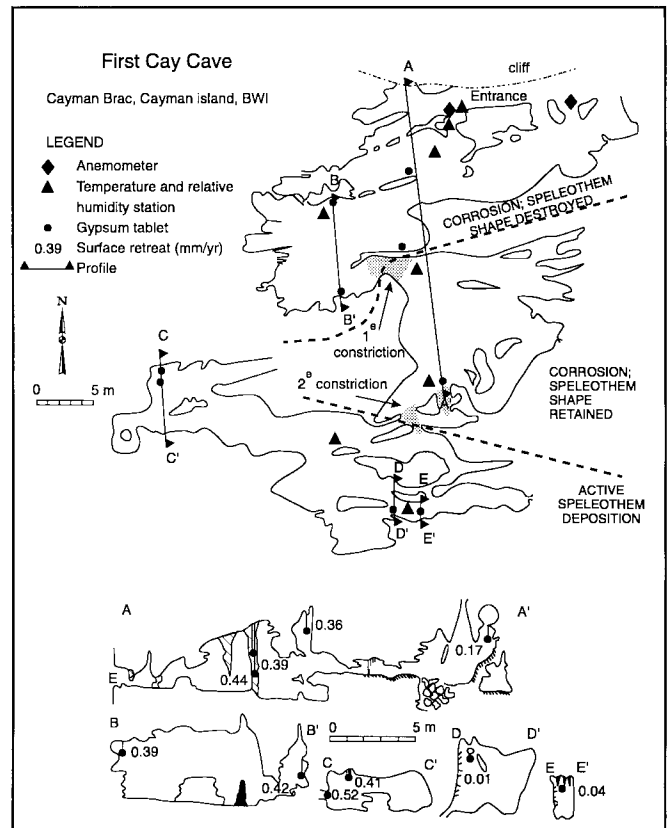


Figure 2. Zonation of speleothem corrosion, meteorological instrument set up, location of gypsum tablets with their surface retreat rates, First Cay Cave, Cayman Brac.

cipitation averages 1025 mm on Cayman Brac and 800 mm on Isla de Mona and is concentrated mainly in the summer months. Proximity to the sea causes comparatively high relative humidity at all times in the caves.

METHODS OF STUDY

Field measurements were taken during two rainy season months (May 1994 and September 1995) in seven caves on Cayman Brac, and in June 1994 in two caves on Isla de Mona (Fig. 1).

TEMPERATURE AND RELATIVE HUMIDITY

Temperature and relative humidity profiles were taken at five caves on Cayman Brac (FC, PC, TC, GC and SC) from the entrances inward, twice daily (~10:00 hr and ~17:00 hr). Wet and dry bulb temperatures were measured with a T-type thermocouple to a resolution of 0.1 °F. The measurements were taken at three heights: 5 cm above the floor, midway between floor and ceiling and about 5 cm below the ceiling (in very high rooms, readings were made at 3.5 m above the floors). The Fahrenheit scale was used to increase the precision of calculation of relative humidity and later converted to degrees Celsius.

Temperature and relative humidity maps were constructed for FC, PC, SC and GC using one-time temperature readings at the three heights at sufficient points to cover all areas of the caves satisfactorily. Due to time limitations, only simpler line (transect) profiles could be constructed for CAS and CAP on Isla de Mona.

In First Cay Cave a more elaborate system was installed, consisting of two anemometers, two wind vanes, and two sets of dry bulb-wet bulb thermocouples connected to a datalogger (Fig. 2). This permitted continuous measurements during the period, September 12 - October 5, 1995. The wind measurements were taken at the two main entrances to the cave, and the psychrometric temperature measurements at 2 m (entrance) and 8 m (middle of the entrance room) inward from the cliff line.

Relative humidity was calculated from the equation:

$$RH = \frac{m \cdot \exp\left\{\frac{aT_w}{T_w + b}\right\} - 6.6 \cdot 10^{-4}(1 + 15 \cdot 10^{-3} T_w) \cdot P \cdot (T_d - T_w)}{m \cdot \exp\left\{\frac{aT_d}{T_d + b}\right\}} \cdot 100 \quad (5)$$

where RH is relative humidity (%), T_w is wet bulb temperature ($^{\circ}$ F), T_d is dry bulb temperature ($^{\circ}$ F), P is barometric pressure (kPa), and m , a and b are empirically-derived coefficients optimized for the 0 to 50 $^{\circ}$ C temperature range ($m = 0.61121$, $a = 17.368$ and $b = 238.88$; Boudreau 1993).

Air density was calculated by the formula of Cigna and Forti (1986):

$$k = [3.484(P - RH \cdot P_w) \cdot (273.15 + T)^{-1}] + RH \cdot k_w \quad (6)$$

where k is air density (kg/m^3), P is atmospheric pressure reduced at 0 $^{\circ}$ C (kPa), RH is relative humidity (1 = for 100%), P_w is vapor partial pressure reduced to 0 $^{\circ}$ C (kPa), T is air temperature ($^{\circ}$ C) and k_w is the vapor density (kg/m^3).

WATER CHEMISTRY

Conductivity was measured with a YSI Model 33 S-C-T (salinity-conductivity-temperature) meter. Measurements were converted to specific conductivity at 25 $^{\circ}$ C using the function:

$$\text{SpC}(25^{\circ}) = 1.81 \cdot \text{SpC}(T) \cdot e^{-0.023T} \quad (7)$$

where SpC (T) is the measured conductivity at T° C, T is the temperature ($^{\circ}$ C). The equation is derived empirically from karst water data in Pennsylvania and is valid between 0 to 40 $^{\circ}$ C (White 1988).

pH was determined with an ATC pH meter with an accuracy of 0.01 pH. The meter was standardized against buffers pH = 4.00 and pH = 7.00 before each series of measurements. Temperature was taken with a dual-sensor digital thermometer having a resolution of 0.1 $^{\circ}$ C and an accuracy of ± 1.0 $^{\circ}$ C in the range -10 to + 50 $^{\circ}$ C. Alkalinity, calcium and total hard-

ness were measured using a Hach Digital Titrator. The saturation indices for calcite and dolomite, the partial pressure of CO_2 with which the water would be in equilibrium and ion balance errors were calculated using the program WCHEM3.

No water analyses were made on Isla de Mona. On Cayman Brac, the caves are quite dry in general and there are few drip sites. Only during heavy rains were the drip rates fast enough to allow satisfactory water collection; on these occasions samples were collected from as many sites as possible.

Condensation was induced by chilling the cave air. Half-gallon plastic milk containers that had been filled with water and then frozen solid were used as condensers. The condensation water was collected in 250 ml sample bottles, via funnels with small apertures to reduce evaporation. In each sample run three bottles were suspended in the selected cave for a minimum of six hours, by which time all the ice had melted; one was placed close to the entrance, one halfway and one close to the back of the cave. A total of 12 condensation experimental runs were completed in six different caves (B2, CC, GC, PC, SC and TC), including up to three repeat runs at the same positions in a given cave on separate days.

GYPNUM TABLETS

Gypsum tablets of known weight were suspended on nylon fishing line away from direct drip sites and walls for 16.5 months (May 1994 to October 1995) in four caves on Cayman Brac (B2, FC, PC and TC) and for 13 months (June 1994 to July 1995) in CAS, Isla de Mona. The tablets were dried overnight at 60 $^{\circ}$ C in an oven before weighing prior to and after exposure. In each cave they were so located as to form a profile perpendicular to the cliff, from the entrance inward (Fig. 2). On each island one sample was retained unexposed to be used as a reference sample. The gypsum was >90% pure $\text{CaSO}_4 \cdot 2\text{H}_2\text{O}$ donated by the Canadian Gypsum Co., Hagersville, Ontario, Canada. Surface retreat rates were calculated by:

$$r = s \cdot 10^{-3} \cdot \rho^{-1} \cdot \epsilon \cdot 365 \quad (8)$$

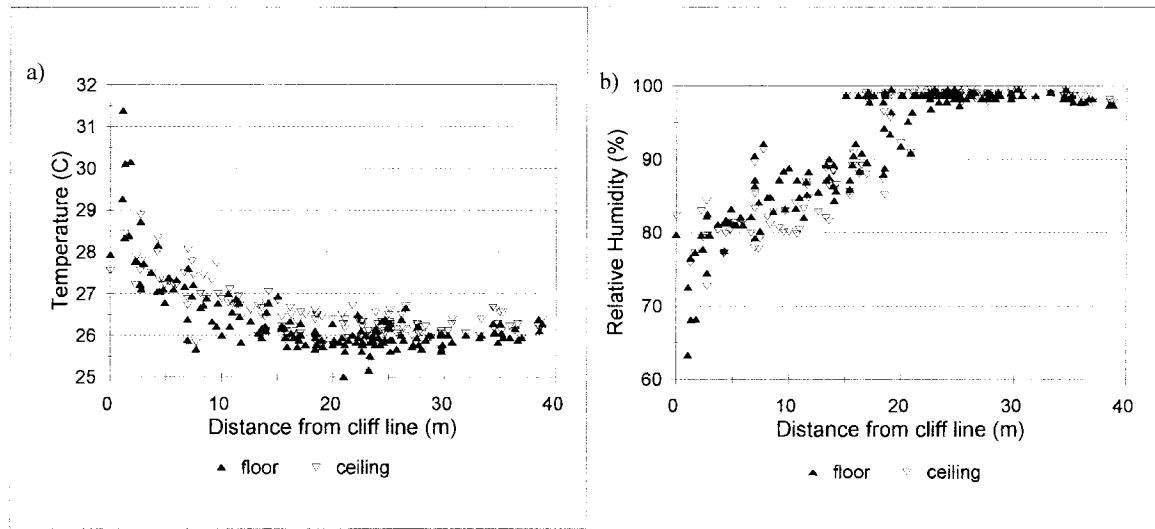
where r is surface retreat rate (mm/a), s is solubility of gypsum (2.5 g/L), ρ is density of gypsum (2.35 g/cm^3) and ϵ is the amount of condensation water accumulated on the surface in one day, expressed as the water film thickness this amount of condensation water would form on the surface of the tablet (mm/day), given by

$$\epsilon = W \cdot (A \cdot t)^{-1} \cdot 10 \quad (9)$$

where A is surface area of the gypsum tablet (cm^2), t is duration of exposure (days) and W is amount of water in thermodynamic equilibrium with gypsum that is needed to dissolve the observed weight loss (cm^3) i.e.

$$W = (w_1 - w_2) \cdot s^{-1} \cdot 10^3 \quad (10)$$

Figure 3.
Temperature
(a) and relative
humidity
(b) profiles in
First Cay
Cave, Cayman
Brac, mea-
sured in May
1994.



where w_1 and w_2 are weight before and after exposure respectively. The minimum amount of condensation water needed per day (C) to dissolve the observed weight loss is thus:

$$C = W/t = \varepsilon \cdot 10^3 \cdot A \quad (11)$$

RESULTS AND DISCUSSION

AIR TEMPERATURE AND RELATIVE HUMIDITY

LONGITUDINAL PROFILES

A constant climate with a temperature of 25.5 to 26.5°C on Cayman Brac and 25 to 25.5°C on Isla de Mona and a relative humidity of 95% to 100% was reached deep inside the larger caves and behind constrictions (Fig. 3). In the smaller caves, the relative humidity did not reach its stable level, but rather remained between 90% and 95% even behind some constrictions (Fig. 4). Both on maps and profiles, it is clear that quite short constrictions in cave passages can substantially reduce the penetration of outside climatic effects.

The entrance zone was the area most affected by the outside climate. The penetration of external influences was greatest near the ceiling and varied with the cave configuration and the temperature and relative humidity differences between the two environments (Fig. 4).

VERTICAL PROFILES

On most occasions, the temperature near the ceiling was greater than the floor temperature. This temperature difference was highest in the entrance zones, which usually consist of large rooms where the air can circulate most readily (Fig. 4 & 5).

During the periods of study, outside daytime temperatures were higher than the inside temperature. Air was drawn into the caves along the ceilings, was cooled down in the interiors and drained out again along the floors. Because warmer air can contain more water vapour, the air along the ceilings had

lower relative humidities than that at the floors (Fig. 5). In areas with poor air exchange (e.g. deep inside the cave or behind constrictions), the relative humidity was either stable up the vertical profile or increased slightly from the floor to the ceiling.

According to the Wigley-Brown model temperature and relative humidity equilibrium will be attained after 5 x_0 to 6 x_0 ; thus, x_0 was calculated by dividing the distance required to arrive at equilibrium in the sample caves by six. On Cayman Brac average $x_0 = 5$ m; however, because of the changing cross-section of the passages in these caves, it varies with distance from the entrance, as illustrated in detail in figure 4. As noted, the Wigley-Brown model was developed for a simple pipe of constant radius. The configuration of the caves on Cayman Brac and Mona is that of series of chambers/high passages separated by constrictions. This configuration is an extreme test of the Wigley-Brown model. Values of x_0 for these caves calculated according to the model are at least one order of magnitude higher than the actual measured average. This discrepancy is most likely explained by the presence of the constrictions. The implication is that the basic Wigley-Brown model needs to be considerably modified into a "chamber-constriction-chamber" model - which was not the objective of this paper.

A quite different pattern of air circulation can be established in these caves by convective processes. Convection may occur if denser air can accumulate initially at the ceilings rather than at the floors and then settle downwards, setting up a vertical cellular circulation. In general this will correspond to cooler air flowing along the ceilings. This pattern is not expected to occur in every cave and is temporary and superimposed on the general circulation described above. In First Cay Cave this situation tended to occur during the nights and early mornings and was recorded at distances up to 30 m from the entrance. It is a consequence of the daytime "hot" general circulation inward at the ceiling and outward along the floor being sustained into the night by inertia. In Peters Cave, one-

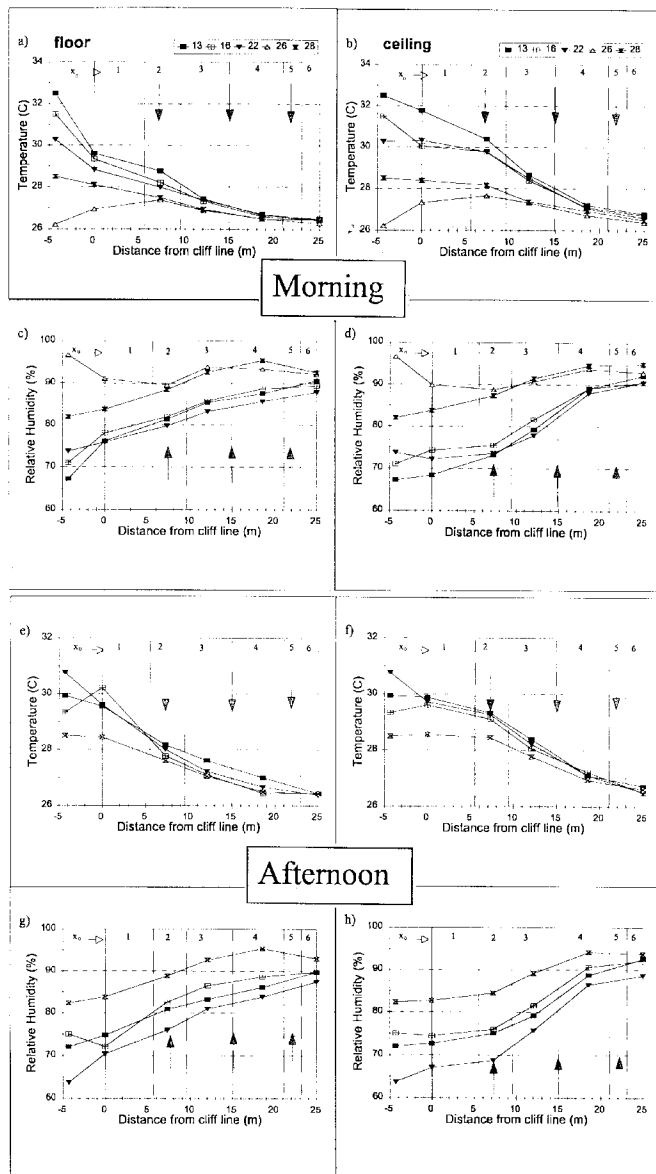


Figure 4. Temperature and relative humidity profiles for September 13, 16, 22, 26 and 28, 1995 in Skull Cave, Cayman Brac. The relaxation lengths, x_0 , are indicated along the top of each profile. Note the varying length of x_0 with distance away from the entrance as a result of the cave configuration. Arrows indicate the location of constrictions. a) Morning temperature profile along the floor; b) Morning temperature profile along the ceiling; c) Morning relative humidity profile along the floor; d) Morning relative humidity profile along the ceiling; e) Afternoon temperature profile along the floor; f) Afternoon temperature profile along the ceiling; g) Afternoon relative humidity profile along the floor; h) Afternoon relative humidity profile along the ceiling.

fifth of the stations used for the temperature and relative humidity maps recorded such temperature inversions (Fig. 6). Convection cells could form at these locations. They were distributed throughout the cave, indicating that the process occurs only on a small scale but it is likely to be of local significance.

As noted in the introduction, the climate on Cayman Brac and Isla de Mona is dominated by diurnal rather than seasonal variations and this permits measurement of the Wigley-Brown parameters within a short period of time. Daytime corresponds with the summer situation, when the wall temperature is less than the outside dew-point temperature and condensation occurs on the walls. At night the situation is similar to the winter condition and inside temperature is greater than the outside dew-point temperature resulting in evaporation. This diurnal variation between condensation and evaporation will be greatest in the area of greatest diurnal temperature and relative humidity differences, i.e. the entrance zones. It is very likely that this alternation plays a major role in condensation corrosion because energy is needed to evaporate water and this will cool the walls. No droplets or sheet flow were observed to occur on the walls, indicating that the condensation water was not substantial enough to form droplets or water films thick enough to overcome the surface tension and flow down, removing dissolved material in the process. During evaporation some material might be removed in the vapour phase, which would explain the high concentrations of calcium and magnesium observed in the condensation waters. At the same time, dissolved material could crystallize as small individual particles when evaporation is fast enough to prevent molecules of the dissolved material from rejoining the crystalline structure of the bedrock. As such, they can then be removed as aerosols by gravity, dislodgment by air circulation or some other process.

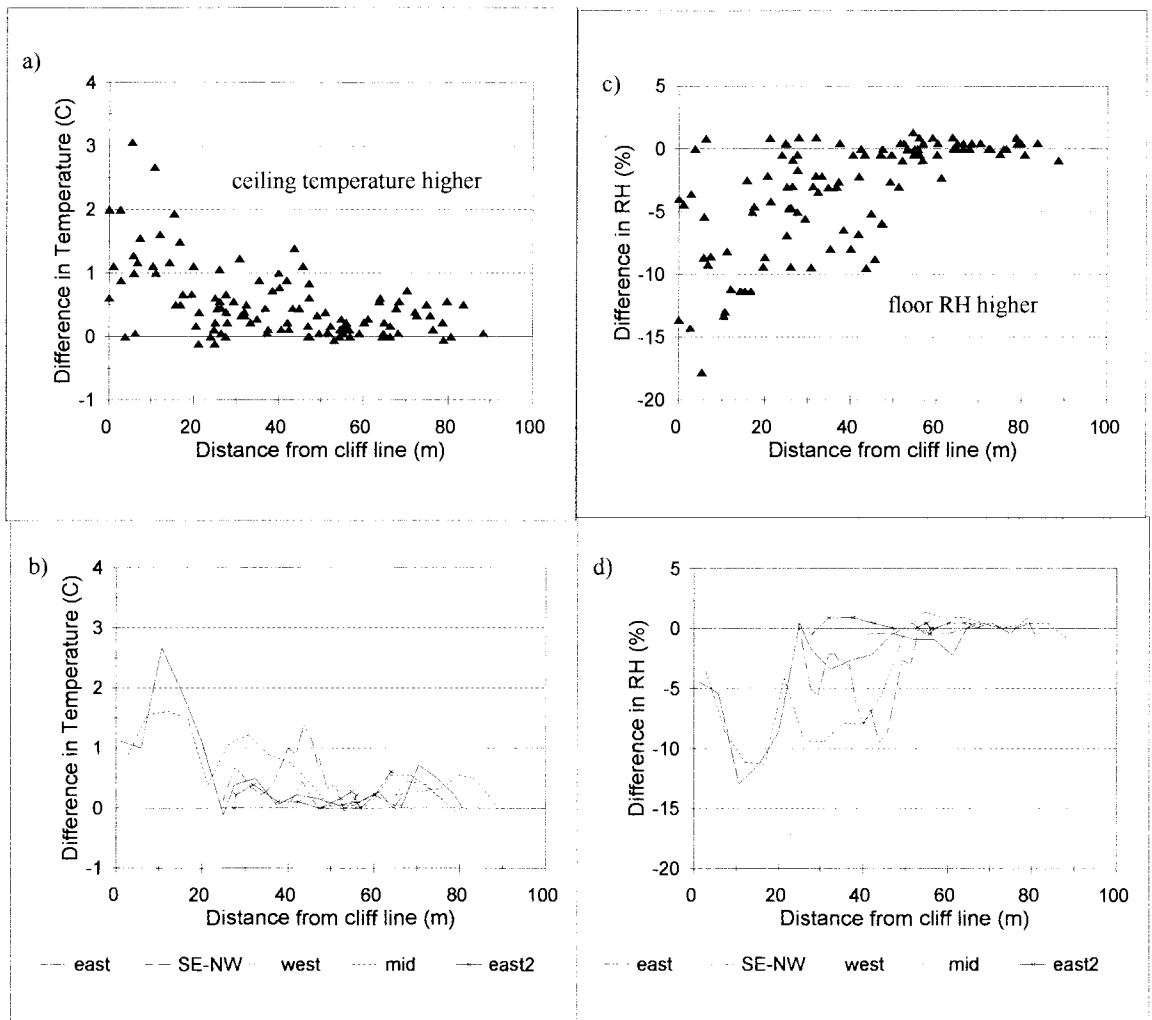
WATER CHEMISTRY

The chemical characteristics of water samples collected on Cayman Brac are presented in Table 1. Drip water could be collected only on rainy days when the drip rates were high. Relative humidity was then close to 100% and thus evaporation, which would increase mineral concentrations in the water, was assumed to be negligible.

Figure 7 compares the specific conductivity (SpC) of the drip waters with their total hardness. The solid line is the relationship between these two parameters that has been established for bicarbonate waters of Pennsylvania by White (1988). The drip waters fall mainly above the bicarbonate water line, indicating that they have a higher SpC due to the presence of significant quantities of ions other than calcium and magnesium. These foreign ions are believed to have come from sea salt particles in the air or deposited on vegetation.

Two different factors each divide the drip waters into distinct groups. First, samples from rains of May 1994 and September 26, 1995, have greater hardness and lower specific conductivity, in general, than the samples of October 3 and 4, 1995 (Fig. 7a). The difference is attributed to different rainfall

Figure 5.
a) Temperature differences between ceiling and floor for all stations, Cueva de Agua Sardinera, Isla de Mona (June 1994);
b) Temperature difference between the ceiling and the floor along selected profiles in the cave. Three transects were made NNE-SSW, one in the western end (west), one in the eastern end (east) and one midway between the two (mid). One transect was almost



perpendicular to the previous three transects (SE-NW) and transect East2 first goes SSW-NNE and then turns SE-NW to join the eastern transect; **c)** Relative humidity difference between ceiling and floor for all stations, Cueva de Agua Sardinera; **d)** Relative humidity difference between the ceiling and the floor along selected profiles in the cave (transect location see 5b).

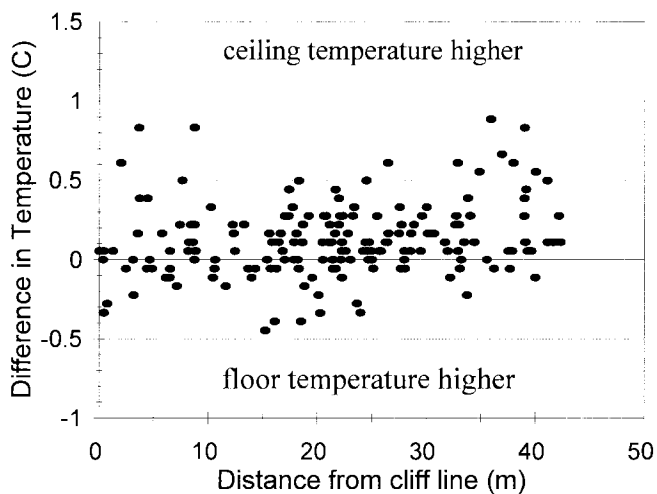


Figure 6. Temperature differences between ceiling and floor for all stations in Peters Cave, Cayman Brac (May 1994).

intensities, duration and amounts. During the night of September 25-26, as well as part of the day it rained steadily, resulting in a mean rainfall of 65 mm for the island. On October 3, the heaviest downpour of the entire study period was experienced due to the influence of Hurricane Opal. Rain fell all day; mean precipitation for the island was 95 mm, varying from 50 mm at the west end to 135 mm in the middle. With a steady rain the amount of water is less and takes longer to penetrate the rock, giving it more time to dissolve the bedrock and, thus, a greater hardness. Heavy downpours will be able to penetrate the bedrock faster and they will flush all the foreign ions through the system as well, increasing the SpC but keeping the hardness relatively low.

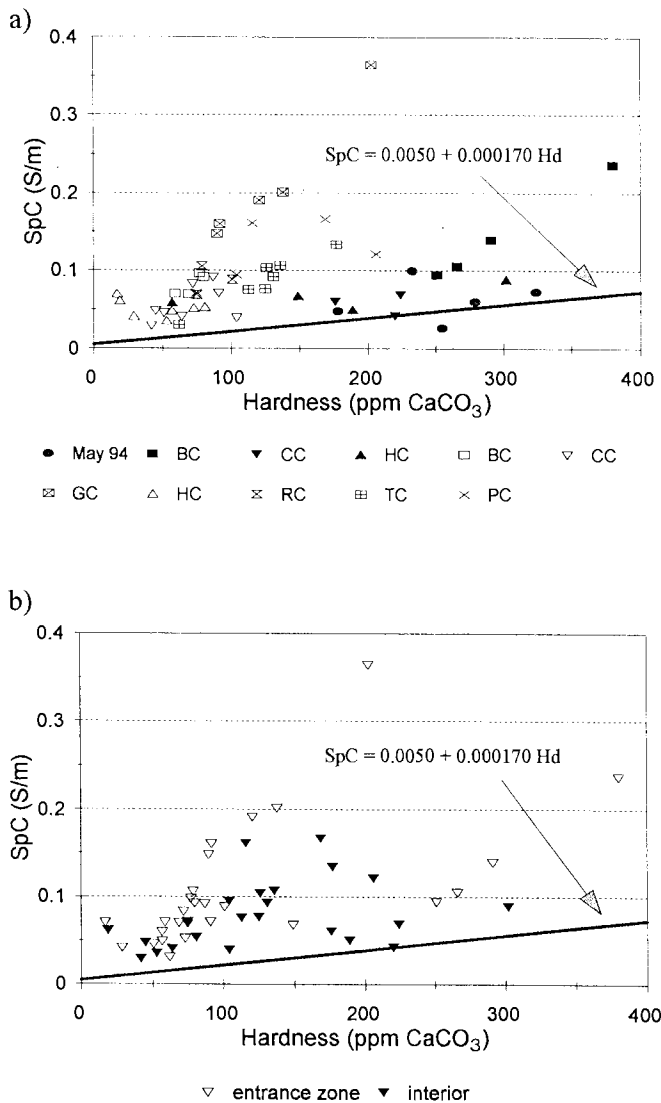


Figure 7. Relationship between specific conductivity and hardness for drip waters. a) Drip waters by cave; closed symbols indicate drip waters from heavy downpours (October 3 and 4, 1995) and open symbols drip waters from steady rain (May 1994 and September 26, 1995); b) Drip waters at the entrances and deep inside caves (Sept-Oct 1995). The solid line is the Pennsylvania water line for inland bicarbonate waters given by White (1988: 137).

As a second effect, these differentiated storm waters also divide in two subgroups according to location within the cave. Waters from the entrance zone have higher SpC for a given hardness than those deep inside, indicating that there is a higher foreign ion content close to the entrances (Fig. 7b). This is in agreement with the temperature and relative humidity observations, which indicated that the entrance zone is most influenced by outside climate. The inflowing air not only conveys heat and moisture into the cave but also sea salt aerosols. Sea

salt aerosols are very hygroscopic and can initiate aqueous condensation at relative humidities as low as 80% (Wells 1986). The presence of these particles may therefore cause condensation in the air, increasing the amount of condensation water and the likelihood of condensation corrosion.

Figure 8 displays the saturation index values of the different water samples with respect to calcite (SI_c) and dolomite (SI_d). It is seen that the induced condensation waters are similar to the intense storm drip waters of October 3 and 4, 1995. Condensation waters were undersaturated with respect to both minerals in 75% of the cases and supersaturated in 25%. The calcite index values are the most significant in this study. Their range was from -1.06 to +0.88, the former representing a water capable of dissolving a speleothem quite rapidly and the latter one that would deposit new calcite upon it.

Some measured relationships between the SI_c of sample condensation waters and their distances from cave entrances are shown in Figure 9. They are quite complex, varying between caves and at different dates in the same cave. To generalize, however, a majority of the traverses detected little change in the SI_c state on a given day at distances up to 25 m from the cliff lines but Tibbetts Turn Cave (TC) gave quite aberrant results. Two traverses deeper than 25 m in Great Cave measured significant increases in SI_c, the waters becoming slightly supersaturated. The need for more research here is evident.

GYP SUM TABLETS

The calculated losses by surface retreat on the gypsum, the condensation film thicknesses and minimum quantities of condensation water needed to achieve those losses are given in Table 2. The two reference samples did not display any loss of material. All other tablets recorded losses, which can be represented as surface retreat rates of up to 0.5 mm/a. There was no correlation between the surface areas of the different gypsum tablets and their retreat rates.

With some exceptions, gypsum tablets that were suspended close to the entrances suffered more dissolution than those further inside the caves. Tablets close to the floors were more affected than those close to the ceilings (Fig. 10). Condensation corrosion is the only feasible mechanism for this dissolution: the gypsum tablet experiments reinforce the conclusion from the meteorological work that condensation occurs preferentially in entrance zones and close to the floors.

The greatest number of tablets were placed in First Cay Cave. The amount of surface retreat decreased rapidly beyond a distance of 30 m from the cliff (second constriction; Fig. 10a). Beyond the first constriction at 17 m, the temperature became nearly invariant and the relative humidity stabilized at around 99% (Fig. 2 & 3). Almost no dissolution occurred on tablets where the relative humidity exceeded 95% and remained constant over time. Substantial dissolution was observed at relative humidities less than 95%, i.e. in the entrance areas. These are the zones with the greatest diurnal climatic variations and where alternation of condensation and

Table 1.
Chemical
analysis of
different
water types on
Cayman Brac.

| | Specific Conductivity (µS/cm) | | | total Ca (mmol/l) | | | total Mg (mmol/l) | | | Saturation Index for calcite (SIc) | | | Saturation Index for dolomite (SI _d) | | |
|--|-------------------------------|-------|-------|-------------------|--------|--------|-------------------|------|--------|------------------------------------|-------|-------|--|-------|-------|
| | max | min | mean | max | min | mean | max | min | mean | max | min | mean | max | min | mean |
| Cayman Brac, May 1994 | | | | | | | | | | | | | | | |
| Sea | 56000 | 46000 | 51660 | 148.13 | 104.91 | 118.73 | 648.56 | 0.50 | 255.98 | 1.86 | 0.72 | 1.32 | 3.62 | 2.96 | 3.30 |
| Well | 2180 | 210 | 1576 | 6.52 | 2.55 | 4.11 | 4.79 | 1.51 | 2.48 | 0.96 | 0.20 | 0.51 | 1.62 | 0.40 | 1.00 |
| Rain | 60 | 24 | 42 | 0.05 | 0.02 | 0.04 | 0.03 | 0.01 | 0.02 | -2.86 | -3.92 | -3.38 | -5.73 | -7.81 | -6.84 |
| Drip | 1050 | 270 | 616 | 1.75 | 0.96 | 1.23 | 2.52 | 0.81 | 1.42 | 0.82 | 0.43 | 0.69 | 2.25 | 1.08 | 1.62 |
| Condensation | 200 | 20 | 103 | 2.76 | 0.16 | 1.11 | 0.98 | 0.00 | 0.31 | 0.68 | -0.98 | 0.05 | 1.54 | -1.97 | 0.02 |
| Cayman Brac, Sept-Oct 1995 | | | | | | | | | | | | | | | |
| Rain | 20 | 9 | 15 | 0.04 | 0.01 | 0.03 | 0.01 | 0.00 | 0.00 | -2.90 | -4.22 | -3.59 | -6.68 | -6.62 | -6.68 |
| Drip | 3646 | 292 | 945 | 2.67 | 0.07 | 0.84 | 1.19 | 0.00 | 0.41 | 1.07 | -1.58 | 0.10 | 1.83 | -2.76 | 0.10 |
| Condensation | 116 | 27 | 50 | 3.32 | 0.24 | 0.98 | 0.46 | 0.00 | 0.19 | 0.77 | -1.06 | -0.42 | 0.58 | -2.87 | -0.89 |
| Drip water for sample caves | | | | | | | | | | | | | | | |
| Peters Cave | 1664 | 718 | 1231 | 1.24 | 0.46 | 0.76 | 0.86 | 0.30 | 0.60 | 0.30 | -0.27 | -0.02 | 0.67 | -0.50 | 0.11 |
| Tibbetts Turn Cave | 1337 | 310 | 887 | 1.15 | 0.45 | 0.85 | 0.65 | 0.14 | 0.41 | 0.46 | -0.13 | 0.17 | 0.88 | -0.51 | 0.23 |
| Cross Island Road Cave | 917 | 292 | 565 | 2.09 | 0.23 | 0.78 | 0.71 | 0.14 | 0.34 | 0.95 | -0.51 | 0.12 | 1.67 | -0.47 | 0.19 |
| Skull Cave | 899 | 359 | 575 | 2.01 | 0.07 | 0.65 | 1.12 | 0.00 | 0.31 | 1.05 | -1.58 | -0.22 | 1.79 | -2.76 | -0.56 |
| Rebecca's Cave | 1060 | 694 | 860 | 0.74 | 0.66 | 0.71 | 0.29 | 0.02 | 0.15 | 0.42 | -0.08 | 0.19 | 0.64 | -0.89 | -0.30 |
| Bats Cave | 2367 | 703 | 1132 | 2.67 | 0.42 | 1.38 | 1.19 | 0.17 | 0.50 | 1.07 | -0.11 | 0.46 | 1.83 | -0.43 | 0.71 |
| Great Cave | 3646 | 1476 | 2130 | 1.04 | 0.56 | 0.73 | 1.03 | 0.33 | 0.58 | 0.40 | 0.06 | 0.19 | 1.04 | 0.18 | 0.49 |
| Condensation water for sample caves | | | | | | | | | | | | | | | |
| Peters Cave | 45 | 27 | 31 | 0.55 | 0.24 | 0.43 | 0.08 | 0.00 | 0.03 | -0.46 | -0.97 | -0.77 | -1.97 | -2.53 | -1.09 |
| Tibbetts Turn cave | 116 | 29 | 59 | 2.94 | 0.41 | 1.16 | 0.42 | 0.00 | 0.22 | 0.31 | -1.06 | 0.50 | -0.17 | -2.87 | -1.18 |
| Great Cave | 107 | 38 | 56 | 3.32 | 0.44 | 1.25 | 0.46 | 0.18 | 0.30 | 0.77 | -0.77 | 0.04 | 0.58 | -1.69 | -0.26 |

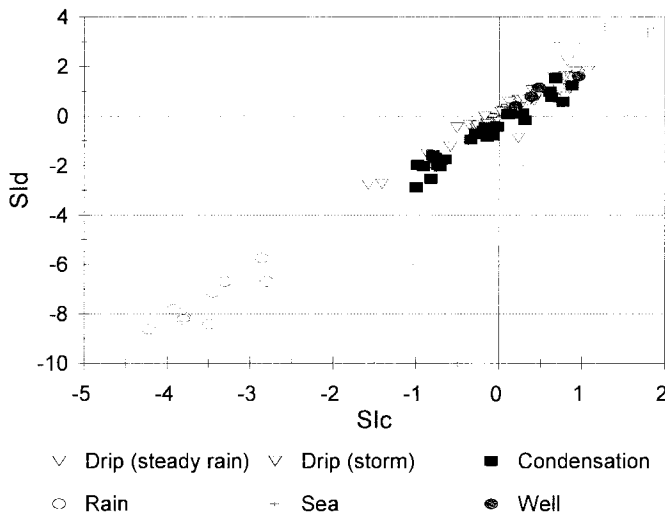


Figure 8. Saturation Index for dolomite (SI_d) versus the Saturation Index for calcite (SI_c) for rain, drip and condensation water on Cayman Brac, 1994 and 1995.

evaporation is believed to occur. As noted above, this cycle of condensation and evaporation might enhance condensation corrosion.

In Peters Cave, the tablets suspended near the ceiling and near the floor displayed similar retreat rates (Fig. 10b). This is believed to be the result of a more homogeneous air mass than in the other caves. The tablets were suspended in the second and third principal passages, which are parallel to the cliff line and in direct contact with the first (or outer) principal passage by an aperture of about 20 cm diameter. The gypsum tablet profile follows a downward slope between the second and third passage. The temperature and relative humidity measurements indicate that convection cells form on a very localized scale in these passages, which might enhance the homogenization of

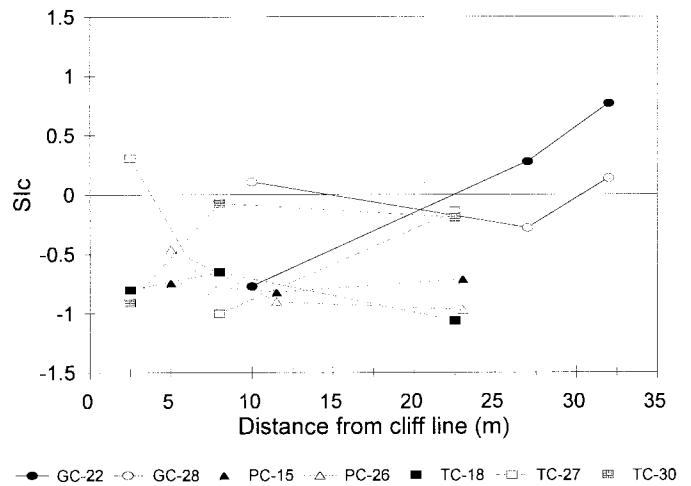


Figure 9. The change in the Saturation Index for calcite (SI_c) of condensation water with distance from the cliff line in three caves on Cayman Brac for September 15, 18, 22, 26, 27, 28 and 30, 1995.

the air mass.

In Cueva de Agua, Sardinera, the highest surface retreat was found on a sample 92 m from the entrance and close to the ceiling (Fig. 10d). A local convection cell might explain this anomaly also, but temperature and relative humidity measurements indicate this was not occurring on the day these measurements were taken. Another possibility might be that the sample was located under or close to an aggressive drip site that was not active at the time of the field measurements.

Excluding the reference samples, the mean surface retreat on the gypsum tablets was 0.36 mm/a. If a ratio of 10:1 is assumed for the ratio of gypsum solubility to calcite solubility (Ford & Williams 1989), the calculated mean calcite (limestone and speleothem) corrosion is 0.036 mm/a or 36 mm/ka.

Table 2. The Gypsum Tablet Experiment.

| Cave | Shortest distance to cliff (m) | Measured surface recession (mm/yr) | | Estimated aqueous condensation (mm/day) | |
|--------------------------|--------------------------------|------------------------------------|------|---|------|
| | | H* | L* | H* | L* |
| Reference samples | | | | | |
| PC | 19 | 0.01 | | 0.02 | |
| CAS | 87 | 0.00 | | 0.00 | |
| Cayman Brac | | | | | |
| B2-Cave | 1 | 0.37 | | 0.94 | |
| | 2 | | 0.08 | | 0.22 |
| First Cay Cave | 9 | 0.39 | 0.44 | 1.00 | 1.14 |
| | 13 | 0.39 | | 1.01 | |
| | 16 | 0.36 | | 0.92 | |
| | 21 | | 0.42 | | 1.07 |
| | 29 | 0.41 | 0.52 | 1.07 | 1.33 |
| | 31 | 0.17 | | 0.43 | |
| | 40 | 0.01 | | 0.02 | |
| Peter's Cave | 19 | | 0.21 | | 0.55 |
| | 23 | 0.47 | 0.45 | 1.21 | 1.16 |
| | 28 | 0.39 | 0.40 | 1.01 | 1.02 |
| | 31 | 0.02 | | 0.05 | |
| | 33 | 0.09 | | 0.23 | |
| | 34 | 0.40 | | 1.03 | |
| Tibbets Turn Cave | 28 | 0.01 | 0.16 | 0.02 | 0.42 |
| | 30 | 0.11 | | 0.28 | |
| | | | 0.01 | | 0.03 |
| | 33 | | | | |
| maximum | | 0.47 | 0.52 | 1.21 | 1.33 |
| minimum | | 0.01 | 0.01 | 0.02 | 0.03 |
| mean | | 0.24 | 0.30 | 0.62 | 0.77 |
| Isla de Mona | | | | | |
| Cueva del Agua | 1 | 0.32 | | 0.82 | |
| | 6 | 0.01 | | 0.02 | |
| | 13 | 0.00 | | 0.00 | |
| | 63 | | | | |
| | 63 | 0.01 | 0.26 | 0.03 | 0.66 |
| | 87 | | 0.02 | | 0.05 |
| | 87 | | | 1.18 | |
| | 92 | 0.46 | | | |
| maximum | | 0.46 | 0.26 | 1.18 | 0.66 |
| minimum | | 0.00 | 0.02 | 0.00 | 0.05 |
| mean | | 0.18 | 0.14 | 0.41 | 0.36 |

H* = close to ceiling; L* = close to floor

This must be reduced by a measure that takes into account the greater porosity of gypsum: 33% would seem a likely maximum for this effect, giving a corrosion rate of ~24 mm/Ka for calcites with porosities below ~5%. This remains a considerable loss rate.

Theoretical condensation corrosion rates were also calculated, using

$$R = \alpha(c_{eq} - c) \quad (12)$$

where R is the dissolution rate in mmol/cm²s, α is the kinetic constant in cm/s, c is the Ca-concentration in the water film and c_{eq} is the equilibrium concentration of calcium in mol/l (= mmol/cm³) with respect to calcite (Buhmann & Dreybrodt 1985; Baker *et al.*, in prep.). An average value of 19 mm/ka was obtained using the Ca-concentrations measured in the induced condensation waters. This corresponds very well with the rates calculated from the gypsum tablet experiments, indicating that (although the methods were crude and the time spans short) the results of the field experiments appear to be meaningful. U-series dating has determined that the growth rates of some larger speleothems on Cayman Brac can be up to 7 mm/Ka but are generally < 1 mm/Ka (Lips 1993). These are far below the corrosion rates that can prevail: thus, for instance, a flowstone 10 cm thick will require about 100,000 years to form and can be dissolved away again in only 4000 - 5000 years.

CONCLUSIONS

Condensation corrosion occurs at present in the entrance zones of caves where the atmospheric variables fluctuate on a daily basis and are highly influenced by the outside climate. The relationships are complicated, however; Figure 11 schematically outlines how they and other environmental variables will contribute to the formation of condensation water and the condensation corrosion inside caves that is a consequence. The climatic variables have both short and long term influences on the climate inside the caves, whereas sea level fluctuations are only of long term importance. The latter influence the size of the entrance, the configuration of the cave and the distance between the sea and the cave.

The physical model for condensation corrosion that is suggested by this investigation is depicted in Figure 12. The typical coastal caves consist of a series of chambers and constrictions. The latter inhibit the free flow of air and dampen the external climatic influences substantially.

The mean condensation corrosion rate was estimated to be ~24 mm/Ka. This corresponds well with a theoretical rate of ~19 mm/Ka that can be calculated from the model of Buhmann and Dreybrodt (1985).

ACKNOWLEDGMENTS

First of all the authors would like to thank Karen Lazzari of the Water Authority for the ever important logistical support on Cayman Brac; Dr. Ashley McLaughlin from the Ministry of Environment of the Cayman Islands for the meteorological data and permission to collect samples of everything we needed; Mr. Floyd Banks of the Mosquito Control unit of Cayman Brac for the meteorological data during the period of study; Pedro Lazzari for showing us the island from a fisherman's point of view; and everybody else on Cayman Brac who helped us in our study of the caves of their island. Very special thanks go to Dale Boudreau for his enormous help with the meteorological equipment and the interpretation of the climatology data. Mike Bagosy, Craig Malis and Dr. Steve Worthington are thanked for being the field assistants and for their helpful discussions. A special thank you to Dr. Brian Jones for introducing us to Cayman Brac. Thanks also go to the anonymous reviewer of this paper for valuable comments and suggestions.

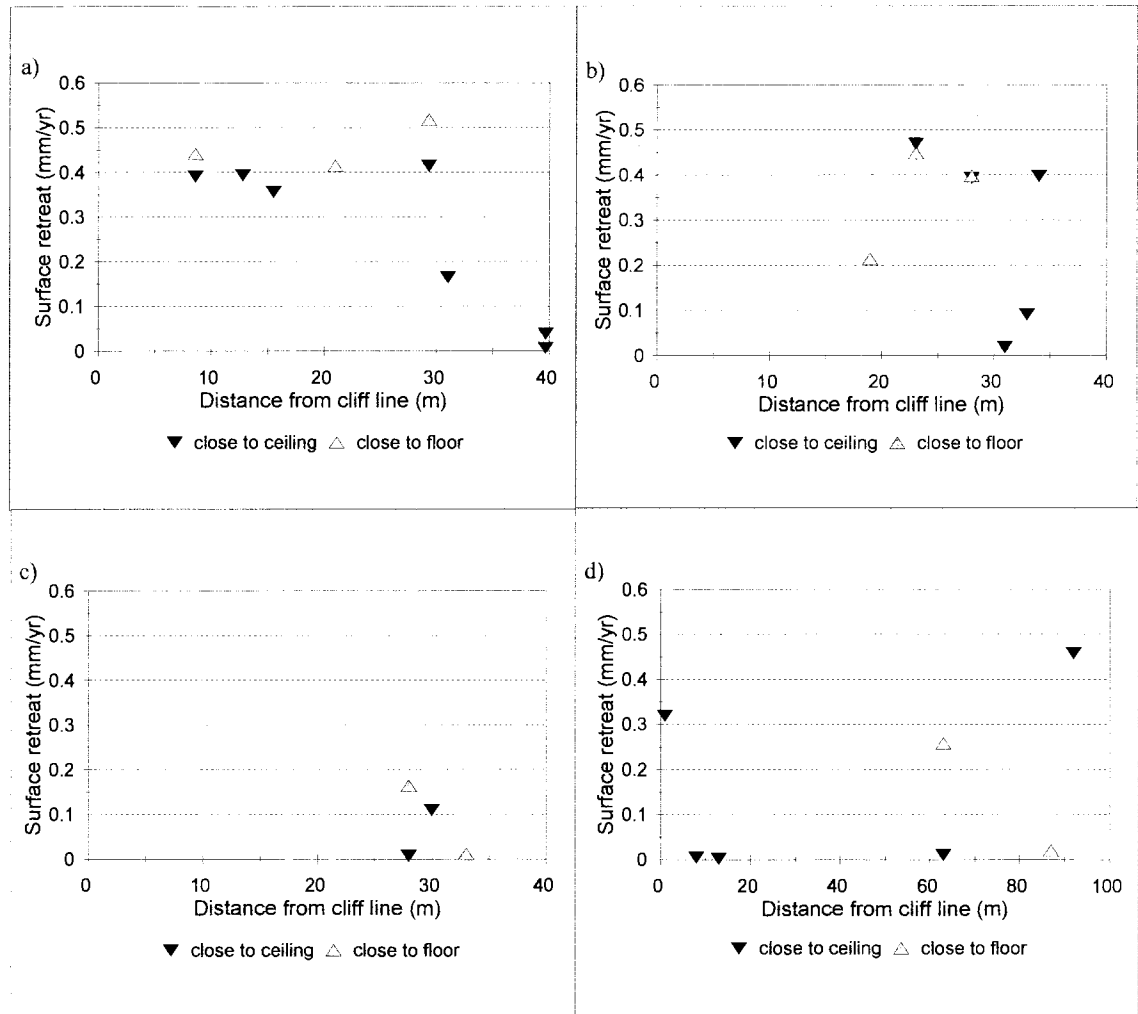
All the organizers of the Isla de Mona expeditions, especially Joe Troester, are thanked very much for the opportunity to study this desolate island and for the well organized trips.

U-series dating by α -spectrometry was done by Nicki Robinson. Karen Goodger and Catharina Jager were very patient teaching the first author the mass spectrometric dating procedures.

The gypsum was donated by the Canadian Gypsum Co., Hagersville, Ontario, Canada.

This work was supported by a Research Grant to Ford from the National Sciences and Engineering Research Council of Canada.

Figure 10.
Surface
retreat of gyp-
sium tablets in
First Cay
Cave (a),
Peters Cave
(b), Tibbetts
Turn Cave (c)
on Cayman
Brac and
Cueva de
Agua (d) on
Isla de Mona.



REFERENCES

Baker, A., Genty, D., Dreybrodt, W., Barnes, W.L., Mockler, N.J. & Grapes, J. (in prep.). Testing theoretically predicted stalagmite growth rates with recent annually laminated samples: implications for past stalagmite deposition.

Boudreau, L.D. (1993). *The energy and water balance of a high sub-arctic wetland underlain by permafrost*. MS thesis, McMaster University, Hamilton, Ontario, Canada: 205 p.

Buhmann, D. & Dreybrodt, W. (1985). The kinetics of calcite dissolution and precipitation in geologically relevant situations of karst areas. 1. Open system. *Chemical Geology* 48: 189-211.

Cigna, A.A. & Forti, P. (1986). The speleogenetic role of air flow caused by convection. First contribution. *International Journal of Speleology* 15: 41-52.

Ford, D.C. & Williams, P.W. (1989). *Karst geomorphology and hydrology*. London (Unwin Hyman): 601 p.

Frank, E.F. (1993). *Aspects of karst development and speleogenesis, Isla de Mona, Puerto Rico: an analogue for Pleistocene speleogenesis in the Bahamas*. MS thesis, Mississippi State University, Starkville, Mississippi, USA: 288 p.

Frank, E.F., Wicks, C.M., Mylroie, J.E., Troester, J.W., Alexander, E.C. Jr. & Carew J.L. (1998). Geology and hydrology of Isla de Mona, Puerto Rico. *Journal of Cave and Karst Studies* 60(2): 69-72.

Hill, C.A. (1987). Geology of Carlsbad Cavern and other caves in the Guadalupe Mountains, New Mexico and Texas. *New Mexico Bureau of Mines and Mineral Resources Bulletin* 117: 150 p.

Jones, B., Hunter, I.G. & Kyser, K. (1994). Stratigraphy of the Bluff Formation (Miocene-Pliocene) and the newly defined Brac Formation (Oligocene), Cayman Brac, British West Indies. *Caribbean Journal of Science*.

Mylroie, J.E. & Carew, J.L. (1990). The flank margin model for dissolution cave development in carbonate platforms. *Earth Surface Processes and Landform* 15: 413-424.

Mylroie, J.E., Carew, J.L., Frank, E.F., Panuska, B.C., Taggart, B.E., Troester, J.W. & Carrasquillo, R. (1994). Comparison of flank margin cave development on San Salvador Island, Bahamas and Isla de Mona, Puerto Rico. *San Salvador, Bahamas, 7th Symposium on the geology of the Bahamas, June 16-20, 1994*.

Taggart, B.E. & González, L.A. (1994). Quaternary geology of Isla de Mona, Puerto Rico: San Juan, Puerto Rico. *Presented at the XX Simposio de los Recursos Naturales, November 16-17, 1994, Puerto Rico Department of Natural and Environmental Resources*.

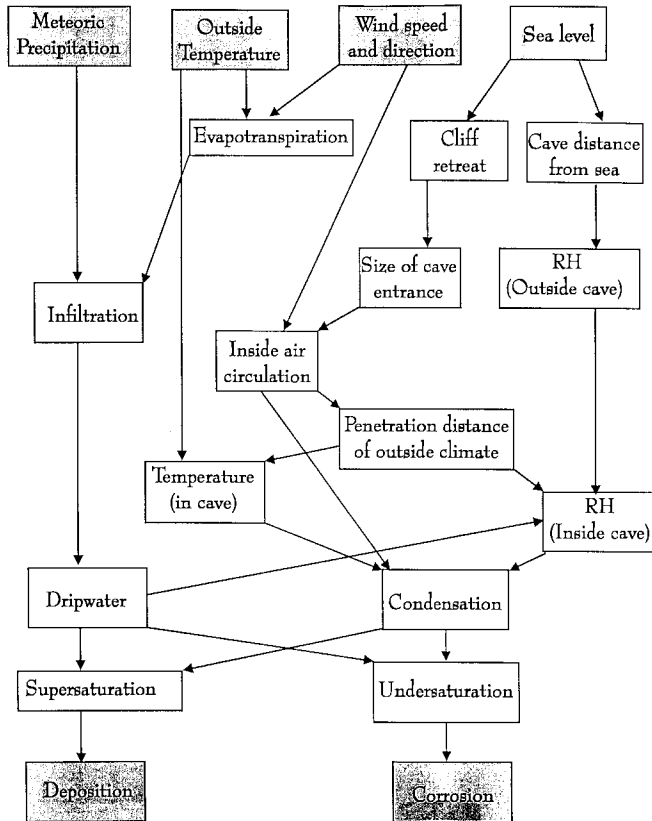


Figure 11. Schematic representation of the interaction between the outside and cave environments.

Wells, N. (1986). *The atmosphere and ocean: a physical introduction*. London (Taylor & Francis): 347 p.
 White, W.B. (1988). *Geomorphology and hydrology of karst terrains*. New York (Oxford University Press, Inc.): 464 p.
 Wigley, T.M.L. & Brown, M.C. (1971). Geophysical applications of heat and mass transfer in turbulent pipe flow. *Boundary-Layer Meteorology 1*: 300-320.
 Woodroffe, C.D., Stoddart, D.R., Harmon, R.S. & Spencer, T. (1983). Coastal morphology and late Quaternary history, Cayman Islands, West Indies. *Quaternary Research 19*: 64-84.

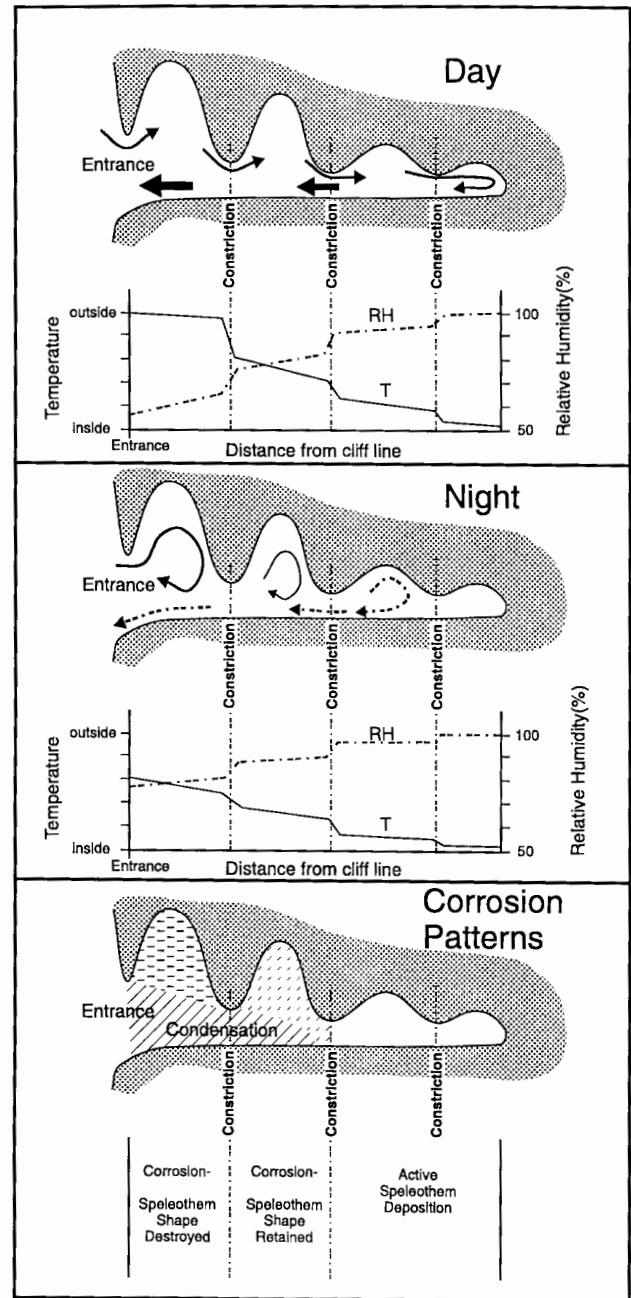


Figure 12. Proposed model of condensation corrosion in coastal caves on small holokarstic oceanic islands with young rocks.

MAGNETOSTRATIGRAPHY OF CUEVA DEL ALEMAN, ISLA DE MONA, PUERTO RICO AND THE SPECIES DURATION OF AUDUBON'S SHEARWATER

BRUCE C. PANUSKA, JOHN M. MYLROIE, DARRELL ARMENTROUT

Department of Geosciences, Mississippi State University, Mississippi State, MS 39762 USA

DONALD MCFARLANE

W.M. Keck Science Center, The Claremont Colleges, 925 North Mills Ave., Claremont, CA 91711 USA

*Magnetostratigraphic analysis of deposits exposed in Cueva del Aleman shows two reversed and two normal chronozones. The lower normal polarity event is observed in a clastic dike and probably predates initial cave formation. Sediments deposited inside the cave proper show a R-N-R sequence and probably date to at least 1.8 Ma. A fossiliferous clastic dike contains normal polarity with an overlying reversed magnetozone. Audubon's Shearwater (bird) bones occur in the dike, which is tentatively correlated with the lower N polarity zone predating cave formation. If this correlation is correct, the Audubon's Shearwater (*Puffinus lherminieri*) range can be extended back to at least 1.8 Ma, the Olduvai subchron.*

The caves of Isla de Mona, Puerto Rico, contain evidence of a rather protracted and complicated history. (See Frank *et al.* 1998, for a description of Isla de Mona.) Many of the caves contain dissolved speleothems, which have been interpreted to indicate at least two separate phreatic events (Mylroie *et al.* 1995). This, in turn, implies considerable age for the cave systems. In an attempt to determine some semi-quantitative constraints on the age of various deposits, a magnetostratigraphic study was undertaken in Cueva del Aleman, a cave displaying unusually well-constrained stratigraphic relationships. Additionally, vertebrate fossils, including the bird, Audubon's Shearwater, have been recovered from well-lithified sediments in the cave.

Audubon's Shearwater, *Puffinus lherminieri*, is a pelagic circumtropical species which breeds in burrows, crevices and caves. The species is known from the West Indian late Quaternary cave deposits on Cayman Brac (Morgan 1994), Barbuda (Brodkorb 1963), Barbados (Brodkorb 1964), Crooked Island, Bahamas (Wetmore 1938) and Mona Island (Kaye 1959). The oldest of these deposits that has been securely dated is from Pattons Fissure, Cayman Brac, with an age of $11,180 \pm 105$ yrs BP (Morgan 1994). Evidence presented here extends the minimum age for this species by 2 orders of magnitude.

CAVE STRATIGRAPHY

Cueva del Aleman (see issue reference map) has been mapped and described by Mylroie *et al.* (1995) and preliminary magnetostratigraphic age inferences were proposed (Panuska *et al.* 1995; Armentrout & Panuska 1995; Mylroie *et al.* 1995). The critical stratigraphic relationships are exposed in the Pasunka Room of Cueva del Aleman, (locality A, Fig. 1; Fig. 2).

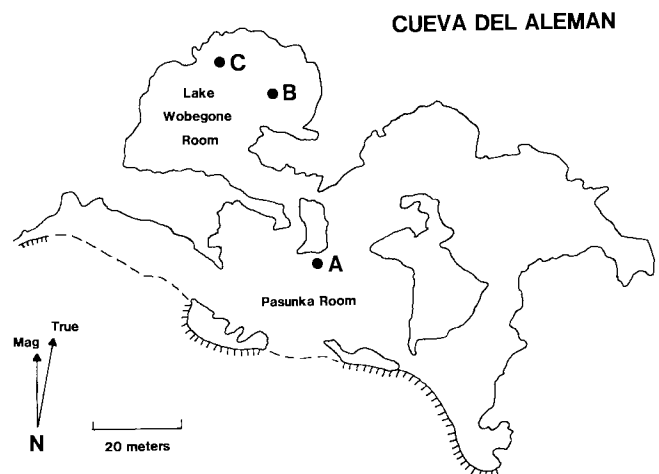


Figure 1. Map of central portion, upper level, of Cueva del Aleman. Letters indicate locations referred to in text. Hachures indicate cliff face; dashed lines indicate cave entrances.

The oldest deposit in Cueva del Aleman is a clastic dike (filled dissolutional fissure) containing red soil derived from the surface. A second red soil wash-in deposit overlies the clastic dike. The very sharp contact between these units is interpreted to be the result of the phreatic event that dissolved the initial cave chamber. Overlying the red cave floor deposit is a dripstone column (here termed Keillors Pillar) of complex origin.

The uppermost portion of the Keillors Pillar consists of vertically laminated flowstone, which can be traced for several meters in the cave ceiling. These laminations appear to be coating the walls of a former fissure in the cave ceiling. Below the vertical laminations is a set of apex-down chevron shaped

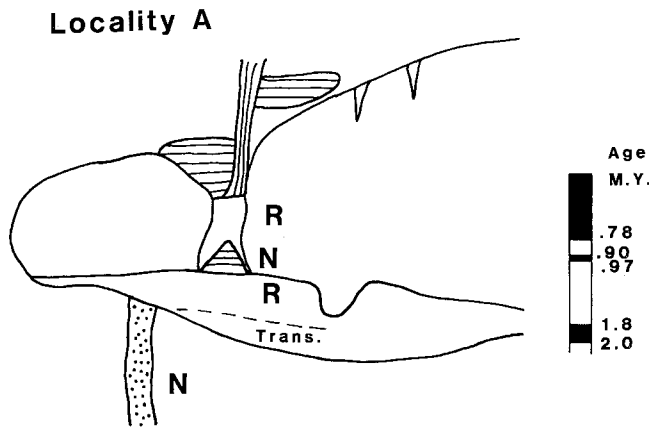


Figure 2. Locality A in Pasunka Room of Cueva del Aleman. N and R indicates normal and reversed magnetic polarity; Trans indicates a paleomagnetic direction transitional between normal and reversed polarity. Black portion of reference time scale is normal polarity; white portion is reversed polarity. See text for a discussion of cave deposits.

laminations, with a thin vertical tube occurring near the center. The chevron laminations are interpreted to be a former stalactite, with the tube forming a soda straw precursor. Chevron laminations give way to crudely laminated to massive carbonate, interpreted to be a dripstone column. The base of the column contains a triangular pocket of horizontally laminated flowstone. These horizontal laminations curve near their margins and become parallel to the side of the pocket. This triangular set of laminations is considered to be a poolstone deposit formed by water dripping from a stalactite overhead. Massive flowstone bounding the poolstone would, thus, be rimstone confining the pool. Cores extracted from beneath the column show red cave floor sediment and red sediment with white flowstone below the poolstone pocket. Thus, the column stratigraphically overlies the cave floor sediment.

The preferred scenario for Pasunka Room speleogenesis begins with soil washing into fissures in the limestone, forming a clastic dike. Phreatic dissolution cross cuts the clastic dike during the opening of the initial cave chamber. Red soil was subsequently washed in during vadose conditions, producing the cave floor sediment. Vadose deposition is favored as the upper portion of the floor sediment consists of interbedded red sediment and white flowstone and since the floor sediment is thicker at the deeper sections of the cave floor, rather than blanketing the floor evenly. Following soil wash-in, a stalactite-poolstone pair formed above the cave floor sediment. Continued dripstone deposition joined the stalactite and poolstone with a column. Although the stalactite and poolstone are penecontemporaneous, a stratigraphic sequence of column-poolstone-cave floor sediment-clastic dike can be established. Following this early phase of speleothem deposition, the cave

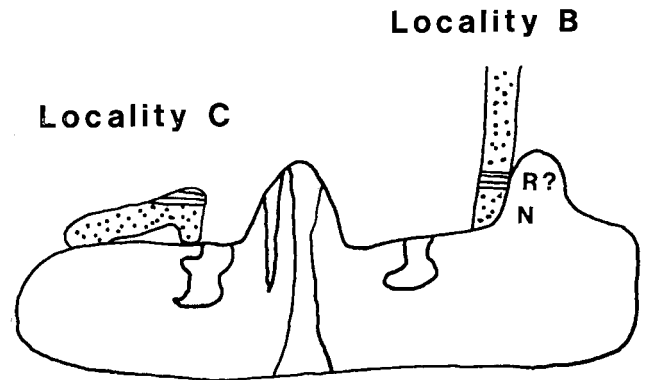


Figure 3. Cross section view of deposits in Lake Wobegon Room. Stipple pattern is red soil redeposited in clastic dikes and dissolution pockets. Parallel lines are laminated flowstone. Irregular roof pendants are phreatically dissolved speleothems. N and R indicates normal and reversed polarity respectively.

was flooded, partially dissolving dripstone formations, and subsequently drained, giving rise to a second stage of vadose dripstone deposition.

A second room, adjoining the Pasunka Room, is depicted in cross section D-D', figure 12A of Mylroie *et al.* (1995). This room, here termed the Lake Wobegon Room (Fig. 1), is important as it contains fossiliferous clastic dikes. The Lake Wobegon Room shows two stages of speleothem deposition, with the older phase being partly dissolved (Fig. 3). Clastic dikes can be seen in the ceiling and walls of this chamber. Cross cutting relationships show at least two stages of dike emplacement; the younger of these dikes is depicted as locality B in figure 3.

The correlation of deposits between the Lake Wobegon and Pasunka Rooms is problematic; however, the clastic dike at locality B can be tentatively correlated with the dike in the floor of the Pasunka Room. Portions of walls confining the clastic dikes have been phreatically dissolved. Moreover, the dikes are associated with phreatically dissolved speleothems. This implies a depositional history where cave chambers were dissolved across pre-existing clastic dikes, vadose conditions then allowed for dripstone deposition, followed by a second phreatic dissolutional event and, finally, cave draining and a second stage of vadose dripstone formation.

VERTEBRATE FOSSILS

Bird bones are present, although sparsely distributed, in the Lake Wobegon Room clastic dikes. Two recovered long bone fragments are indistinguishable from *Puffinus lherminieri*, a species whose fossil and subfossil remains are superabundant in and on younger, unconsolidated cave deposits in Cueva

Aleman and many other Isla de Mona caves.

P. lherminieri apparently made extensive use of the Mona caves as breeding sites, but is now extirpated from the island. The species has also been extirpated from Cayman Brac (Morgan 1994). The surficial nature of the bone deposits in Cueva Negra, Isla de Mona, and their loose association with anthropogenic charcoal deposits led Kaye (1959) to propose that the species had been a major prey for Taino Indians. However, the absence of any burning of the bones themselves, the absence of other taxa known to have been consumed by the Taino, and the absence of any evidence of Taino use in other Isla Mona caves containing *P. lherminieri* deposits argues against a catastrophic human predatory impact on the species.

Holdaway & Worthy (1994) have studied the extirpation and extinction of *Puffinus* species in the New Zealand archipelago. These authors have noted the susceptibility of *Puffinus* sp. to predation by *Rattus exulans*. Holdaway (1997) has further noted a correlation between *Puffinus* egg size and *Rattus* body mass. It seems likely that *P. lherminieri* on Isla Mona, and on the other West Indian islands from which it has been extirpated, is a casualty of nest predation by introduced *Rattus rattus*.

PALEOMAGNETIC DATA

Approximately 50 samples were collected from red sediment and speleothems. (All sample holes were filled with similar color material and restored to original contour. One year after initial backfill techniques were employed, cave researchers had to be shown the extraction points before they could recognize that samples had been collected.) Standard paleomagnetic specimens (2.5 cm diameter, 2 cm high) were measured on a Schonstedt SSM-1a spinner magnetometer. Some of the more weakly magnetized specimens (flowstones, less than 10^{-7} emu/cm³) were measured on cryogenic magnetometers at the University of Alaska, Louisiana State University and the University of Pittsburgh. Specimens were cleaned using standard alternating field (AF) techniques.

Normal secondary components could be especially pronounced in the reversely magnetized specimens (Fig. 4), being stronger than the characteristic component. However, most secondary components were no more than about 10% of the signal. In nearly all cases, AF was sufficient to remove secondary components of magnetization allowing the characteristic components to be isolated. Full details of the paleomagnetism will be given in Armentrout (in prep.).

At locality A, 5 samples in the lower clastic dike are normally magnetized. The upper portion of the cave floor sediment is reversely magnetized (10 samples), whereas the lower portion shows a variety of directions (15) with VGPs (virtual geomagnetic poles) located in eastern China to the Indian Ocean. These anomalous directions are interpreted to be a record of a transitional geomagnetic field. It is not possible to tell whether this is a N→R transition or a R→R excursion of the field. Two specimens from the poolstone above the floor

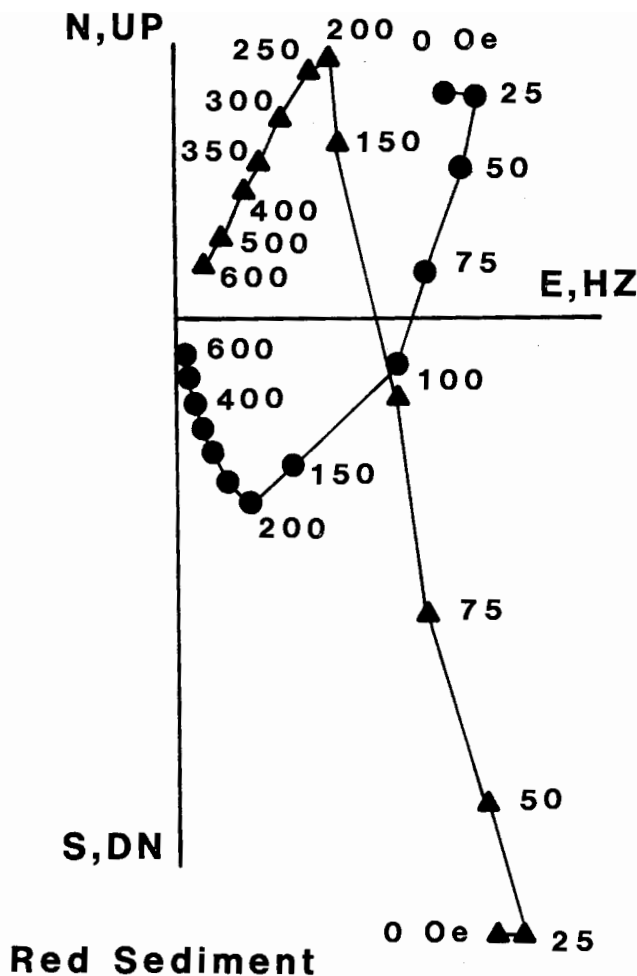


Figure 4. Demagnetization diagram showing primary and secondary components of magnetization. Dots indicate magnetic declination plotted in N, E, S (north, east, south) coordinates. Triangles represent magnetic inclination plotted in UP, DN, HZ (up, down, horizontal) coordinates. Numbers show alternating field demagnetization intensity in Oersteds (Oe). Note that the normal secondary component is removed by 200 Oe demagnetization step.

sediment record normal polarity and two specimens from the column above the poolstone are reversely magnetized.

To infer age, the magnetozone is assigned to the youngest reasonable chronozones. The reversed dripstone column is assigned to the uppermost portion of the Matuyama reversed zone older than 783 Ka (Baksi *et al.* 1992), the normal poolstone is correlated to the 70 Ky long Jaramillo event and the normally magnetized clastic dike would be the Olduvai event (1.8-2.0 Ma) (Baksi 1994). The initial cave passage was formed after the lower clastic dike, in post-Olduvai time. If the transitional zone in the cave floor sediment is inferred to be a N→R record, the age of the cave is 1.8 Ma. The N→R correlation is considered to be more likely than a R→R Matuyama excursion.

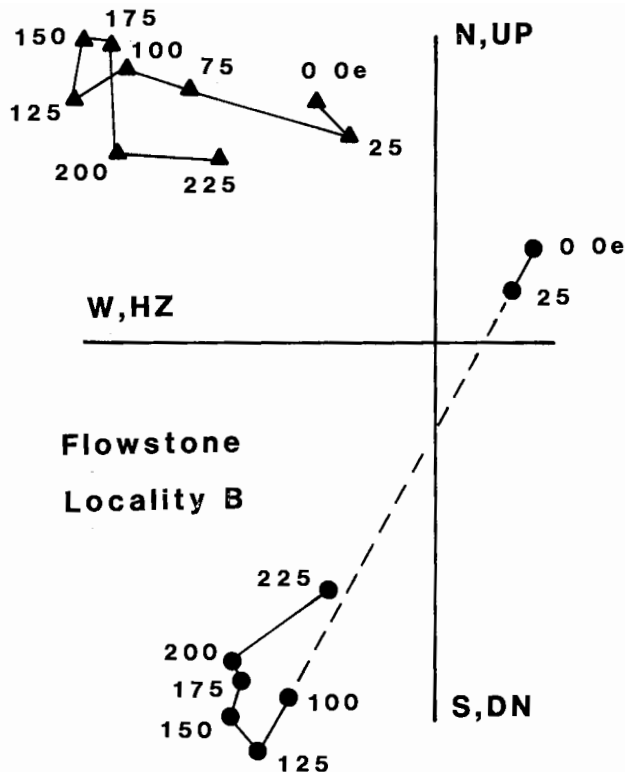


Figure 5. Demagnetization diagram of flowstone sample from locality B. See figure 4 caption for plotting conventions. Secondary components appear to be removed by 125 Oe demagnetization. While the characteristic direction is not well-defined, all measurements between 200 and 350 Oe shows a southwest (S, W) and negative (UP) direction, a reversed magnetization.

At locality B, the clastic dike has a lower normally magnetized section, with a probable reversed flowstone overlying the clastic dike wash-in sediment. The magnetization of the flowstone is problematic as only one sample was strong enough to be measured. While this sample does not display a well-defined characteristic direction (Fig. 5), the 200-350 Oe demagnetization steps show directions which are southwest and negative, a reversed direction. Even without acceptance of the reversed flowstone, the dike at locality B can be correlated with the clastic dike in the floor of locality B, as both cave chambers show evidence of two phreatic events, with the dikes predating initial cave dissolution. Thus, the age of the Audubon's Shearwater fossils may be taken as 1.8 - 2.0 Ma. It must be emphasized that these ages should be considered minimum ages, in the absence of independent age constraints.

CONCLUSIONS

A magnetostratigraphic study was undertaken in Cueva del Aleman. Pre-cave clastic dikes show a normal polarity. Sediment and speleothems deposited inside the cave show a R-

N-R sequence. Conservative assignment of the reversals to standard chronozones suggests that the cave formed during the Matuyama epoch, a minimum of 1.1-1.8 Ma. Pre-cave clastic dikes date at least to the Olduvai normal event. Audubon's Shearwater bones recovered from some of these dikes would then be 1.8-2.0 Ma. The establishment of a two million year tenure of this species on Isla de Mona and the probable correlation of its extirpation with the introduction of *Rattus rattus* further illustrates the extreme fragility of small island ecosystems.

ACKNOWLEDGMENTS

Discussions in the field with Calvin Alexander, James Carew and Joseph Troester were most informative and greatly appreciated. B.P. is indebted to Roosmarijn Tarhule-Lips for discussion of the depositional sequence, assistance with core sample collection and her patient instruction in speleothem deposition. We would like to thank David Stone, University of Alaska, Chad McCabe, Louisiana State University, and Bill Harbert, University of Pittsburgh, for allowing us use of their paleomagnetic laboratories and their hospitality during our visit. The manuscript was greatly improved by suggestions made by Carol Wicks and an anonymous reviewer. Support and assistance provided by the U.S. Geological Survey is gratefully acknowledged.

REFERENCES

- Armentrout, D.L. (in prep.). *Paleomagnetism of Cueva del Aleman, Puerto Rico*. M.S. Thesis, Mississippi State University.
- Armentrout, D.L. & Panuska, B.C. (1995). Preliminary minimum age constraints on a vertebrate fossil bearing cave, Isla de Mona, Puerto Rico. *Geological Society of America Abstracts With Programs* 27(6): A-345.
- Baksi, A.K. (1994). Concordant sea-floor spreading rates obtained from geochronology, astrochronology and space geodesy. *Geophysical Research Letters* 21(2): 133-136.
- Baksi, A.K., Hsu, V., McWilliams, M.O. & Farrar, E. (1992). $^{40}\text{Ar}/^{39}\text{Ar}$ dating of the Brunhes-Matuyama geomagnetic field reversal. *Science* 256: 356-357.
- Brodkorb, P. (1963). Catalogue of fossil birds: Part 1 (*Archaeopterygiformes* through *Ardeiformes*). *Bulletin, Florida State Museum, Biological Sciences* 7(4): 179-293.
- Brodkorb, P. (1964). Fossil birds from Barbados, West Indies. *Journal of the Barbados Museum and Historical Society* 31: 3-10.
- Frank, E.F., Mylroie, J.E., Troester, J.W., Alexander, Jr., E.C. & Carew, J.L. (1998). Karst Development and Speleogenesis, Isla de Mona, Puerto Rico. *Journal of Cave and Karst Studies* 60(2): 73-83.
- Holdaway, R.N. (1997). Differential vulnerability in the New Zealand vertebrate fauna. In Mac Phee, R.D. *Humans and other catastrophes: a new look at extinction and extinction process*. Plenum Press.
- Holdaway, R.N. & Worthy, T.H. (1994). A new fossil species of Shearwater *Puffinus* from the late Quaternary of the South Island, New Zealand, and notes on the biogeography and evolution of the *Puffinus gavia* subspecies. *Emu* 94: 201-215.

- Kaye, C.A. (1959). Geology of Isla Mona and notes on the age of Mona Passage. *United States Geological Survey Professional Paper 317C*: 141-178.
- Morgan, G.S. (1994). Late Quaternary fossil vertebrates from the Cayman Islands. In Brunt, M.A. & Davies, J.E. (eds). *The Cayman Islands: Natural History and Biogeography*. Kluwer Academic Publishers, Netherlands: 465-508.
- Myroie, J.E., Carew, J.L., Frank, E.F., Panuska, B.C., Taggart, B.E., Troester, J.W., & Carrasquillo, R. (1995). Development of flank margin caves on San Salvador Island, Bahamas and Isla de Mona, Puerto Rico. In Boardman, M. (ed.) *Proceedings of the Seventh Symposium on the Geology of the Bahamas, Bahamian Field Station, San Salvador Bahamas*: 49-81.
- Panuska, B.C., Lips, R., Myroie, J.E., Troester, J.W. & Armentrout, D.L. (1995). A pre-Brunhes age for Cueva del Aleman, Isla de Mona, Puerto Rico. *Geological Society of America Abstracts with Programs* 27(2): 79.
- Wetmore, A. (1938). Bird remains from the West Indies. *Auk* 5: 51-55.

A RADIOCARBON DATE OF 380 ± 60 BP FOR A TAINO SITE, CUEVA NEGRA, ISLA DE MONA, PUERTO RICO

EDWARD F. FRANK

Department of Geology and Geophysics, University of Minnesota, Minneapolis, MN 55455 USA

Charcoal fragments were collected from a mixed charcoal and bone deposit from a chamber in Cueva Negra, Isla de Mona Puerto Rico. Radiocarbon dating yielded a conventional ^{14}C age of 380 ± 60 Radiocarbon Years before present. Considering the standard deviation in the ^{14}C data, the range in possible calendar dates is from 1480 to 1655 AD. This time period encompasses the first contact between Taino population and Europeans, and the subsequent removal of the last of the Taino from the island to Puerto Rico in 1578.

Charcoal fragments and bird bone samples were collected from a mixed charcoal and bone deposit in a back chamber of Cueva Negra, Isla de Mona, Puerto Rico on August 1995 for identification and radiocarbon dating. The sample area is located in the distal end of a 40 m long by 5 m wide chamber. This chamber is located in complete darkness several hundred meters, and around several bends, from the nearest entrance. The sample site itself consists of a 2.5 to 7.5 cm layer of mixed charcoal, bird bone, and silt, atop a 15 cm bed of yellowish silt. Kaye (1959: 166) first described this deposit: "Bones of what must be literally thousands of birds are contained in the floor deposit of the chamber and all of them are more or less intimately mixed with small charcoal fragments. The abundance of charcoal fragments within the cave, it seems to the writer, cannot be ascribed to natural causes." Kaye (1959) reported these bones to be exclusively those of Audubon's shearwater (*Puffinus lherminieri*). This identification is consistent with bird bones collected during the 1995 sampling. Kaye (1959: 166) further suggested, based upon the location and characteristic of the deposit, "the bird bones constitute a midden built with the refuse of many feasts, probably during Indian occupancy of the cave, and that the charcoal represents scattered ashes from the fires. Why the Audubon's shearwater was exclusively favored in these feasts is not known."

The charcoal and bone samples were collected from a 2-m-wide flowstone ledge on the eastern side of the chamber, and the charcoal was submitted to Beta Analytic for radiocarbon analysis (sample #Beta-86999, November 1995). After mechanical and chemical pre-treatment, less than one gram of suitable carbon remained. That carbon was analyzed with extended counting to enhance precision. The sample yielded a conventional ^{14}C age of 380 ± 60 Radiocarbon Years BP with a $\Delta^{13}\text{C}$ of -29.6 relative to PDB-1 (Beta Analytic sample #Beta-86999, November 1995). The error represents the one standard deviation statistic, 68% probability. Using the Stuiver and Pearson (1993) radiocarbon calibration curves, this ^{14}C age corresponds to a nominal calendar date of 1525 AD. Considering the standard deviation in the ^{14}C data, the range in

possible calendar dates is from 1480 to 1655 AD.

Collected from the top surface of the deposit, the sample may represent the youngest material in the sequence. The time period is one of significant transition for the Taino population of the island. It spans the first contact between the island inhabitants and Europeans and the subsequent decimation and removal of that native population. The island was first sighted by Columbus on November 22, 1493, while sailing across the Mona Passage from Puerto Rico to Hispaniola on his second voyage to the New World (Morison 1944). Landfall on the island was made later on the same voyage by Columbus on September 24, 1494. Herrera y Tordesillas (1625, as translated by Stevens 1740, reprinted 1973: 137) states, "They next touch'd at the Island Mona, which is ten leagues from Hispaniola, and eight from the Island of St. John, being six leagues in compass, and on it grow most delicious melons, as big as a jar of oil that will hold six quarts." The island was described by de las Casas as being very rocky, but containing many holes filled with very fertile red soil. Cassava grew so large in some of these holes that an Indian could only carry two of them at a time on his back (Kaye 1959). Columbus provided his ship with fresh water, melons, and cassava during his short stay from supplies provided by the Taino Indians inhabiting the island (Wadsworth 1973). In 1508, Juan Ponce de Leon landed on the island with fifty men and spent several days there. They were supplied by the local population of 80 Taino Indians with water, cassava, and cloth made from wild cotton.

Isla de Mona was recognized as a productive source of supplies and changed governorship several times in the early 1500s. Soon, French pirates trying to disrupt this line of supply subjected the island to raids. These raiding parties took a grave toll on the Taino Indians. In 1578, the remaining Taino Indian population of ~10-30, down from a high of 152 reported in 1517, was transferred to Puerto Rico to protect them (Wadsworth 1973). This 1578 date of removal of the Taino Indian population from the islands provides a possible upper limit on the age of the bone and charcoal deposit.

Circumstantial evidence suggests that the bone and charcoal deposit is of Taino Indian origin; however, Europeans could have been responsible.

Prior to contact with Europeans in 1494, the island had been an important link in the travel patterns of the peoples of the Caribbean for possibly 2,000 years. It was a stopover on the long voyage between Hispaniola and Puerto Rico. There have been two archaeological excavations on the island. The first was the excavation of a village site in the Sardinera region at the west end of the island. This village was likely the same one found by Columbus in 1494. The village site is still evidenced by shell heaps and potsherds in the area (Santana 1973). The second excavation was conducted in Cueva de los Caracoles (Davila 1991). Stone implements, beads, amulets, and pieces of shell were recovered from the cave. Pictographs and petroglyphs are in several caves on the island (Frank 1993). These are carved into the cave walls or flowstone or they consist of black charcoal or mud drawings on the cave walls. Two "ball courts" are present on the island at Bajura de las Cerezos and at Los Corrales de los Indios (Alegria 1983). The ball court at Los Corrales de los Indios is oriented north-south and bounded by aligned stones at its margins. It measures 27 m wide by 35 m long. The ball court at Bajura de los Cerezos is 27 m by 40 m. The archaeological evidence clearly indicates that a population of Taino Indians were present on the island long prior to European contact. The event marked by the analyzed charcoal sample may represent the terminal phase of a long tradition on the island.

In Cueva Negra, Kaye (1959), described evidence of occupancy by man in the form of fragments of early Spanish colonial and Indian pottery, old glass, and conch shells (*Strombus gigus*). No evidence of this pottery or glass was found in the sample area. He also describes Indian petroglyphs and historical writings found on the cave walls made by finger tracing marks onto the soft limestone surface. Petroglyphs originally found in the walls adjacent to the bone and charcoal deposit in the cave have been nearly destroyed by vandalism. Most of the large caves in the island were mined for guano in the late 1800s and early 1900s. This mining disturbed large areas in these caves and destroyed many potentially rich archaeological sites. Vandalism in easily accessible caves is also taking a toll. Sites, such as Cueva Negra, need to be adequately documented before they are lost.

ACKNOWLEDGMENTS

I would like to thank the Cave Research Foundation, the University of Minnesota's Department of Geology and Geophysics, and their George and Orpha Gibson Endowment for financial assistance in conducting field work on Isla de Mona and laboratory processing of samples collected from the island.

REFERENCES

- Alegria, R.E. (1983). Ball courts and ceremonial plazas in the West Indies. *Yale University Publications in Anthropology* 79: 1-185.
- Davila, O. (1991). Cueva de las Caracoles, un sitio preceramico de la Isla de Mona. *XVII Simposio de los recursos naturales, 13 y 14 de Noviembre de 1991*: 87-104.
- Frank, E.F. (1993). *Aspects of karst development and speleogenesis Isla de Mona, Puerto Rico: An analogue for Pleistocene speleogenesis in the Bahamas*. MS thesis, Mississippi State University: 1- 282 pp.
- Herrera y Tordesillas, A. de (1625). *Historia general de los hechos de los castellano*. Abridged English translation by Capt. John Stevens, 1740, London: reprinted AMS Press, New York, NY, 6 volumes.
- Kaye, C.A. (1959). Geology of Isla Mona, Puerto Rico, and notes on the age of the Mona Passage. *U.S. Geological Survey, Professional Paper 317C*: 141-178.
- Morison, S.E. (1944). *Admiral of the ocean sea, a life of Christopher Columbus*. Little, Brown, and Company, Boston, MA: 1-679.
- Santana, P.M. (1973). La Isla de Mona en los tiempos Precolumbinos, Appendice M. *Junta de Calidad Ambiental, Las Islas de Mona y Monito: Una evaluacion de sus Recursos Naturales e Historico, volume 2*: M1-M9..
- Stuvier, M. & Pearson, G.W. (1993). High-precision bidecadal calibration of the radio-carbon time scale, AD 1950-500 BC, and 2500-6000 BC. *Radiocarbon* 35 (1): 1-23.
- Wadsworth, F.W. (1973). The historical resources of Mona Island, Appendix N. *Junta de Calidad Ambiental, las Islas de Mona y Monito: Una evaluacion de sus recursos naturales e historicos, volume 2*: N1-N37.

VERTEBRATE PALEONTOLOGY OF ISLA DE MONA, PUERTO RICO

EDWARD F. FRANK AND RICHARD BENSON

*University of Minnesota, Department of Geology and Geophysics, and Bell Museum of Natural History,
Minneapolis, MN 55455 USA*

*Vertebrate fossil materials were collected from over a dozen cave localities on Isla de Mona, Puerto Rico. Guano deposits at these localities were excavated and sifted to recover bone materials. The predominant vertebrate fossils recovered at every sifting site were Audubon's shearwater (*Puffinus lherminieri*) bones. Fragmentary undifferentiated lizard bones were also found sporadically in the sifted material. Fossil skeletal bones and fresh bones from other bird species were found on the surface of the cave floors at several localities. Extensive fossil guano deposits on the island are interpreted to be of mixed origin with deposits near entrances primarily derived from bird guano, and deposits from the darker interiors of the caves derived from bat guano.*

Isla de Mona is a small, isolated island located in the Mona Passage, 68 km west of Puerto Rico and 60 km east of Hispaniola. There are a limited number of native, non-flying, vertebrate species extant on Isla de Mona. These include nine species of terrestrial reptiles (six lizards and three snakes), one species of amphibian (coqui tree frog), and two species of native mammals, both bats (Wiewandt 1973). Five species of sea turtle live in the Caribbean region. Hawksbill, leatherback, and green turtles nest on Isla de Mona and the others may nest there occasionally, as well.

Mammals on the island presently include rats, mice, goats, pigs, and wild house cats, and in the recent past have also included dogs, burros, and cattle. All non-native species were brought to the island by settlers, miners, and pirates (Wiewandt 1973). Remains of a large rodent (*Isolobodon potoricensi*) were reported from the island by Anthony (1926) and later workers, but always in association with Taino archaeological sites. These rodents were a common item in the diet of the Taino Indians and could easily be carried by them from one island to another (Wiewandt 1973). Rafaele (1973) provides a list of 97 species of birds that have been observed on the island, but only 14 have significant breeding populations. Similar patterns of endemism and cross-island affinities are apparent in the vegetation on the island (Woodbury 1973) and terrestrial arthropods (Velez 1973; Martorell 1973; Peck & Kuklova-Peck 1981). The particular terrestrial species represented and the limited diversity, or depauperate nature are characteristic of island populations established by waif dispersal as described most recently by Stehli and Webb (1985) and Perfit and Williams (1989). In waif dispersal, animals are carried to oceanic islands primarily by clinging to floating debris that has been washed out to sea or carried by flying birds or bats to the island.

PALEONTOLOGICAL INVESTIGATIONS

There have been few investigations of Isla de Mona verte-

brate paleontology. The earliest work of note was by H.W. Anthony in 1926 (Anthony 1926, Goodwin 1926). Anthony was interested in finding mammal bones on that expedition, but met with little success. He found isolated fragments of *Isolobodon sp.*, but all were associated with Taino sites. Fragments of unidentified bird bones were found in indurated crevice fill material. Fish bones were in a phosphate bed within extensive guano deposits. He attributed the origin of this deposit as altered guano from a fish-eating bat (*Noctilio leporinus mastivus*). The most significant discovery was tortoise bones from two localities on the eastern side of the island. The first was from an unidentified crevice fill, the second was a more complete skeleton from the Cathedral Chamber in Cueva del Lirio at Punta Este. The material from the later skeleton (*Geochelone (Monachelys) monesis*) was first described by Williams (1952), revised by Auffenberg (1967). The reconstructed skull was 6 cm long, suggesting a shell size of ~0.5 m. *Geochelone* is the only genus yet found in the fossil record in the Caribbean. *Geochelone* specimens have been found in Cuba, Sombrero Island, New Providence Island, Navassa, Curacao, and Antigua (Auffenberg 1967; Pregill 1991).

Kaye (1959) described a deposit of bones from the Audubon's Shearwater (*Puffinus lherminieri*) intermingled with charcoal in the back of Cueva Negra on the southwestern side of the island. He hypothesized the remains to be a midden refuse deposit from paleo-Indian feasts. Recent radiocarbon dating of the associated charcoal remains yielded a conventional radiocarbon age of 380 ± 60 , or a corrected nominal calendar age of 1525 AD, with a one deviation range of 1480 to 1655 AD (Frank 1998a). This age is consistent with Kaye's interpretation. This represents the period encompassing the contact between Taino populations and Europeans. Circumstantial evidence suggests that this deposit was a Taino midden, but a European origin can not be completely ruled out. None of the other samples collected in 1995 were associated with Taino archaeological materials and may be substantially older.

More recently Nieves-Rivera *et al.* (1995) described sample collected from a water-filled portion of Cueva de Agua (Punta los Ingleses). Three species were identified from the samples: 1) Audubon's Shearwater (*Puffinus lherminieri*); 2) Mona Island Ground Iguana (*Cyclura stejnegeri*) and 3) Blainville's Leaf-chinned Bat (*Moormops blainvilli*). Ages of the deposits could not be specifically determined, but the authors estimated them to be on the order of tens of years rather than hundreds of years.

PRESENT INVESTIGATIONS

In 1995, sampling localities included Cueva de los Losetas on the east side, Bat Cave on the south side, Cueva Negra on the southwest side, and several sites within Cueva del Diamante on the west side of the island. Materials were also collected from grab sites in several other caves. At these sites guano and detrital material was dug from the cave floor and sifted on site through a shake table of 1/4" mesh wire screen. Bone material was picked from the screen surface and from the sifted tailings below. Samples of associated loose sediment and phosphate crust material were collected, as well as some specimens of *Cerion sp.* (snail shells), likely carried into the site by hermit crabs. Where practical, some of the material was re-sifted through finer mesh screens.

Identifications were made on the basis of specimens in the avian skeletal collection of the Bell Museum of Natural History, University of Minnesota. Most identified bird bones are Audubon's Shearwater (*Puffinus lherminieri*), the family Procellariidae. Audubon's Shearwater, which presently occurs on Isla de Mona (Raffaele 1973), is the only shearwater of any genus of its small size to occur in the Caribbean (del Hoyo *et al.* 1992).

A single humerus of the Black-capped Petrel (*Pterodroma hasitata*), another member of the procellariid family, also occurs among the collected specimens. The humeri of this species differ from Audubon's Shearwater in being larger and having a less compressed shaft. The Black-capped Petrel is the only petrel inhabiting the Caribbean (del Hoyo *et al.* 1992). Other specimens include Red-footed and Brown Boobies (*Sula sula* and *Sula leucogaster*), the latter represented by a hatchling age individual. Both of these species nest on Isla de Mona (Raffaele 1973). A single humerus of a large passerine bird, missing its proximal end, also occurs among the collected bones. The specimen is of a kingbird, the size of a Loggerhead or Gray Kingbird (*Tyrannus caudfasciatus* or *T. dominicensis*).

DISCUSSION

Aside from a few fragmentary, undifferentiated, lizard skeletal specimens, the samples collected were almost exclusively Audubon's Shearwater skeletal remains. Skeletal fragments from that species were found at all entrance locations and, surprisingly, in a completely dark chamber in the back of Cueva del Diamante. The Audubon's Shearwater specimens

collected from Cueva Negra, Site C, in bag 108, are from the same locality as those collected by Kaye (1959) which he identified as exclusively Audubon's Shearwater. Audubon's Shearwater historically has nested in small numbers on Isla de Mona, and may presently be nesting on Isla Monito, Isla de Mona's small sister island (Raffaele 1973). It is the only representative of the family Procellariidae in Puerto Rico and the Virgin islands and is fast becoming extirpated from its few nesting cays in the Virgin Islands as a result of over-hunting or poaching (Raffaele 1973). The wide distribution of bones from this species suggests that it once was much more common, and possibly the predominant species of sea bird on the island.

Surface samples from various localities also included several other bird species: Red-footed Booby (*Sula sula*), Kingbird (*Tyrannus sp.*), Black-capped Petrel (*Pterodroma hasitata*), and Brown Booby (*Sula leucogaster*) which are still present in the area. These bones may be of recent origin.

A small vertebra, less than 1 cm in length, in a sample from Cueva de los Losetas (Bag 133) is tentatively identified as crocodile vertebrae based upon typical procoelous characters. This is the first report of crocodile remains from Isla de Mona, although crocodylidae presently live, or have been found in the fossil record, from other Caribbean localities including: Cuba, Hispaniola, Jamaica, Isla de Juventud, Cayman Islands, Grenada, and New Providence Island, Bahamas (Pregill 1981, 1982). The cave itself is atop a 45 m high, overhung cliff above the sea and kilometers in distance from any presently easy sea level access.

The caves where these skeletal materials were found contain extensive fossil guano deposits. In the late 1880s and early 1900s, ~150,000 metric tons of guano were commercially mined from caves on the island (Kaye 1959; Frank 1998b). Determining the origin of these fossil guano deposits, bat or bird, was one of the goals of the sampling effort. Bat bones were not found in any of the sifted fossil guano material. However sifting fresh guano from an active bat colony in Bat Cave also yielded no bat bones. Bat bones are digested by chemical and biological activity within the fresh guano deposits and do not survive incorporation into the fossil record. The thickness of the fossil guano deposits in entrance areas, the numbers of Audubon's Shearwater bones, hermit crab claws, and associated *Cerion sp.* shells suggests that the deposits in these areas are primarily derived from bird guano. The bulk of the cave deposits, however, are in twilight to total darkness. Given that there are no remains of echolocating birds, such as the Oil-Bird (*Steatornis caripensis*) of South America, we interpret these deposits as bat guano.

Whatever the origin of the deposits, a significantly larger population of bats and birds than currently on the island would be required to produce deposits of this volume. ¹⁴C dating was not performed on the guano deposits from these Isla de Mona caves because geomorphologic evidence indicates that many of the deposits are probably on the order of hundreds of thousands of years old, beyond the range of ¹⁴C dating. Individual

deposits may vary from over 2 Ma to recent and dating would not yield information of significant interpretive or diagnostic value. Also, Audubon's Shearwater fossils are not particularly age diagnostic.

If migration of species across the Caribbean Islands took place by dispersal from populations originating in South America, North America, Central America, or Cuba, then the fossil record of Isla de Mona species might be expected to include examples of species that migrated from Puerto Rico to Hispaniola or from Hispaniola to Puerto Rico, and some species that are on only one or the other of the islands. Isla de Mona is a stepping stone bridging one of the longest gaps in the migration routes from island to island in the Lesser and Greater Antillies island chains. Because of deep water on all sides of Isla de Mona, during past low sea level stands the length of this gap would not be significantly different than it is today. The lack of a diversified fossil faunal record is likely a combination of three major factors: (1) the fossils could be pre-

sent, but simply have not been found yet, (2) specific species may have moved from one large island to the other bypassing Isla de Mona, or (3) the transient species may not have established a breeding population on Mona because of its small size, or lack of appropriate habitat.

A persistent problem when evaluating vertebrate fossil records from the Caribbean is determining the ages of the specimens. Many of the prime fossil localities are within caves or infilled karst features. Uranium-thorium dates (Ruiz 1993) and paleomagnetic investigations (Panuska 1998) provide evidence that many of the caves on Isla de Mona may be in excess of 2 Ma. Williams (1952) tentatively assigned a sub-recent age for the tortoise fossil from Cueva del Lirio. There is no empirical basis for this age assignment, and we would suggest the specimen may potentially be as old as 2 Ma or as young as sub-recent.

Some fossil materials preserved in these caves and other fossil bearing caves on other islands similarly may be upwards

Table 1. Identifications, Minimum Number of Individuals (MNI) tabulations, and general listings of avian bone material collected on Isla de Mona, Puerto Rico, July 1995.

Cueva Negra Site C, Bag 08; (Specimens are charred).

Puffinus lherminieri (Audubon's Shearwater)

MNI=5, based on 5 distal ends of right humeri.

ID based on distal end of a left humerus with procellariid characters. Also present are a pair of left and right carpometacarpi.

Bat Cave, surface material, Bag 67.

Tyrannus sp. (Kingbird)

MNI=1, based on distal end of a right humerus.

ID based on distal end of a right humerus of a large tyrannid.

Tyranni, family unidentified

MNI=1

The proximal end of a right ulna of another, but smaller, subsocial passerine, not yet identified, is also present.

Cueva del Diamante, southernmost entrance, Bag 113 and 115.

Puffinus lherminieri

MNI=11, based on 11 right humeri.

ID based on a complete procellariid right femur, left ulna and carpometacarpus, manual phalanges, and right tibiotarsus. Also present are procellariid sacrum and pelvis, scapula, humeri, ulnae, carpometacarpi, manual phalanges, and tibiotarsi, and 5 tarsometatarsi.

Cueva del Diamante, back of cave in dark, Bags 123 and 124.

Puffinus lherminieri

MNI=5, based on 5 proximal ends of left humeri.

ID based on a left coracoid and humerus, a right tibiotarsus, a tarsometatarsus, right humerus and ulna, left carpometacarpus, and right tibiotarsus and tarsometatarsus of a procellariid. Specimens are very encrusted, so that surface details are obliterated; identification is by general outline and size.

Cueva de Espinal, Pictograph Room, Bag 117.

Pterodroma hasitata (Black-capped Petrel)

MNI=1, based on distal end of right humeri.

ID based on the single specimen in bag, the distal end of a right humerus.

Cueva de Espinal, Pictograph Room, Bag 118.

Sula leucogaster (Brown Booby)

MNI=1.

ID based on the extremely unossified partial skeleton of a hatchling.

Cueva de los Losetas, Layer 5, Bag 112.

2 unidentified long-bone shafts.

Cueva de los Losetas, Bag 119.

Sula sula (Red-footed Booby)

MNI=1, based on 1 sulid pelvis.

ID based upon a sulid pelvis.

Cueva de los Losetas, from surface, Bag 111.

Puffinus lherminieri

MNI=1, based on distal end of a left humerus.

ID based on distal end of a left humerus identical to that listed for Bag 08 above.

Sula sula

MNI=1, based on a pair of right and left sulid radii.

ID based upon a pair of sulid radii. The left radius is complete, however only the proximal end of the right radius is present. Also present is a clavicular fragment of a furcula.

Cueva de los Losetas, Crunchy Room, Bag 126.

Puffinus lherminieri

MNI=1, based on the proximal ends of a pair of left and right tarsometatarsi.

ID based upon the proximal ends of a pair of left and right tarsometatarsi.

Cueva de los Losetas, 2nd phosphate layer, Bag 127.

Puffinus lherminieri

MNI=4, based on 4 left and right proximal ends of humeri.

ID based on procellariid humeri and tarsometatarsi. Also present are the ventral fragments of a right coracoid and a right ulna.

Cueva de los Losetas, 2nd phosphate layer, Bag 128.

Puffinus lherminieri

MNI=3, based on 3 left proximal ends of humeri.

ID based on coracoids and humeri of the type identified as this species.

Cueva de los Losetas, Bag 131.

Puffinus lherminieri

MNI=3, based upon 3 left humeri.

ID based upon procellariid humeri, radius, femur, and tibiotarsi.

Cueva de los Losetas, Bag 133.

Puffinus lherminieri

MNI=3, based on 3 left coracoids.

ID based on procellariid coracoids, humeri, left ulna and left femur. Also present is a symphyseal fragment of a furcula consistent with a *Puffinus* of this size.

Cueva de Esquelito, Bag 120.

Puffinus lherminieri

MNI=2, based on 2 left humeri.

ID based on left humerus and tarsometatarsus.

Cueva de Esquelito, Bag 122.

Puffinus lherminieri

MNI=2, based on 2 right coracoids.

ID based on left and right humeri, left carpometacarpus, sacrum, and right femur and tibiotarsus.

of several million years old. The speed of karst processes is highly variable. We urge other researchers to consider that many fossil deposits may be older than they first appear and to interpret the available stratigraphic and empirical dating information accordingly. Paleontologists and karst scientists can both benefit from working more closely together to better establish ages for fossil localities and time lines for trans-island migrations.

ACKNOWLEDGMENTS

We thank the Cave Research Foundation, the University of Minnesota's Department of Geology and Geophysics, their George and Orpha Gibson Endowment in hydrogeology, and the University of Minnesota, Bell Museum of Natural History for financial assistance in conducting field work on Isla de Mona or laboratory processing of samples collected from the island. We would also like to thank E. Calvin Alexander, Jr. and Susan Magdeline for their assistance in the field work.

REFERENCES

Anthony, H.E. (1926). *Field notes of the 1926 expedition to Mona and other West Indian Islands*. Unpublished manuscript, American Museum of Natural History, New York.

Auffenberg, W. (1967). Notes on West Indian tortoises. *Herpetologica* 23: 34-44.

del Hoyo, J., Elliott, A., Sargatal, J. (eds.). (1992). *Handbook of the birds of the world, Volume 1*. Lynx Edicions, Barcelona: 320 pp.

Frank, E.F. (1998a). A radiocarbon date of 380 ± 60 years BP for a Taino site, Cueva Negra, Isla de Mona, Puerto Rico. *Journal of Cave and Karst Studies* 60(2): 101-102.

Frank, E.F. (1998b). History of the guano mining industry, Isla de Mona, Puerto Rico. *Journal of Cave and Karst Studies* 60(2):121-125.

Goodwin, G. (1926). *Field notes of 1926 trip to Mona Island, 28 February to 13 March*. Unpublished manuscript, American Museum of Natural History, New York.

Kaye, C.A. (1959). Geology of Isla Mona, Puerto Rico, and notes on the age of the Mona Passage. *U.S. Geological Survey, Professional Paper* 317C: 141-178.

Martorell, L.F. (1973). The insects of Mona Island, P.R., Apendice J. In Junta de Calidad Ambiental, *Las Islas de Mona y Monito: Una evaluacion de sus Recursos naturales y historicos* 2: J1-J7.

Nieves-Rivera, A.M., Mylroie, J.E., MacFarlane, D.A. (1995). Bones of *Puffinus lherminieri* Lesson (Aves: Procellariidae) and two other vertebrates from Cueva de Agua, Mona Island, Puerto Rico (West Indies). *National Speleological Society Bulletin* 57: 99-102.

Panuska, B.C., Mylroie, J.E., and McFarlane, D. (1998). Magnetostratigraphy at Cueva de Aleman, Isla de Mona, Puerto Rico. *Journal of Cave and Karst Studies* 60(2): 96-100.

Peck, S.B. & Kukalova-Peck, J. (1981). The subterranean fauna and conservation of Mona Island, Puerto Rico. *National Speleological Society Bulletin* 43(3): 59-68.

Perfit, M.R. & Williams, E.E. (1989). Geological constraints and biological retrodictions in the evolution of the Caribbean Sea and its islands. In Woods, C.A. (ed.), *Biogeography of the West Indies, past, present, and future*. Florida Museum of Natural History, Sandhill Crane Press, Gainesville, Florida: 46-102.

Pregill, G.K. (1981). Late Pleistocene herpetofaunas from Puerto Rico. *Miscellaneous Publications of the University of Kansas Museum of Natural History* 71: 1-72.

Pregill, G.K. (1982). Fossil amphibians and reptiles from New Providence, Bahamas. In Olsen, S.L. (ed.), *Fossil vertebrates from the Bahamas. Smithsonian contributions to paleobiology* 48:8-21.

Raffaele, H. (1973). Assessment of Mona Island avifauna, Apendice K. In Junta de Calidad Ambiental, *Las Islas de Mona y Monito: Una evaluacion de sus Recursos naturales y historicos* 2: K1-K32.

Ruiz, H.M. (1993). *Sedimentology and diagenesis of Isla de Mona, Puerto Rico*. MS thesis, University of Iowa, Iowa City, Iowa: 86 pp.

Shirihai, H., Sinclair, I. & Colston, P.R. (1995). A new species of *Puffinus* shearwater from the western Indian Ocean. *Bulletin of the British Ornithologists' Club* 115: 75-87.

Stehli, F.G. & Webb, S.D. (1985). A kaleidoscope of plates, faunal and floral dispersals, and sea level changes; In Stehli, F.G. & Webb, S.D. (ed.), *The great American biotic interchange*. Plenum Press, New York: 3-16.

Velez, M.J. Jr. (1973). The terrestrial arthropoda (exclusive of insects and crustacea) of Mona Island, Puerto Rico, Apendice I. In Junta de Calidad Ambiental, *Las Islas de Mona y Monito: Una evaluacion de sus Recursos naturales y historicos* 2: I1-I14.

Wiewandt, T.A. (1973). Mona amphibians, reptiles, and mammals, Apendice L. In Junta de Calidad Ambiental, *Las Islas de Mona y Monito: Una evaluacion de sus Recursos naturales y historicos* 2: L1-L12.

Williams, E.E. (1950). *Testudo cubensis* and the evolution of western hemisphere tortoises. *Bulletin American Museum of Natural History* 95(1): 1-36.

Williams, E.E. (1952). A new fossil tortoise from Mona island, West Indies and a tentative arrangement of the tortoises of the world. *Bulletin American Museum of Natural History* 99(9): 547-561.

Woodbury, R.O. (1973). The vegetation of Mona Island, Apendice G. In Junta de Calidad Ambiental, *Las Islas de Mona y Monito: Una evaluacion de sus Recursos naturales y historicos* 2: G1-G2.

GROUNDWATER GEOCHEMISTRY OF ISLA DE MONA, PUERTO RICO

CAROL M. WICKS

Department of Geological Sciences, University of Missouri, Columbia, MO 65211 USA

JOSEPH W. TROESTER

U.S. Geological Survey, GSA Center, 651 Federal Drive, Suite 400-15, Guaynabo, PR, 00965

In this study, we explore the differences between the hydrogeochemical processes observed in a setting that is open to input from the land surface and in a setting that is closed with respect to input from the land surface. The closed setting was a water-filled passage in a cave. Samples of groundwater and of a solid that appeared to be suspended in the relatively fresh region of saline-freshwater mixing zone were collected. The solid was determined to be aragonite. Based on the analyses of the composition and saturation state of the groundwater, the mixing of fresh and saline water and precipitation of aragonite are the controlling geochemical processes in this mixing zone. We found no evidence of sulfate reduction. Thus, this mixing zone is similar to that observed in Caleta Xel Ha, Quintana Roo, also a system that is closed with respect to input from the land surface.

The open setting was an unconfined aquifer underlying the coastal plain along which four hand-dug wells are located. Two wells are at the downgradient ends of inferred flowpaths and one is along a flow-path. The composition of the groundwater in the downgradient wells is sulfide-rich and brackish. In contrast, at the well located along a flow line, the groundwater is oxygenated and brackish. All groundwater is oversaturated with respect to calcite, aragonite, and dolomite. The composition is attributed to mixing of fresh and saline groundwater, CO₂ outgassing, and sulfate reduction. This mixing zone is geochemically similar to that observed in blue holes and cenotes.

In coastal carbonate aquifers, the saline-freshwater mixing zone is an area of enhanced calcite dissolution, aragonite neomorphism, and dolomitization (Back *et al.* 1979; Randazzo & Bloom 1985; Randazzo & Cook 1987; Smart *et al.* 1988; Budd 1988; Stoessell *et al.* 1989; Whitaker *et al.* 1994). The water-rock interactions that occur in the mixing zone can lead to changes in the chemical composition of the groundwater, the mineralogical composition of the bedrock, and the porosity and permeability of the aquifer. Summarizing the geochemical reactions in saline-freshwater mixing zones and their role in the evolution of carbonate-aquifer systems, Hanshaw and Back (1980) conclude that mineral dissolution and precipitation in the mixing zone could enhance, or at least redistribute, porosity and permeability.

Physical heterogeneities, such as cenotes, blue holes, and caves, are common on the low-lying carbonate islands of the Caribbean. These features can be flooded by fresh, brackish, or saline water. Cenotes and blue holes are collapse depressions that are directly open to the earth's surface, thus rainfall and detritus can enter cenotes and blue holes directly (Mylroie *et al.* 1995, Ford & Williams 1989). A subaqueous cave passage has a roof and is not as open to the earth's surface as are cenotes or blue holes. Therefore, subaqueous cave passages probably do not directly receive rainfall or detritus material inputs.

In a series of studies of the blue holes of Andros Island, Bahamas, Smart *et al.* (1988) and Bottrell *et al.* (1991) demon-

strated that pervasive dissolution of carbonate wall rock was driven by mixing of fresh and saline groundwater and by bacterial processes. Organic matter was observed suspended on the saline-freshwater interface. In detailed studies of the cenotes and blue holes in the Yucatan, Stoessell *et al.* (1993) found that dissolution was enhanced by bacterial-driven processes. It seems that in cenotes and blue holes that are open to the earth's surface, bacterial reactions influence processes within the mixing zone.

From detailed sampling along a subaqueous cave passage, Back *et al.* (1986) determined that mixing of fresh and saline groundwater in the Yucatan Peninsula resulted in dissolution of the carbonate bedrock and the development of caves and crescent-shaped beaches. Three of the five groundwater samples collected from a cave system were in equilibrium with respect to aragonite (Back *et al.* 1986). Subsequently, Stoessell *et al.* (1989) showed that aragonite was dissolved in the Xcaret Cave. In the studies based on the Xcaret Cave, no mention of bacterial-driven processes is given. In subaqueous cave passages, bacterial processes appear to be of minor importance.

In our study, we explore the contrasts between the hydrogeochemical processes observed in open and closed settings and seek a better understanding of the controls on the geochemical processes that occur in these two distinct settings. In this study, we document the mixing and geochemical processes that control the composition of groundwater in the saline-freshwater mixing zone on Isla de Mona, Puerto Rico.

FIELD SITE DESCRIPTION

Descriptions of the geologic setting and history of Isla de Mona are found in Frank *et al.* (1998), Ruiz (1993), and Kaye (1959). Frank *et al.* (1998) includes a map showing the location of the island in the Caribbean.

COASTAL PLAIN AREA

Access to the water table is limited to hand-dug wells (Pozo del Aeropuerto, Pozo del Playa las Mujeres, Pozo del Portugués, and Pozo de Playa del Uvero) located along the coastal plain (Fig. 1). The wells intersect carbonate sand and reef deposits (Jordan 1973). The description of the configuration of the water table is based on the results of a geophysical survey (TEM and TC) on the island (Richards *et al.* 1998; Richards *et al.* 1995; Martinez *et al.* 1995). A groundwater mound exists near the center of the coastal plain and flowpaths were constructed from the groundwater mound outward in all directions (Martinez *et al.* 1995) (Fig. 1). Where the coastal plain abuts the meseta, Martinez *et al.* (1995) have constructed flowpaths that originate under the meseta and divert around the coastal plain. This behavior was attributed to the lower permeability of coastal plain sediments compared to the permeability of the karstified rocks of the meseta. Thus, the coastal plain sediments are thought to act as a barrier preventing groundwater flow from the plateau to the coastal plain (Martinez *et al.* 1995). Vacher (1978) and Wallis *et al.* (1991) report that regions with different hydraulic conductivity influence the shape and position of the freshwater lens. The vege-

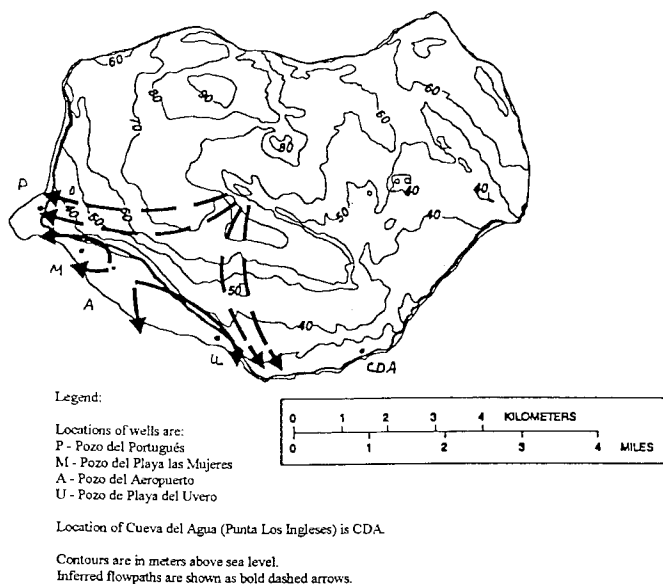


Figure 1. Map of Isla de Mona, Puerto Rico, located in the Mona Passage midway between Puerto Rico and Hispaniola showing the coastal plain that is along the southern and southwestern edge of the plateau. The sampling locations are noted. Flowpaths are based on the work by Martinez *et al.* (1995) and Richards *et al.* (1995).

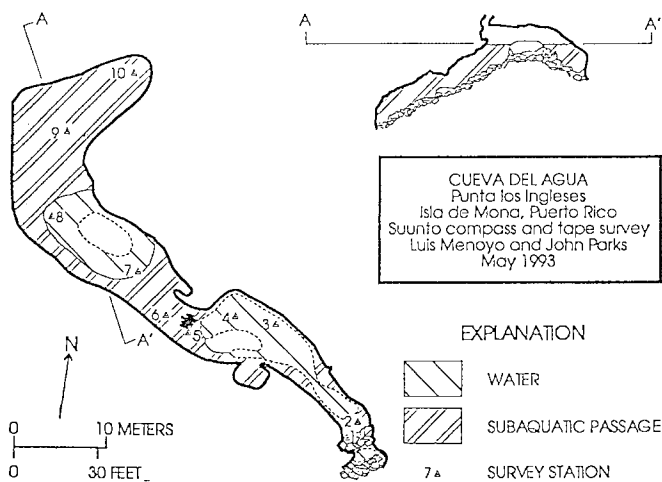


Figure 2. Map of Cueva de Agua (Punta Los Ingleses).

tation of the coastal plain consists of a coastal lowland forest and mahogany plantation, which form closed canopies, and a Casuarai plantation, which has an open canopy (Cintron & Rogers 1991).

MESETA AREA

Access to the water table is limited to Cueva de Agua (Punta los Ingleses) that penetrates through Mio-Pliocene carbonates (Frank 1993) (Fig. 1). This cave is thought to have formed during the substage 5-e sea level highstand about 125 Ka (Frank *et al.* 1998). The cave has been referred to as Cueva de Agua Playa Brava in Nieves-Rivera *et al.* (1995). The main cave passage extends into the island and under the meseta. The cave passage is generally flat-lying with a series of air bells (Fig. 2). There is one steeply sloping passage located toward the seaward edge of the cave where the saline-freshwater mixing zone is intersected. Groundwater flow is outward from the central portion of the meseta (Richards *et al.* 1998; Richards *et al.* 1995; Martinez *et al.* 1995) (Fig. 1). About 94% of the meseta is covered with a dry forest and shrublands, which is an open association of shrubby trees (Cintron & Rogers 1991). Soil coverage is greater along the western portion of the meseta than along the eastern portion of the meseta (Briggs & Seiders 1972). Along the eastern portion and overlying Cueva de Agua (Punta los Ingleses), the meseta surface is either exposed bare rock or covered with cacti (Briggs & Seiders 1972; Frank *et al.* 1998).

METHODS

Samples of groundwater were collected from the wells along the coastal plain in May 1992, May 1993, and June 1994, from the Caribbean in May 1993, and from Cueva de Agua (Punta los Ingleses) in May 1993 and June 1994. The amount of precipitation delivered to Isla de Mona during the months of the sampling trips were 30, 11, and 3 cm in May 1992, May 1993, and June 1994, respectively (NOAA 1996).

Table 1. The chemical composition (in mmol/L, mixing ratio (MR), specific conductance (Cond, $\mu\text{S}/\text{cm}$), dissolved oxygen concentration (DO, in mg/L), sulfide concentration (H_2S , mg/L), log of the partial pressure of CO_2 , and saturation indices with respect to calcite (SI_c), aragonite (SI_a) and dolomite (SI_d) of the groundwater collected from Isla de Mona, Puerto Rico.

| | depth | cond | pH | MR ¹ | Cl ⁻ | SO ₄ ²⁻ | HCO ₃ ⁻ | Ca ²⁺ | Mg ²⁺ | Na ⁺ | K ⁺ | DO ³ | H ₂ S | logCO ₂ ² | SI _c | SI _a | SI _d |
|--------------------------|--------------------|-----------------|------|-----------------|-----------------|-------------------------------|-------------------------------|------------------|------------------|-----------------|----------------|-----------------|------------------|---------------------------------|-----------------|-----------------|-----------------|
| 1993 | | | | | | | | | | | | | | | | | |
| Cueva del Agau | | | | | | | | | | | | | | | | | |
| 5 | 2.0 | 5000 | 7.37 | 0.00 | 82. | 2.8 | 5.07 | 3.4 | 8.6 | 67. | 1.5 | 7. | 0 | -1.97 | 0.20 | 0.06 | 1.00 |
| 7 | 4.0 | 6100 | 7.32 | 0.03 | 96. | 4.2 | 5.16 | 3.7 | 10. | 78. | 1.8 | 6. | 0 | -1.92 | 0.17 | 0.03 | 1.00 |
| 6 | 6.0 | 8200 | 7.24 | 0.14 | 150. | 6.3 | 4.95 | 5.2 | 16. | 120. | 3.1 | 7. | 0 | -1.88 | 0.14 | 0.02 | 1.00 |
| 3 | 8.0 | 11000 | 7.29 | 0.23 | 200. | 8.5 | 4.77 | 5.4 | 19. | 170. | 3.3 | 6. | 0 | -1.96 | 0.14 | 0.00 | 1.02 |
| 2 | 10.0 | 18000 | 7.27 | 0.44 | 310. | 16. | 3.70 | 8.5 | 35. | 260. | 6.4 | 4. | 0 | -2.09 | 0.12 | -0.02 | 1.10 |
| 4 | 12.0 | 24500 | 7.30 | 0.62 | 400. | 20. | 3.20 | 10. | 43. | 330. | 8.4 | 4. | 0 | -2.21 | 0.13 | 0.00 | 1.10 |
| 1 | 14.0 | 47000 | 7.21 | 0.86 | 520. | 24. | 2.64 | 13. | 56. | 430. | 10. | 4. | 0 | -2.22 | .02 | -0.12 | 0.90 |
| SW ¹ | 33.7% ² | | 8.24 | 1.00 | 592. | 31.3 | 3.54 | 14.0 | 66. | 480. | 13. | 8. | 0 | -3.25 | 1.06 | 0.92 | 2.99 |
| 1994 | | | | | | | | | | | | | | | | | |
| Cueva del Agau | | | | | | | | | | | | | | | | | |
| 1 | 1.21 | 8200 | 7.33 | 0.00 | 68. | 3.1 | 5.11 | 3.4 | 7.2 | 45. | 1.5 | 4. | 0 | -1.92 | 0.20 | 0.05 | 0.88 |
| 2 | 2.74 | 10200 | 7.30 | 0.03 | 81. | 3.9 | 5.15 | 3.8 | 9.8 | 150. | 1.7 | 6. | 0 | | | | |
| 6 | 5.79 | 15000 | 7.22 | 0.16 | 150. | 6.7 | 5.07 | 4.6 | 14. | 92. | 1.9 | 4. | 0 | | | | |
| 5 | 4.27 | 16500 | 7.23 | 0.17 | 150. | 8.0 | 5.02 | 5.0 | 15. | 101. | 2.2 | 6. | 0 | -1.86 | 0.11 | -0.03 | 0.88 |
| 4 | 7.62 | 27400 | 7.21 | 0.42 | 260. | 13. | 4.20 | 8.5 | 27. | 181. | 5.1 | 2. | 0 | -1.96 | 0.14 | 0.00 | 0.96 |
| 7 | 9.14 | 44500 | 7.28 | 0.95 | 500. | 26. | 1.25 | 12. | 44. | 460. | 9.5 | 1. | 0 | -2.63 | -0.28 | -0.42 | 0.18 |
| 3 | 10.4 | 45200 | 7.24 | 0.99 | 520. | 26. | 2.55 | 12. | 46. | 440. | 9.8 | 1. | 0 | -2.27 | 0.00 | -0.14 | 0.77 |
| 1992 | | | | | | | | | | | | | | | | | |
| Pozo | | | | | | | | | | | | | | | | | |
| Aeropuerto | nd | 1400 | 7.54 | 0.00 | 8.7 | 0.49 | 4.09 | 1.4 | 1.5 | 7.0 | 0.25 | 4.8 | 0 | -2.20 | 0.15 | 0.10 | 0.49 |
| Portugues-u ³ | nd | 2300 | 7.32 | 0.04 | 31. | 1.9 | 3.77 | 2.1 | 3.2 | 29. | 1.9 | 3.1 | 0 | -2.00 | -0.05 | -0.19 | 0.06 |
| Portugues-u ³ | nd | 4300 | 7.24 | 0.02 | 16. | 1.0 | 4.10 | 1.8 | 1.9 | 14. | 0.31 | 2.7 | 0 | -1.90 | -0.12 | -0.26 | 0.10 |
| Portugues-u ³ | nd | 3200 | 7.26 | 0.02 | 24. | 1.5 | 4.92 | 2.5 | 2.6 | 2.0 | 0.31 | 1.6 | 0 | -1.80 | 0.11 | -0.03 | 0.40 |
| Uvero | nd | 3250 | 7.53 | 0.02 | 21. | 2.0 | 5.25 | 2.4 | 2.8 | 19. | 1.4 | 3.8 | 1 | -2.10 | 0.37 | 0.23 | 0.99 |
| 1993 | | | | | | | | | | | | | | | | | |
| Aeropuerto | | | | | | | | | | | | | | | | | |
| Portugues-1 ⁴ | 1.34 | 2430 | 7.63 | 0.02 | 19. | 1.1 | 4.10 | 1.9 | 2.1 | 17. | 0.41 | 1.0 | 0 | -2.30 | 0.34 | 0.20 | 0.91 |
| Portugues-2 | 1.70 | 3250 | 7.59 | 0.02 | 20. | 1.0 | 3.77 | 2.0 | 2.3 | 17. | 0.41 | 0.8 | 0 | -2.30 | 0.24 | 0.10 | 0.71 |
| Uvero | nd | 5% ² | 7.63 | 0.11 | 73. | 3.0 | 8.03 | 5.0 | 7.8 | 56. | 2.2 | <0.2 | 1 | -2.00 | 0.83 | 0.69 | 2.00 |
| 1994 | | | | | | | | | | | | | | | | | |
| Aeropuerto | | | | | | | | | | | | | | | | | |
| Portugues-1 | 1.10 | 2900 | 7.36 | 0.01 | 48.2 | 2.17 | 4.10 | 2.89 | 3.7 | 15.4 | 0.31 | 1.0 | 0 | -1.95 | 0.87 | 0.73 | 2.00 |
| Portugues-2 | 1.71 | 6000 | 7.34 | 0.07 | 16.6 | 18.7 | 3.68 | 2.36 | 2.28 | 49.6 | 0.29 | 0.8 | 0 | -2.00 | 0.12 | -0.02 | 0.62 |
| Mujeres | 1.20 | 15200 | 7.85 | 0.19 | 118. | 1.0 | 11.1 | 5.67 | 13.6 | 75.5 | 1.8 | <0.2 | 1 | -2.10 | 1.20 | 1.0 | 2.92 |
| Uvero ⁵ | 2.25 | 12500 | 7.72 | 0.20 | 119. | 4.45 | 88. | 1.61 | 7.4 | 12.4 | 0.15 | | | -2.09 | 1.06 | 0.92 | 2.53 |

1. SW is Caribbean seawater

2. Salinity is reported instead of conductivity.

3. Sampled several times during rain event on 5-22-93 at 10am (1), on 5-22-93 at 12 pm (2), and on 5-25-93 at 11 am (3).

4. Pozo del Portugues is often stratified. Samples collected from the upper water body are number 1 and those from the lower water body are number 2.

5. Represents an average composition of samples collected hourly over a 26-hour period.

All samples of water were filtered and split for subsequent analyzes of cations (acidified to pH < 2) and anions. Due to the remoteness of Isla de Mona, water samples could not be refrigerated. In the field, potentiometric titrations were performed for determination of bicarbonate alkalinity. The concentration of dissolved oxygen in each water sample was determined using a Hach® kit*. The temperature and conductivity of each groundwater were also measured. Upon return to the laboratory, the concentrations of calcium, magnesium, sodium, and potassium were determined by atomic absorption spectrophotometry, and the concentrations of chloride and sulfate were determined by ion chromatography. The total inorganic carbon content and the partial pressure of carbon dioxide were calculated using the numerical model, PHREEQE (Parkhurst *et al.* 1990). The quality of the chemical analyses was affirmed

by fifty-one of the fifty-three samples having a charge balance error of less than 10% (Tables 1 & 2) and only those fifty-one samples were used in the interpretation of water-rock interactions.

Theoretical mixing calculations were performed based on a presumed linear relationship between the solute concentrations in the fresh endmember and the saline endmember. This relationship results from conservative mixing with all solutes remaining in solution, that is, with no mineral dissolution or precipitation reactions and no gas exchange. For the groundwater collected from the wells in the coastal plain, the freshest groundwater collected (Pozo del Aeropuerto sample collected in 1992) and Caribbean seawater were used as the fresh and saline endmembers, respectively (Table 1). For the water collected from Cueva de Agua (Punta los Ingleses), the freshest groundwater (CDA1-94 sample collected in 1994) and Caribbean seawater were used as the fresh and saline end-

*The use of trade names in this article is for descriptive purposes only and does not imply endorsement by the University of Missouri or the U.S. Government.

Table 2. The mixing ratio(MR), the pH and calcium concentration in theoretical mixtures of fresh and saline endmembers (CDA1-94 and Seawater), the mass of aragonite that could be removed from each mixture at equilibrium with respect to aragonite (Δ), and the concentration of calcium of each mixture at equilibrium with respect to aragonite.

| MR | Ca ²⁺ _{init} (mM) | Ca ²⁺ _{final} (mM) | Δ (mmol/kg) | pH _{final} |
|------|--|---|-----------------------|---------------------|
| 0 | 3.43 | 3.39 | 0.038 | 7.29 |
| 0.05 | 3.97 | 3.93 | 0.041 | 7.29 |
| 0.1 | 4.5 | 4.45 | 0.050 | 7.29 |
| 0.15 | 5.03 | 4.97 | 0.064 | 7.29 |
| 0.2 | 5.56 | 5.48 | 0.080 | 7.29 |
| 0.25 | 6.10 | 6.00 | 0.098 | 7.29 |
| 0.35 | 7.16 | 7.02 | 0.138 | 7.29 |
| 0.4 | 7.69 | 7.53 | 0.158 | 7.29 |
| 0.45 | 8.23 | 8.05 | 0.180 | 7.29 |
| 0.5 | 8.76 | 8.55 | 0.202 | 7.30 |
| 0.55 | 9.29 | 9.07 | 0.224 | 7.30 |
| 0.6 | 9.82 | 9.57 | 0.247 | 7.30 |
| 0.65 | 10.4 | 10.0 | 0.271 | 7.30 |
| 0.7 | 10.9 | 10.6 | 0.293 | 7.31 |
| 0.75 | 11.4 | 11.1 | 0.318 | 7.32 |
| 0.8 | 11.9 | 11.6 | 0.342 | 7.33 |
| 0.85 | 12.5 | 12.1 | 0.367 | 7.33 |
| 0.9 | 13.0 | 12.6 | 0.392 | 7.34 |
| 0.95 | 13.6 | 13.1 | 0.418 | 7.36 |
| 1 | 14.1 | 13.6 | 0.448 | 7.37 |

members, respectively. Concentrations of solutes observed in the groundwater were compared to concentrations predicted by theoretical mixing calculations based on the mixing ratio of each groundwater. The mixing ratio was calculated based on the chloride concentrations of the groundwater and of the fresh and saline endmembers (Plummer & Back 1980). Differences between the observed concentrations of solutes in the groundwater and the concentrations predicted based on theoretical mixing were attributed to sources or sinks for the various solutes (Plummer & Back 1980). For each groundwater and for each theoretical mixture, the saturation state of the sample with respect to calcite, aragonite, and dolomite were calculated using PHREEQE (Parkhurst *et al.* 1990). The saturation state of a groundwater was compared to the saturation state of a theoretical mixture with the same mixing ratio. The difference between the saturation state observed in the groundwater and the saturation state of the theoretical mixture was attributed to water-rock interactions (Plummer & Back 1980).

In theoretical calculations, the amount of mineral that could be dissolved (if the conservative mixture is undersaturated) or precipitated (if the conservative mixture is oversaturated) from a conservative mixture was calculated using PHREEQE (Parkhurst *et al.* 1990). By forcing a conservative mixture to equilibrium with respect to the specified mineral, the mass of mineral added to or removed from solution was calculated.

The change in the concentration of Ca²⁺ and total inorganic carbon and of the pH in the conservative mixture as a result of the dissolution or precipitation was also calculated using PHREEQE (Parkhurst *et al.* 1990).

In December 1996, a Campbell CR10[®] data logger, which was equipped with Druck[®] pressure transducers and Campbell[®] conductivity and temperature probes, was installed at Pozo de Playa del Uvero to monitor the water level in the well and the temperature and conductivity of the groundwater. Also recorded was the tidal signal of the Caribbean. (Precipitation data from December 1996 were not available.) All sensors were sampled every second and averaged for 5 minutes. The 5 minute averages were recorded in the data logger. The tidal data were smoothed using a one-hour running average. Both the tidal data and the water-level response of Pozo de Playa del Uvero were normalized to the overall average of the entire set of data. We do not know the elevation of Pozo de Playa del Uvero relative to sea level. The data were reduced using a Fourier transform to determine the peak amplitude.

RESULTS

COASTAL PLAIN AREA

The composition of the groundwater from the coastal plain wells ranged from 1.5 to 19% seawater and represented a relatively fresh-water environment (Table 1). The concentration of dissolved oxygen in the groundwater ranged from 0.2 mg/L to 1.0 mg/L. On a Piper diagram, the composition of the groundwater falls within the Na-K-Cl-SO₄ field (Fig. 3) and the compositions cluster near the theoretical mixing line.

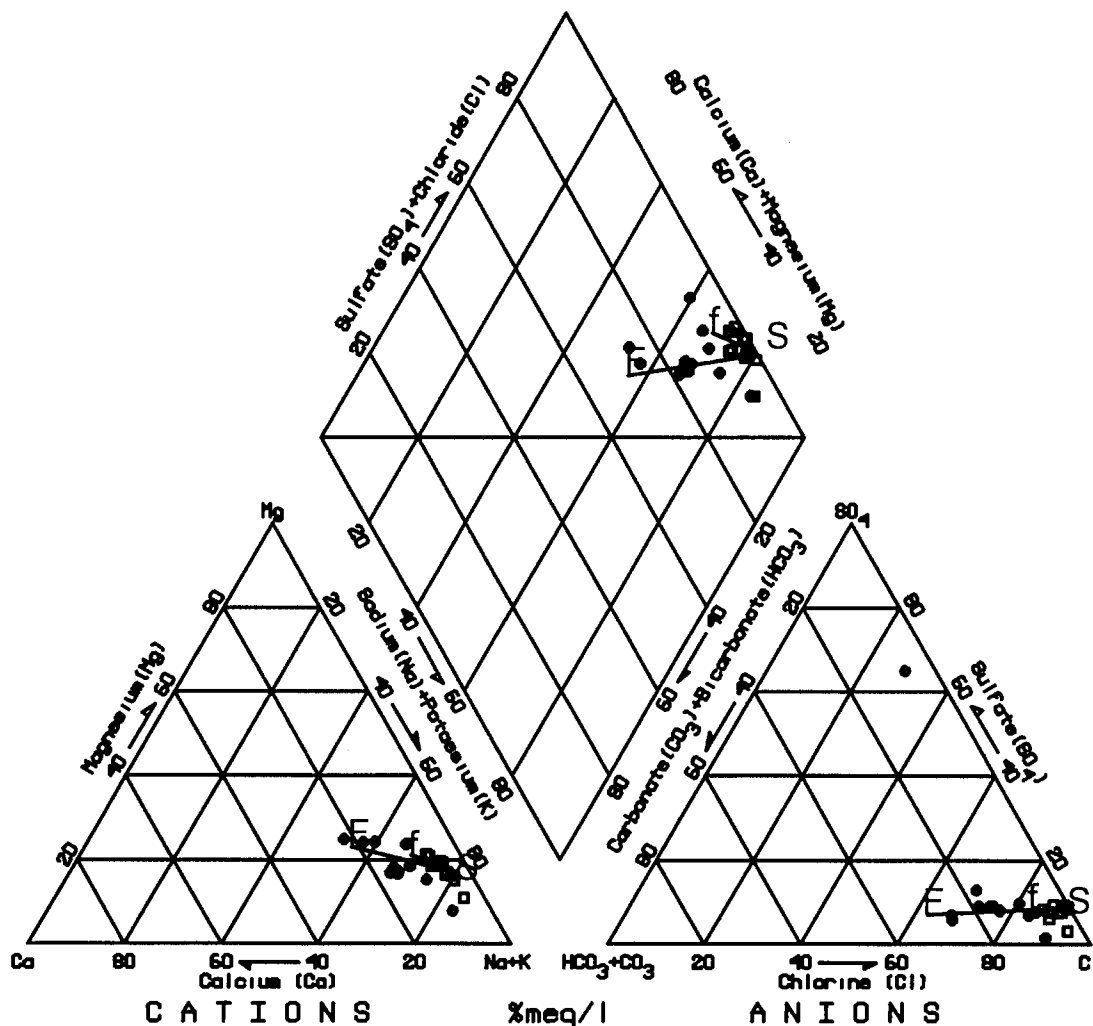
Most of the groundwater was oversaturated with respect to calcite, aragonite, and dolomite (Fig. 4). Over the limited range of mixing ratios that include samples from the wells, the theoretical mixing curves are basically flat. The saturation index (SI = log IAP/Kt) of most groundwater with respect to calcite, aragonite, and dolomite was greater than that predicted by theoretical mixing calculations.

The results from the December 1996 tidal monitoring showed that the depth to the water table exhibited a tidal cycle. The peak amplitudes of the water-level response and of the tidal data indicate both are 26.7 hours (Fig. 5). The tidal cycle response (peak amplitude of 26.7 hours) is also apparent in the temperature and conductivity data (Fig. 5). Based on the method and assumptions outlined in Erskine (1991), the ratio of storativity (specific yield) to the transmissivity of the aquifer is $5.2 \times 10^{-3} \pm 6.1 \times 10^{-3}$ day/m² (n = 28). Assuming a storativity of 0.01, the transmissivity would be 1.9×10^2 m²/day.

MESETA AREA

The cave divers noted that a material appeared to be suspended in the water column along the flat-lying passage inland from the first air bell in Cueva de Agua (Punta los Ingleses) (Fig. 2). They collected samples of the material during the dive in May 1993. The samples were analyzed by XRD and

Figure 3.
A piper diagram showing the composition of the groundwater. Observations from Cueva de Agua (Punta Los Ingleses) are plotted as hollow squares and from wells along the coastal plain as solid circles. The lines are theoretical mixing lines between the fresh and saline endmembers. The E, f, and S denote the composition of the fresh endmember for the coastal plain, the fresh endmember for Cueva de Agua (Punta Los Ingleses), and the saline endmember for both settings, respectively.



found to be aragonite (R. Deike, pers. comm. 1994).

Samples of groundwater were collected at different depths as the divers traversed from near the surface to the bottom of the cave along the steeply sloping passage (Fig. 2). The conductivity of the groundwater along the steeply sloping passage increased from 5000 $\mu\text{S}/\text{cm}$ (measured 10 cm below the surface of the water) to 47000 $\mu\text{S}/\text{cm}$ (measured 10 cm above the bottom of the cave) (Table 1). The concentration of dissolved oxygen in the groundwater ranged from 2 to 14 mg/L with the concentration decreasing as the salinity increased. The composition of the groundwater ranged from relatively fresh to nearly saline and closely matched the composition of the theoretical mixtures and, on a Piper diagram, cluster near the theoretical mixing line (Table 1 & Fig. 3). Some differences in observed compositions relative to the mixing line were noted, and they fell on either side of the line.

Most groundwater was in equilibrium with respect to aragonite and slightly oversaturated with respect to calcite up to a mixing ratio of 0.6 (Fig. 4). For mixing ratios greater than 0.8, the groundwater was undersaturated with respect to aragonite

and approximately in equilibrium with respect to calcite. All groundwater was oversaturated with respect to dolomite. The saturation index of theoretical mixtures of fresh and saline endmembers with respect to aragonite, calcite, and dolomite increases as the mixing ratio increases. The observed saturation state of the water with respect to calcite, aragonite, and dolomite was less than that predicted by theoretical mixing calculations.

DISCUSSION

The groundwater geochemistry as observed on the island, and particularly underlying the coastal plain, may not reflect long-term conditions. The island was formerly known as a watering port and now, the water resources of the island are supplemented to provide drinking water for the few rangers that reside on the island. Further, the geochemistry is probably not representative of the chemistry of the water during the development of the unconfined aquifers or of the chemistry of the water during the development of the caves that ring the

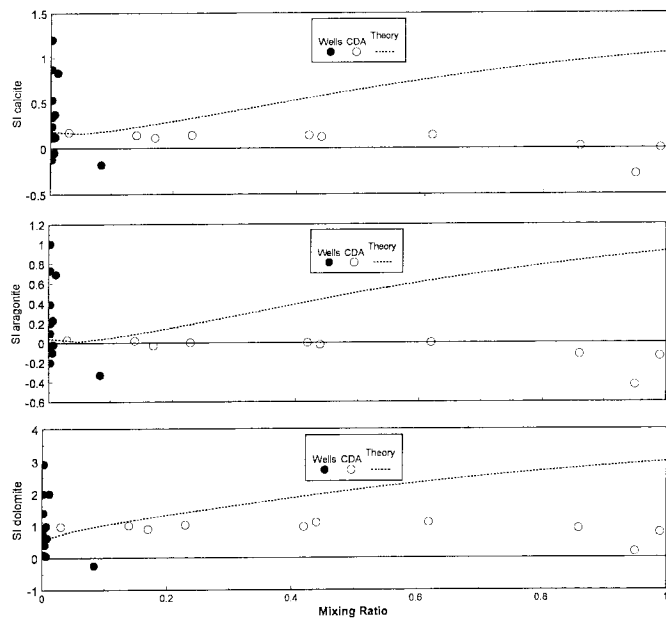


Figure 4. Graph of the saturation indices of the groundwater with respect to (a) calcite, (b) aragonite, and (c) dolomite plotted against the mixing ratio. Observations from Cueva de Agua (Punta Los Ingleses) are plotted as hollow circles and from the coastal plain as solid circles. The curves (dashed) are the theoretical mixing curves between the fresh and saline endmembers.

island. However, it does represent the conditions during the sampling events and probably current conditions.

COASTAL PLAIN AREA

The observed compositions and saturation states are consistent with an interpretation of mixing fresh and saline endmembers, outgassing of carbon dioxide, and reduction of sulfate to sulfide. We suggest that outgassing occurs from the

surface of the water in the large-diameter open-bore hand-dug wells, and that results in sampled waters that are more oversaturated with respect to the carbonate minerals than predicted by conservative mixing alone (Fig. 4). These samples might not represent the composition of the groundwater due to the large open-bore nature of the wells. However, installation of sampling wells along the coastal plain was not feasible.

Changes in the chemistry of the groundwater were observed over tidal periods and over the three-year study period. The change in the composition of the groundwater at a particular well relative to the three sampling periods showed the influence of the yearly weather pattern on the composition (Table 1). In the wet year of 1992, the groundwater was the freshest observed and the chloride concentration of the groundwater collected at Pozo del Aeropuerto was 8.7 mM. Whereas, the concentration was 20 mM in 1993 (a normal precipitation year) and 24.5 mM in 1994 when there was a drought on Isla de Mona. These observed changes in the composition of the groundwater with annual fluctuations in precipitation suggest that a strong evaporative flux could change the composition of the water in the large-diameter open-bore wells. The correlation between the tidal fluctuation, the water level in the well, and the changes in the temperature and conductivity of the water allow us to conclude that tidal pumping is the cause of those changes. The coastal plain aquifer appears to be transmissive and to respond to changing hydrological boundary conditions (tidal and evaporative) readily.

MESETA AREA

The chemical composition of the groundwater was closely matched by theoretical mixing alone (Fig. 3), whereas the saturation states of the groundwater were not accurately reproduced by theoretical mixing alone (Fig. 4). Theoretically, all mixtures are oversaturated with respect to aragonite (Fig. 4). However, the saturation state of the groundwater is in equilibrium with respect to aragonite (Fig. 4). These two interpretations suggest that aragonite has precipitated from the ground-

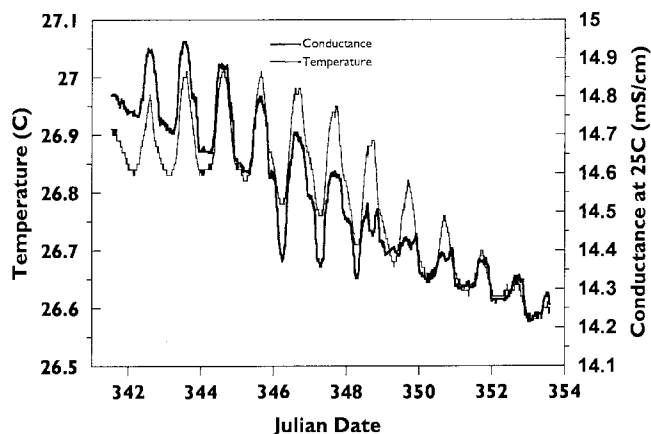
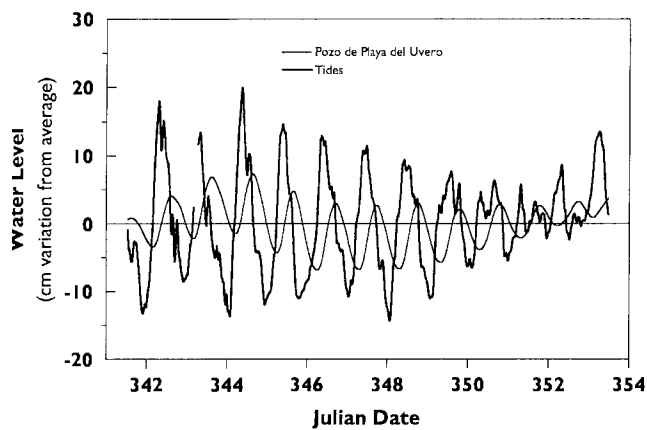


Figure 5. Graph of the results of the tidal monitoring effort of December 1996 showing (a) the response of the tides and the elevation of the water table and (b) the conductivity and temperature of the groundwater.

water in Cueva de Agua (Punta los Ingleses). However, if aragonite had precipitated from the groundwater in the cave, the composition of the water should have been depleted in calcium and total inorganic carbon relative to theoretical mixing. This was not observed (Fig. 3).

This discrepancy can be understood using geochemical modeling. Based on mixing of the fresh and saline endmembers, the mass of aragonite that would be precipitated from a theoretical mixture and the resultant composition of that mixture were calculated using PHREEQE (Parkhurst *et al.* 1990). The mass of aragonite could be theoretically precipitated ranged from 0.038 to 0.448 mmol/kg (Table 2). Precipitation of that amount of aragonite from a mixture results in a proportional change in the concentration of calcium in that mixture (Table 2). A loss of 0.038 mmol/L of calcium from the fresher groundwaters and of 0.448 mmol/L of calcium from the more saline groundwaters in the Cueva de Agua (Punta los Ingleses) represents a loss of two to three percent of the calcium in the groundwaters (Table 1). A 3-4% deviation in the composition of the groundwater is within the charge-balance error and is therefore not detectable.

The pH of the mixtures that were forced to equilibrium with respect to aragonite ranged from 7.29 to 7.37 (Table 2). The pH of the groundwater in Cueva de Agua (Punta los Ingleses) ranged from 7.21 to 7.37 (Table 1). The agreement between the expected pH of the mixtures in equilibrium with respect to aragonite and the measured pH of the groundwater supports the idea that aragonite has precipitated within the mixing zone in Cueva de Agua (Punta los Ingleses).

In Cueva de Agua (Punta los Ingleses), it appears that the saturation state of the groundwater is a more sensitive indicator of water-rock interactions than is the composition of the groundwater. Stoessell *et al.* (1989) also concluded that the saturation state of the groundwater was a more sensitive indicator of water-rock interactions based on their results from the Yucatan Peninsula. The composition of the saline-freshwater mixing zone underlying the meseta of Isla de Mona appears to be controlled by mixing of the fresh and saline endmembers and precipitation of aragonite. There were no indications that microbial processes were occurring in this mixing zone.

OPEN AND CLOSED SYSTEMS

In blue holes and cenotes, the water becomes sulfidic because of sulfate reduction (Bottrell *et al.* 1991; Smart *et al.* 1988; Stoessell *et al.* 1993). This bacterial process is driven by an abundance of sulfate (seawater source) and organic matter (for example, Berner 1980). The seawater, and therefore sulfate, enters into the cenotes and blue holes through either subaqueous cave passages or diffuse groundwater flow. The organic matter seems to added to the blue holes and cenotes from the land surface as detritus material. The blue holes and cenotes represent an open system with respect to input from the land surface. Subaqueous cave passages are open to the entry of seawater through the subaqueous passages but are closed with respect to input from the land surface. In these

systems, there is source of sulfate to the mixing zone. However, the roof of the cave prevents or reduces the delivery of detrital organic matter to the mixing zone. Therefore microbially driven sulfate reduction cannot occur as there is no organic matter available.

On Isla de Mona, it appears that the geochemistry of the coastal plain aquifer more closely resembles that of cenotes or blue holes. The source of sulfate is the seawater and the source of organic matter is the abundant plant communities (mahogany, lowland forest, and Casuarai) on the coastal plain. We believe that dissolved organic carbon is delivered to the groundwater environment through infiltration through the soil zone. As oxygen is consumed by organic matter degradation along a flowpath, the dissolved oxygen concentration decreases. At the terminus of flowpaths (Fig. 1), the groundwater becomes sulfidic and similar to that of cenotes and blue holes. This represents a different hydrologic setting than the blue holes and cenotes, but similar microbial and geochemical reactions occur (Bottrell *et al.* 1991; Smart *et al.* 1988).

On Isla de Mona, it appears that the geochemistry of the groundwater in Cueva de Agua (Punta los Ingleses) closely resembles that of other subaqueous cave passage (Back *et al.* 1986; Stoessell *et al.* 1989 & 1993). These systems are closed with respect to input from the land surface. Sulfate is delivered into Cueva de Agua (Punta los Ingleses) by seawater, yet very little organic matter can enter the cave because of the roof. Further, given the lack of plant communities and the presence of bare rock on the overlying meseta, there is very little organic matter that could be decayed, dissolved in soil water, and delivered to the groundwater. There is no indication that any sulfate reduction is occurring in the mixing zone of Cueva de Agua (Punta los Ingleses). The observations of the groundwater geochemistry and the geochemical modeling have lead us to conclude that mixing and precipitation of aragonite control the carbonate geochemistry. This is similar to the mixing zone studied in a Xcaret Cave in the Yucatan (Back *et al.* 1986; Stoessell *et al.* 1989 & 1993).

CONCLUSIONS

In our study, we explored the differences between the hydrogeochemical processes observed in open and closed settings and sought a better understanding of the controls on those geochemical processes. We documented that the geochemistry of the groundwater in the coastal plain aquifer represents a system open to input from the land surface and influenced by microbial processes, similar to blue holes and cenotes. We documented that the geochemistry of the groundwater in the meseta aquifer represents a system that is closed to input from the land surface and that is not influenced by microbial processes, similar to other subaqueous caves.

ACKNOWLEDGMENTS

We especially thank the cave divers, Donald McFarlane, Luis Menoyo, and John Parks, for their assistance with sample collection. We gratefully acknowledge Ed Frank, Calvin Alexander, and Scott Alexander for the data provided to us from the December 1996 sampling event. Acknowledgement is made to the Donors of The Petroleum Research Fund, administered by the American Chemical Society, for partial support of this research. We also thank Laura Sacks, William Ward, Ward Sanford, James Carew, Chris Agate, Myrna Iris Martínez, Janet Herman, and John Mylroie for helpful comments on this manuscript.

REFERENCES

- Back, W., Hanshaw, B.B., Pyle, T.E., Plummer, L.N. & Weidie, A.E. (1979). Geochemical significance of groundwater discharge and carbonate solution to the formation of Caleta Xel Ha, Quintana Roo, Mexico. *Water Resources Research* 15: 1521-1535.
- Back, W., Hanshaw, B.B., Herman, J.S. & Van Driel, J.N. (1986). Differential dissolution of a Pleistocene reef in the ground-water mixing zone of coastal Yucatan, Mexico. *Geology* 4: 137-140.
- Berner, R.A. (1980). *Early Diagenesis: A theoretical approach*. Princeton University Press, Princeton, NJ: 241 pp.
- Bottrell, S.H., Smart, P.L., Whitaker, F.F. & Raiswell, R. (1991). Geochemistry and isotope systematics of sulphur in the mixing zone of Bahamian blue holes. *Applied Geochemistry* 6: 97-103.
- Briggs, R.P. & Seiders, V.M. (1972). Geologic map of the Isla de Mona quadrangle, Puerto Rico. *U.S. Geological Survey Miscellaneous Geologic Investigations Map I-718, scale 1:20,000*.
- Budd, D.A. (1988). Aragonite to calcite transformation during fresh-water diagenesis of carbonates: Insights from pore-water chemistry. *Geological Society of America Bulletin* 100: 1260-1270.
- Cintron, B. & Rogers, L. (1991). Plant communities of Mona Island. In *Acta Científica. Asociación de Maestros de Ciencia de Puerto Rico* 5(1-3): 10-64.
- Erskine, A.D. (1991). The effect of tidal fluctuation on a coastal aquifer in the UK. *Ground Water* 29: 556-562.
- Ford, D. & Williams, P. (1989). *Karst Geomorphology and Hydrology*. Unwin Hyman Publishing: 601 pp.
- Frank, E.F. (1993). *Aspects of karst development and speleogenesis Isla de Mona, Puerto Rico: An analogue for Pleistocene speleogenesis in the Bahamas*. MS thesis, Mississippi State University: pp. 132.
- Frank, E.F., Wicks, C.M., Mylroie, J.M., Troester, J.W., Alexander, E.C. Jr. & Carew, J.L. (1998). Geology of Isla de Mona, Puerto Rico. *Journal of Cave and Karst Studies* 60(2): 69-72.
- Hanshaw, B.B. & Back, W. (1980). Chemical mass-wasting of the northern Yucatan Peninsula by groundwater dissolution. *Geology* 8: 222-224.
- Jordan, D.G. (1973). A summary of the actual and potential water resources Isla de Mona, Puerto Rico. In *Isla de Mona - Volume II: Junta de Calidad Ambiental*: D1-8.
- Kaye, C.A. (1959). Geology of Isla Mona Puerto Rico, and notes on age of Mona Passage. *U.S. Geological Survey Professional Paper 317-C*: 178.
- Martínez, M.I., Troester, J. W. & Richards, R.T. (1995). Surface electromagnetic geophysical exploration of the ground-water resources of Isla de Mona, Puerto Rico, A Caribbean carbonate island. *Carbonates and Evaporites* 10 (2): 184-192.
- Mylroie, J.E., Carew, J.L., Frank, E.F., Panuska, B.C., Taggart, B.E., Troester, J.W. & Carrasquillo, R. (1995). Development of flank margin caves on San Salvador Island, Bahamas and Isla de Mona, Puerto Rico. In Boardman, M.R., (ed.), *Proceedings of the Seventh Symposium on the Geology of the Bahamas: San Salvador Island, Bahamas, Bahamian Field Station*: 49-81.
- Nieves-Rivera, A.M., Mylroie, J.E. & McFarlane, D.A. (1995). Bones of *Puffinus lherminieri* Lesson (Aves: Procellariidae) and two other vertebrates from Cueva de Agua, Mona Island, Puerto Rico (West Indies). *National Speleological Society Bulletin* 57: 99-102.
- National Oceanic and Atmospheric Association. (1996). National Climatic Data Center World Wide Web, www.ncdc.noaa.gov/pub/data/coop-precip/others.txt.
- Parkhurst, D.L., Thorstenson, D.C. & Plummer, L.N. (1990). PHREEQE - a computer program for geochemical calculations. *U.S. Geological Survey Water Resources Investigations* 80-96: 210 p.
- Plummer, L.N. & Back, W. (1980). The mass balance approach: Application to interpreting the chemical evolution of hydrologic systems. *American Journal of Science* 280: 130-142.
- Randazzo, A.F. & Bloom, J.I. (1985). Mineralogical changes along the freshwater/saltwater interface of a modern aquifer. *Sedimentary Geology* 43: 219-239.
- Randazzo, A.F. & Cook D.J. (1987). Characterization of dolomitic rocks from the coastal mixing zone of the Floridan aquifer, USA. *Sedimentary Geology* 54: 169-192.
- Richards, R. T., Troester, J.W. & Martínez, M.I. (1998). An electromagnetic geophysical survey of the freshwater lens of Isla de Mona, Puerto Rico. *Journal of Cave and Karst Studies* 60(2): 115-120.
- Richards, R. T., Troester, J.W. & Martínez, M.I. (1995). A comparison of electromagnetic techniques used in a reconnaissance of ground-water resources under the coastal plain of Isla de Mona, Puerto Rico. *The symposium on the Applications of Geophysics to Environmental and Engineering Problems (SAGEEP'95) Proceeding, Orlando, Florida*: 251-260.
- Ruiz, H.M. (1993). *Sedimentology and diagenesis of Isla de Mona, Puerto Rico*. MS thesis, University of Iowa: 86p.
- Smart, P.L., Dawans, J.M. & Whitaker, F. (1988). Carbonate dissolution in a modern mixing zone. *Nature* 335: 881-813.
- Stoessell, R.K., Ward, W.C., Ford, B.H. & Schuffert, J.D. (1989). Water chemistry and CaCO₃ dissolution in the saline part of an open-flow mixing zone, coastal Yucatan Peninsula, Mexico. *Geologic Society of America Bulletin* 101: 159-169.
- Stoessell, R.K., Moore, Y.H. & Coke, J.G. (1993). The occurrence and effect of sulfate reduction and sulfide oxidation on coastal limestone dissolution in Yucatan cenotes. *Ground Water* 31: 566-575.
- Vacher, H.L. (1978). Hydrogeology of Bermuda - Significance of an across-the-island variation in permeability. *Journal of Hydrology* 39: 207-226.
- Wallis, T.N., Vacher, H.L. & Stewart, M.T. (1991). Hydrogeology of freshwater lens beneath a holocene strandplain, Great Exuma, Bahamas. *Journal of Hydrology* 125: 93-109.
- Whitaker, F.F., Smart, P.L., Vahrenkamp, V.C., Nicholson, H. & Wogelius, R.A. (1994). Dolomitization by near-normal seawater? Field evidence from the Bahamas. *Special Publications of the International Association of Sedimentology* 21: 111-132.

AN ELECTROMAGNETIC GEOPHYSICAL SURVEY OF THE FRESHWATER LENS OF ISLA DE MONA, PUERTO RICO

RONALD T. RICHARDS AND JOSEPH W. TROESTER

U.S. Geological Survey, 651 Federal Dr., Suite 400-15, Guaynabo, Puerto Rico 00965

MYRNA I. MARTÍNEZ

*Department of Geosciences, The Pennsylvania State University, University Park, Pennsylvania 16802
Now at CSA Architects and Engineers, Mercantile Plaza, Mezzanine Suite, San Juan, Puerto Rico 00918*

An electromagnetic reconnaissance of the freshwater lens of Isla de Mona, Puerto Rico was conducted with both terrain conductivity (TC) and transient electromagnetic (TEM) surface geophysical techniques. These geophysical surveys were limited to the southern and western parts of the island because of problems with access and cultural metallic objects such as reinforced concrete roadways on the eastern part of the island. The geophysical data were supplemented with the location of a freshwater spring found by scuba divers at a depth of about 20 m below sea level along the northern coast of the island. The geophysical data suggest that the freshwater lens has a maximum thickness of 20 m in the southern half of the island. The freshwater lens is not thickest at the center of the island but nearer the southwestern edge in Quaternary deposits and the eastern edge of the island in the Tertiary carbonates. This finding indicates that the ground-water flow paths on Isla de Mona are not radially symmetrical from the center of the island to the ocean. The asymmetry of the freshwater lens indicates that the differences in hydraulic conductivity are a major factor in determining the shape of the freshwater lens. The porosity of the aquifer, as determined by the geophysical data is about 33%.

Isla de Mona is an uninhabited 55-km² island located between Puerto Rico and Hispaniola. The island consists of a nearly circular carbonate plateau that has been uplifted and is bounded by vertical cliffs that range from 40 to 80 m msl. A narrow 3 km² coastal plain abuts the plateau to the southwest (Fig. 1). Most of the island is composed of carbonate rocks, with little insoluble residue, of marine origin that were first considered to be Miocene (Kaye 1959; Briggs & Seiders 1972). The coastal plain attains an elevation of 10 m msl and is composed of Pleistocene to Holocene reef and beach deposits (Briggs & Seiders 1972; Taggart 1992).

The density difference between ocean water and freshwater is such that 41 volumes of freshwater have the same mass as 40 volumes of ocean water. The Ghyben-Herzberg principle, which assumes hydrostatic conditions (Vacher 1988), states that for each unit of elevation the water table is above sea level there will be 40 units of freshwater below sea level. The overall thickness of the freshwater lens is the sum of the part below sea level and the part above, but as 98% of the freshwater is below sea level, the contribution above sea level is frequently ignored.

The shape of the saline-freshwater interface is a sensitive measure of aquifer characteristics integrated over large areas (Vacher 1988). In the absence of pumping, the shape of the saline-freshwater interface is determined by the distribution of the ratio of recharge to hydraulic conductivity (Vacher 1988). If recharge is uniform and hydraulic conductivity is isotropic and homogeneous then the shape of the freshwater body floating on the saline water will be that of a lens, thin near the coast and thickening inland. Because of its shape, the freshwater

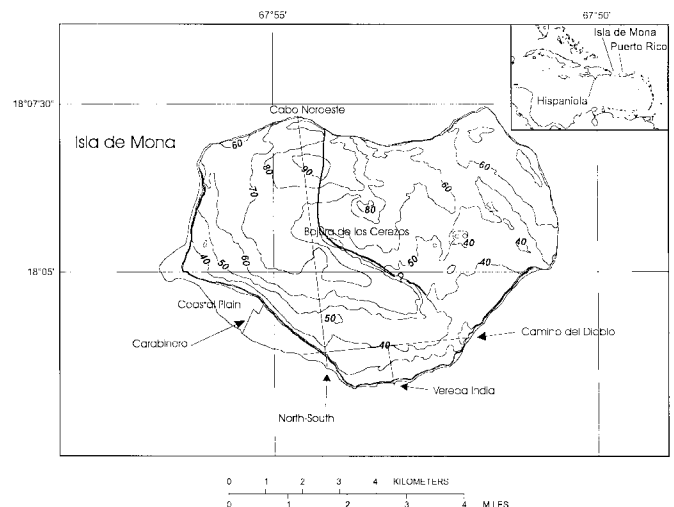


Figure 1. Location and topographic map of Isla de Mona, Puerto Rico. Elevations are in meters above sea level. The principal physiographic areas of the island are the coastal plain and the plateau, which includes the Bajura de los Cerezos and Cabo Noroeste. The four transects are Carabinero, Vereda India, Camino del Diablo, and North-South. The 10-, 20-, and 30- m contours are obscured at this scale because of their proximity to one another. The geologic fault mapped by Briggs and Seiders (1972) is shown as a heavy line.

part of an island aquifer is frequently referred to as a “lens.” If recharge and hydraulic conductivity are heterogeneous, then

the lens will be thicker where the recharge is greater or where the hydraulic conductivity is lower.

Information about the distribution of recharge and hydraulic conductivity in the aquifer can be inferred from studying either the water table or the saline-freshwater interface. According to the Ghyben-Herzberg principle, the two surfaces should mirror each other but with features magnified 40 times in the saline-freshwater interface. Regions of high hydraulic conductivity will have low gradients of hydraulic head. If this region is connected to the ocean, then the heads will be above sea level but lower than in other areas with lower hydraulic conductivity. Consequently, in the region of high hydraulic conductivity the saline-freshwater interface is relatively high.

Rocks saturated with saline water are more electrically conductive than rocks saturated with freshwater. Electromagnetic methods are sensitive to conductors so the saline-freshwater interface makes a good geophysical target. Limestone saturated with freshwater or air is resistive, so that the water table is a poor target for electromagnetic methods (Kauahikaua 1987).

By measuring the electrical conductivity of the earth as a function of depth, electromagnetic geophysics can map the relative thickness of the freshwater lens. The transition from freshwater to saline water in the aquifer is a zone of rapidly rising bulk electrical conductivity. Inversion of electromagnetic geophysical data usually locates this transition zone as a sharp interface without providing any information about its thickness (Kauahikaua 1987). An example of a study where TC data were used to map the thickness of the freshwater lens on a carbonate island and compared to the lens thickness as mapped from well data can be found in Wightman *et al.* (1990).

Current ground-water development on Isla de Mona consists of five hand-dug wells, one of which is occasionally pumped to provide water for showers and sanitary purposes. The deepest of the five hand-dug wells is 3 m deep with the water table at about 2.2 m below land surface. The electrical conductivity of the water in the five wells ranges from 240 to 1500 mS/m (1 mS/m = 10 μ S/cm). Cave divers have measured groundwater conductivities in subaqueous caves along the southeastern coast of the island ranging from 900 to 4000 mS/m (Richards *et al.* 1995).

Jordan (1973) calculated a water budget for Isla de Mona. Average rainfall is 810 mm/a and he estimates evapotranspiration to be 710 mm, which leaves an average of 100 mm/a available for runoff and to recharge the aquifer. By assuming a ground-water gradient similar to that of northern Puerto Rico, Jordan arrived at a hypothetical maximum thickness of the freshwater lens of 76 m. His map of the hypothetical freshwater lens assumes that hydraulic conductivity is isotropic and homogenous and, thus, the contours are concentric versions of the coastline.

A heavy rainfall event was observed in May 1992 when 230 mm of rain fell in 72 hours. Ponding occurred on large sections of the coastal plain and water was observed cascading

off the cliff face. Some of the water cascading off the cliff face would flow directly into the ocean while some could enter the aquifer on the coastal plain. A similar flood occurred in 1994 (Felix López, U.S. Fish and Wildlife Service, written communication 1997).

This study of the hydrogeology of Isla de Mona was conducted by the U.S. Geological Survey in cooperation with the Puerto Rico Department of Natural and Environmental Resources. As part of this study, electromagnetic surface geophysical data were collected to gain a better understanding of the shape of the freshwater lens on the island. Inferences about ground-water flow paths are then made based on the shape of the freshwater lens as defined by surface geophysics. The shape of the saline-freshwater interface under the coastal plain was described by Richards *et al.* (1995). The TEM data on the north-south transect of the plateau were published by Martínez *et al.* (1995). This report includes the TC data from the plateau as well as more data from divers. The effect of these additions is to give a much broader picture of the shape of the saline-freshwater lens under the plateau than was previously available.

METHODS

Both of the electromagnetic geophysical techniques used in this study use induction to measure the electrical conductivity of the earth as a function of depth. The TC technique is a frequency-domain system where the secondary magnetic field is measured by the receiver coil continuously as it is being induced by the transmitter coil. The TC equipment used in this study was the EM34-3 produced by Geonics Limited*. This instrument transmits at frequencies of 400, 1600, and 6400 Hz; the frequencies are coupled with coil spacings of 40, 20, and 10 m, respectively. At each coil spacing, a measurement is taken with the coils in vertical and horizontal orientations. This produces six data points with various depths of penetration. The dipole of the electromagnetic field produced by the coil is at right angles to that coil. A more complete description of the theory of the equipment can be found in McNeill (1980).

The TEM technique is a time-domain method in which a current in a transmitter loop is abruptly shut off and the collapse of the electromagnetic field around the transmitter loop induces a transient current in the ground. The TEM equipment used in this study was the EM47, produced by Geonics Limited. The receiver coil measures the time decay of this transient current. The induced current disperses outward with time and, thus, the information from later times is from deeper depths (Fitterman & Stewart 1986). In this study two transmitter loop sizes were used. On the coastal plain where the elevation of the land surface is less than 10 m, a 5 m by 5 m, 8-turn transmitter loop that has 200 m² of effective area was used. On the plateau where the elevation of the land surface ranges from 30 to 90 m msl, a 100 m by 100 m transmitter loop

*The use of brand names is for identification only and is not an endorsement by the U.S. Geological Survey.

was used. The larger loop takes considerably more time to set up but allows for greater penetration depths.

Each TEM data set consists of 20 readings of apparent conductivity at different times after current shut off and at each of two transmitter repetition frequencies: 285 and 30 Hz. By decreasing the transmitter repetition frequency, readings are taken at later times after the current is shut off, thus allowing the definition of a different section of the time-decay curve. The data from the two transmitter repetition frequencies overlap so the apparent conductivity is known at a total of only 30 different times. The TEM data collected in the field are the voltages in the receiver coil versus time that then are converted at the time of measurement to apparent resistivity (which is the reciprocal of apparent conductivity - the conductivity that the equipment would read if the earth were a homogenous half space). Each data set was repeated six times. The TEM data are examined to see if the curve of apparent resistivity versus time is smooth and that the six readings produced repeatable results. The theory behind this technique is described by Fitterman and Stewart (1986).

The TC and TEM techniques result in 6 and 30 apparent conductivities at each site, respectively. The greater data density gives the TEM better vertical resolution. The TC method, however, is much faster. TC readings can be collected in 5 to 8 minutes while the TEM requires about 45 minutes for the smaller loop.

The computer programs used to interpret the TC and TEM data were the EMIX34 and the TEMIX47, respectively, by Interpex Limited. The programs are similar in function and use the changes in apparent conductivity with depth to find a layered earth solution (Interpex 1988ab). The interpreter enters an initial geoelectric model. Through an iterative process, the program varies the thickness and electrical conductivity of each layer, but not the number of layers, until it finds a final geoelectric model that statistically best fits the data. Estimating the number of layers in the initial model and their values requires the use of geologic or hydrologic data. An example of using TC data and the EMIX34 program to measure the elevation of the saline-freshwater interface on a small oceanic island can be found in Anthony (1992). In this study, two-layer models were used to interpret the electromagnetic geophysical data. The upper layer represents the unsaturated zone and the freshwater-saturated zone whereas the lower layer represents the saline water-saturated zone. The thickness of the first layer represents the depth of the saline-freshwater interface below the land surface. The geoelectric modeling of electromagnetic geophysical data does not always result in unique solutions. The problem of non-unique solutions becomes more significant when the number of layers is increased.

No geophysical data were collected on the northern half of the island because it is inaccessible. The only evidence of the thickness of the freshwater lens on the northern half of the island is from reports by scuba divers. Freshwater discharges from submarine springs were encountered by divers while con-

ducting research on the Hawksbill turtle (*Eretmochelys imbricata*) that inhabits the waters around Isla de Mona. The index of refraction of water is a function of its salinity. The mixing of waters of different salinities produces a blurry area that can be visually identified by divers.

RESULTS

In May and September 1993, a total of 147 TC data sets were collected at 126 sites on the island; 123 on the coastal plain and 24 on the plateau. In July 1994, 21 TEM data sets were collected; 16 on the coastal plain and 5 on the plateau (Fig. 3) (Richards *et al.* 1995; Martínez *et al.* 1995). On the coastal plain most data, both TC and TEM, were collected on unpaved roads and the grass landing strip. On the plateau the TC data were collected along an unpaved road, the Camino del Diablo, and a trail, the Vereda India. The TEM data were collected along the trail to the Bajura de los Cerezos.

Table 1 shows the average interpreted conductivities of the two-layer geoelectric models that resulted from the inversion of the initial geoelectric models. First layer conductivities decreased dramatically between the coastal plain and the plateau.

Table 1. Average results of geoelectric models.

| | Coastal Plain | | Plateau | |
|---------|-----------------------------------|--------------------------|-------------------------|--------------------------|
| | Averaged Interpreted Conductivity | | | |
| | TC method in mS/m | TEM method in mS/m | TC method in mS/m | TEM method in mS/m |
| Layer 1 | 24 | 33 | 1.8 | 2.4 |
| Layer 2 | 540 | 480 | 430 | 610 |

At TC sites where measurements were repeated on different days the average difference of the interpreted thickness of the first layer was 24%. At the single TEM site where the measurement was repeated, the difference in the first layer thickness was 20%. All of the repeat measurements were done on the coastal plain.

The four cross sections in figure 2 show the elevation of the land surface and the interpreted position of the saline-freshwater interface. Note that for clarity, the vertical scales are different above and below sea level. In addition to the geophysical data, the north-south cross section includes data from turtle investigators. Between 1994 and 1996, they report that while diving they repeatedly found colder, fresher water entering the ocean at a number of sites with depths up to 20 m below the water surface. The deepest spring is at the base of a large boulder at Cabo Noroeste. No samples were taken and the exact salinity of this water is unknown (Robert Van Dam, written communication 1997).

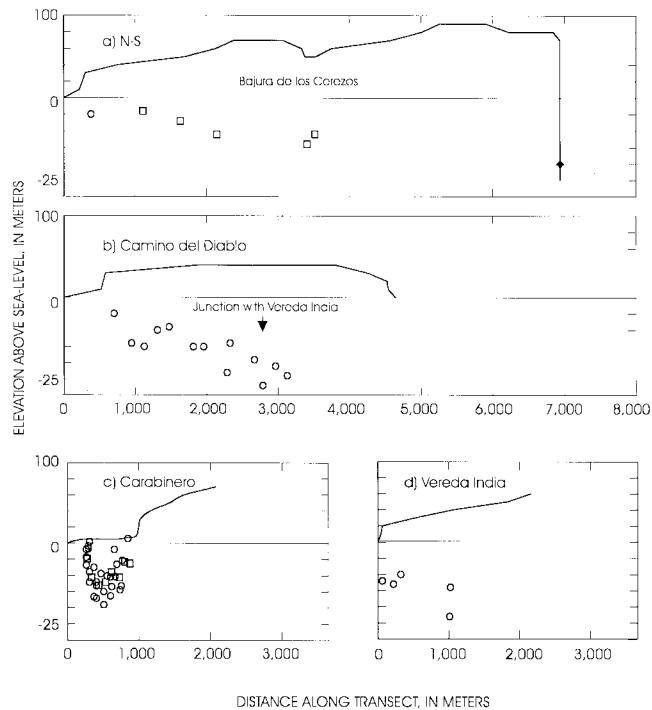


Figure 2. Elevation of the land surface and the interpreted elevation of the saline-freshwater interface at Isla de Mona, Puerto Rico along the transects indicated in figure 1. The four transects are A) North-South, B) Camino del Diablo, C) Carabinero, and D) Vereda India. Circles are terrain conductivity data, squares are transient electromagnetic data and the diamond is diving data. To show the saline-freshwater interface more clearly, the vertical scales are different above and below sea level. Vertical exaggeration of the land surface is 11:1. Vertical exaggeration of the saline-freshwater interface is 44:1.

The Carabinero transect includes both TC and TEM data. The interpreted elevation of the saline-freshwater interface is similar with both methods. The data on the Carabinero transect was collected over 14 months and there is no evidence that the thickness of the freshwater lens changed over this time.

The TC method has less vertical resolution than the TEM method so it is not surprising that the TC data appear noisier than the TEM data. On the plateau, the TC data on the Camino del Diablo are noisier than the TEM data on the north-south line. The speed of operation of the TC makes it practical to reduce noise problems by collecting more data.

The freshwater lens is thickest under the Camino del Diablo in the southeastern section of the plateau. The last six TC readings ranged from -14 to -27 m msl with an average of -21 m msl. By comparison the two TEM data points taken in Bajura de los Cerezos, which is at the center of the island, are -11 and -14 m msl. The elevation of the submarine spring at Cabo Noroeste is -20 m msl, a lower elevation than the elevations for a majority of the geophysical data.

DISCUSSION

In Table 1, the lower electrical conductivity of the first layer is probably due to the change in the ratio between the thickness of the unsaturated and saturated zones. In the center of the coastal plain the typical depth to saline water is about 15 m, of which about 5 m is unsaturated and about 10 m is saturated with freshwater. On the plateau the typical depths are about 50 m to saline water, of which about 40 m is unsaturated and about 10 m is saturated with freshwater. These estimates of the thicknesses of the unsaturated and freshwater saturated zones assume that the Ghyben-Herzberg principle applies.

In the absence of clay, the quantitative relationship between the electrical conductivity of a formation, the electrical conductivity of the pore fluid, and the porosity of the formation is given by the following equation:

$$c_f = c_w p^m$$

where c_f is the electrical conductivity of the formation, c_w is the electrical conductivity of the pore fluid, p is the porosity, and m is a factor that in unconsolidated material is a function of particle shape. In this study, m is assumed to be equal to two. This is a modified version of Archie's Law (McNeill 1990). Table 1 lists the interpreted electrical conductivities of the second layer of the geoelectric models. The electrical conductivity of the saline water in the lagoon at the northwest end of the coastal plain was measured at 4800 mS/m. If layer 2 is assumed to be saturated with a pore fluid with an electrical conductivity of 4800 mS/m, then the interpreted porosities of the formation ranges from 30-36% with an average of 33%.

The Ghyben-Herzberg principle allows us to infer the shape of the water table from knowledge of the elevation of the saline-freshwater interface. On the southern and western parts of the island, the elevation of the water table of Isla de Mona is less than 1 m.

Assuming that there is an inverse relation between the elevations of the saline-freshwater interface and the water table when the saline-freshwater interface is at lower elevation, the water table must be at higher elevation in the same location. A minimum in the saline-freshwater elevation is a maximum in the water table, which is a ground-water divide. The geophysical data in this paper define three ground-water divides on Isla de Mona. They are the coastal plain, the northern half of the island between Bajura de los Cerezos and Cabo Noroeste, and the eastern half of the Camino del Diablo.

The divide on the coastal plain is documented on both sides with both TC and TEM data. From the center of the coastal plain, flow is radially outward with some flow paths that flow towards the plateau and then parallel to the coastline for a considerable distance before the water enters the ocean (Fig. 2c).

At the submarine spring at Cabo Noroeste, there is northward flowing water 20 m below sea level. The salinity of this water is unknown and the spring may be discharging from the

transition zone. At the Bajura de los Cerezos, the elevation of the saline-freshwater interface is no more than -14 m msl, the groundwater cannot flow towards a spring at deeper depth and must flow in the other direction, probably to the south or west (Fig. 2a).

On the Camino del Diablo, we have no information about the eastern limb of the saline-freshwater interface (Fig. 2b). The data from the Camino del Diablo and Vereda India indicate flow to the south or west. It is not logical to assume that this continues to the eastern shore of the island. At some point it must have an easterly component but exactly where cannot be determined. The saline-freshwater interface is not symmetrical and the divide is much closer to the eastern than the western side of the island. There are not enough data to determine if the northern divide is continuous with the eastern divide or not.

The shape of the freshwater lens is neither symmetrical nor a smoothed version of the coastline (Fig. 3). This indicates that the distribution of the ratio of recharge to hydraulic conductivity is not homogenous. Long-term rainfall data from Isla de Mona are available from only one location and it is not known if rainfall differs significantly across the island (Jordan 1973). The plateau has only broad, shallow relief, and it is not known if the plateau generates an orographic effect.

Using groundwater models, Vacher (1988) shows that the shape of a hypothetical freshwater lens is more sensitive to realistic changes in hydraulic conductivity than to recharge. Large changes in hydraulic conductivity are more likely than large changes in recharge. In a karst environment, it is reason-

able for hydraulic conductivity to vary over several orders of magnitude. The hydraulic conductivity of the carbonate rocks on Bermuda varies over four orders of magnitude (Vacher 1989). The zones of high hydraulic conductivity that are acting as drains to the aquifer could be large cave systems or they could consist of small but well connected tubes or fractures.

At the contact between the plateau and the coastal plain, the direction of the ground-water flow from the plateau changes and groundwater diverts around the coastal plain. Somewhere in the area of the contact between the coastal plain and the plateau there must be an area of relatively high hydraulic conductivity that drains water from the center of the island and diverts it around the coastal plain. Three possible causes for this drainage pattern include; (1) there could be a flank margin cave along the contact; or (2) the younger rocks of the coastal plain could have lower hydraulic conductivity; or (3) there could be structural reasons that cause hydraulic conductivity to be anisotropic and higher to the northwest and southeast than to the southwest. Some evidence supports all three of these hypotheses. A small, presumably flank margin, cave was found by at the contact between the plateau and the coastal plain while the authors were collecting geophysical data. The cave did not appear to reach the water table but it was not fully explored due to a lack of time. In the Bahamas and Bermuda, the increase in hydraulic conductivity with age has been documented (Vacher 1989). The last possibility is supported by a number of structural features that run from northwest to southeast; the contact between the coastal plain and the plateau, the Bajura de los Cerezos, and numerous pits on the trail to the Bajura de los Cerezos show elongation in a northwest-southeast direction (Frank *et al.* 1998).

The flow of groundwater on the plateau is to the south and west. The dip of the rocks is also to the southwest and this may be influencing the direction of flow. The spring at Cabo Noroeste is near a mapped fault (Briggs & Seiders 1972), and there may be a zone of high hydraulic conductivity along the fault.

CONCLUSIONS

TC and TEM geophysical methods were used to map the shape of the saline-freshwater interface on Isla de Mona. Data from scuba divers provide information from a part of the aquifer that was not studied by surface geophysics. Interpretation of the surface geophysical data gives a conceptual model of the freshwater lens of Isla de Mona. By establishing probable flow paths and depths to saline water, the model developed gives insights that can guide other data-collection activities. The surface geophysical data indicate that the maximum thickness of the freshwater lens is 20 m on the eastern edge of the plateau. In the center of the island the freshwater lens is no more than 14 m thick and 10 m thick on the coastal plain. Divers found water of unknown salinity discharging into the ocean at -20 m msl on the northern half of the island where it was impossible to collect geophysical data.

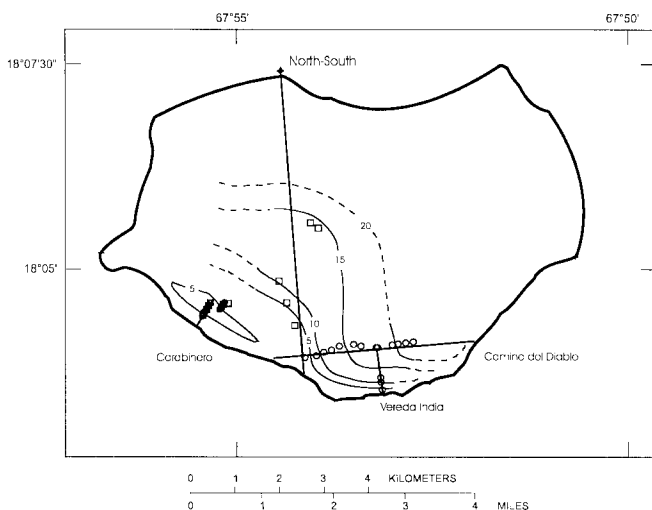


Figure 3. Elevation of the saline-freshwater interface as interpreted from geophysical and diving data, dashed where approximate, Isla de Mona, Puerto Rico. Elevations are in meters below mean sea level. Interval between contour lines is 5 m. The 5 m contour on the coastal plain is drawn based on more data than are shown here. Circles are terrain conductivity data, squares are transient electromagnetic, and the diamond is diving data.

The asymmetrical shape of the freshwater lens indicates that hydraulic conductivity is heterogenous. Groundwater tends to flow around the coastal plain. There probably is a contrast in hydraulic conductivity between the relatively low coastal plain and the higher conductivity under the plateau. The exact form of this contrast cannot be determined.

REFERENCES

- Anthony, S.S. (1992). Electromagnetic methods for mapping freshwater lenses on Micronesian atoll islands. *Journal of Hydrology* 137: 99-111.
- Briggs, R.P. & Seiders, V.M. (1972). Geologic map of the Isla de Mona quadrangle, Puerto Rico. *U.S. Geological Survey Miscellaneous Geologic Investigations Map I-718, scale 1:20,000*.
- Fitterman, D.V. & Stewart, M.T. (1986). Transient electromagnetic sounding for groundwater: *Geophysics* 51: 905-1005.
- Frank, E.F., Mylroie, J.E., Troester, J.W., Alexander, Jr., E.C. & Carew, J.L. (1998). Karst development and speleogenesis, Isla de Mona, Puerto Rico. *Journal of Cave and Karst Studies* 60(2): 73-83.
- Interpex Limited, (1988a). *EMIX34 Users Manual*: 97 p.
- Interpex Limited, (1988a). *TEMIX-G Users Manual*: 128 p.
- Jordan, D.G. (1973). A summary of actual and potential water resources of Isla de Mona, Puerto Rico. *Junta de Calidad Ambiental, las islas de Mona y Monito: Una evaluación de sus recursos e históricos*: D1-D8.
- Kauahikaua, J. (1987). Description of a freshwater lens at Laura Island, Majuro Atoll, Republic of the Marshall Islands using electromagnetic profiling. *U.S. Geological Survey Open-File Report 87-582*: 32 p.
- Kaye, C.A. (1959). Geology of Isla de Mona, Puerto Rico, and notes on the age of the Mona Passage. *U.S. Geological Survey Professional Paper 317C*: 141-178.
- Martínez, M.I., Troester, J.W. & Richards, R.T. (1995). Electromagnetic surface geophysical exploration of the ground-water resources of Isla de Mona, Puerto Rico: A Caribbean carbonate island. *Carbonates and Evaporites* 10(2): 184-192.
- McNeill, J.D. (1980). Electromagnetic terrain conductivity measurement at low induction numbers. *Geonics Limited*: 15 p.
- McNeill, J.D. (1990). Use of electromagnetic methods for ground-water studies. In Ward, S.H. (ed.). *Geotechnical and Environmental Geophysics v. 2 Environmental and Groundwater, Society of Exploration Geophysics*: 191-217.
- Richards, R.T., Troester, J.W. & Martínez, M.I. (1995). A comparison of electromagnetic techniques used in a reconnaissance of the ground-water resources under the coastal plain of Isla de Mona, Puerto Rico. *The Symposium on the Applications of Geophysics to Environmental and Engineering Problems (SAGEEP'95) Proceedings*, Orlando, Florida: 251-260.
- Ruiz, H.M. (1993). *Sedimentology and diagenesis of Isla de Mona, Puerto Rico*. MS thesis, University of Iowa, Iowa City, Iowa: 86p.
- Taggart, B.E. (1992). *Tectonic and eustatic correlations of radiometrically dated marine terraces in northwestern Puerto Rico and Isla de Mona*. PhD dissertation, University of Puerto Rico, Mayagez, Puerto Rico: 252 p.
- Vacher, H.L. (1988). Dupuit-Ghyben-Herzberg analysis of strip-islands. *Geological Society of America Bulletin* 100: 580-591.
- Vacher, H.L. & Bengtsson, T.O. (1989). Effect of hydraulic conductivity on the residence time of meteoric groundwater in Bermudian- and Bahamian-type islands. *Proceedings of the 4th Symposium on the Geology of the Bahamas, San Salvador, Bahamas, Bahamian Field Station*: 337-351.
- Wightman, M.J., Stewart, M.T. & Vacher, H.L. (1990). Geophysical mapping and hydrogeologic analysis of fresh-water lenses at Big Pine Key, Florida. *Proceedings of the International Symposium on Tropical Hydrology, San Juan, Puerto Rico*: 301-309.

HISTORY OF THE GUANO MINING INDUSTRY, ISLA DE MONA, PUERTO RICO

EDWARD F. FRANK

Department of Geology and Geophysics, University of Minnesota, Minneapolis, MN 55455 USA

Isla de Mona, Puerto Rico is ringed by hundreds of flank margin caves (Frank 1993; Mylroie et al. 1995). In the late 1800s and early 1900s, ~150,000 metric tons of phosphorite, altered bat guano, were mined from the caves. A high phosphate content made the phosphorite a valuable fertilizer (Wadsworth 1973). Briggs (1974) indicates the guano deposits have been exhausted from seven of the eight largest known cave systems on the island. Many relics from the guano mining days are still present in the caves and surrounding areas today.

In the mid-1800s, guano deposits in the caves on Isla de Mona were viewed as important economic resources. Numerous applications for exploitation had been received by the Spanish government by 1854. In 1856, two American vessels illegally loaded guano from the island. In response, the Puerto Rico Governor sent the warship, Bazan, to investigate the island later that year. The Bazan returned several times in the next two years, collected samples of guano, Taino Indian relics, and mapped the island, including 17 caves [maps are lost] (Wadsworth 1973). Two concessions granted in the 1870s to mine guano lapsed unused. It was not until the third concession, given in 1877 to Miguel Porrata Doria of Fajaro, Puerto Rico and Juan Contreras Martinez of Spain, that the first legal guano extraction from the island took place. The

mining headquarters set up near Cueva de Pájaros (Vasconi y Vasconi 1883) included facilities for sun drying, screening, and processing over 100 metric tons per day (Fig. 1 & 2). The guano was dug with picks, bars, and shovels and transported in wheel barrows to the processing areas. In the largest caves, tramcars on rails were also used. From cave mouths directly above water, such as in Cueva del Lirio, guano was lowered by basket to waiting ships and transported to Playa de Pájaros for processing. The major part of the first mining operation was completed by 1884 with Cueva de Pájaros nearly worked out.

A second mining venture began in 1890 when Anton Mobins of Germany subleased the mining rights. During this period all but the most remote caves on the north coast of the island were mined. These were the first operations to reach the

Figure 1.
Panorama of
the guano
processing
facilities at
Playa Pájaros
(from Vasconi
y Vasconi,
1883).

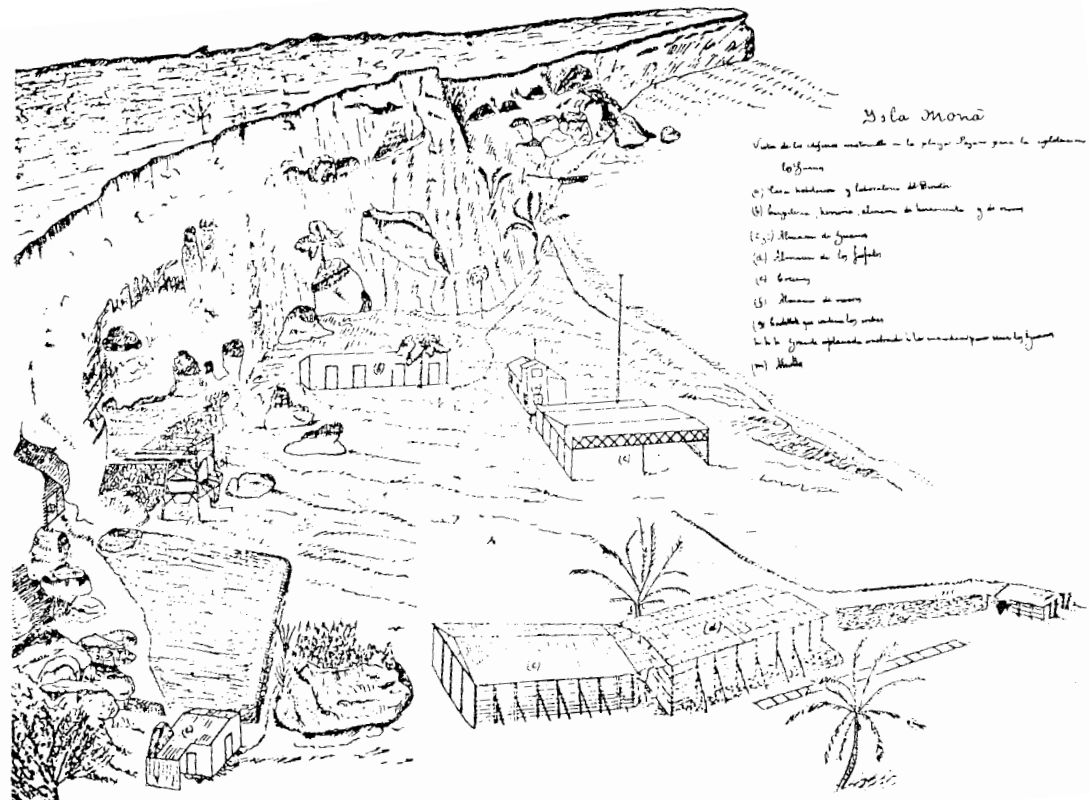
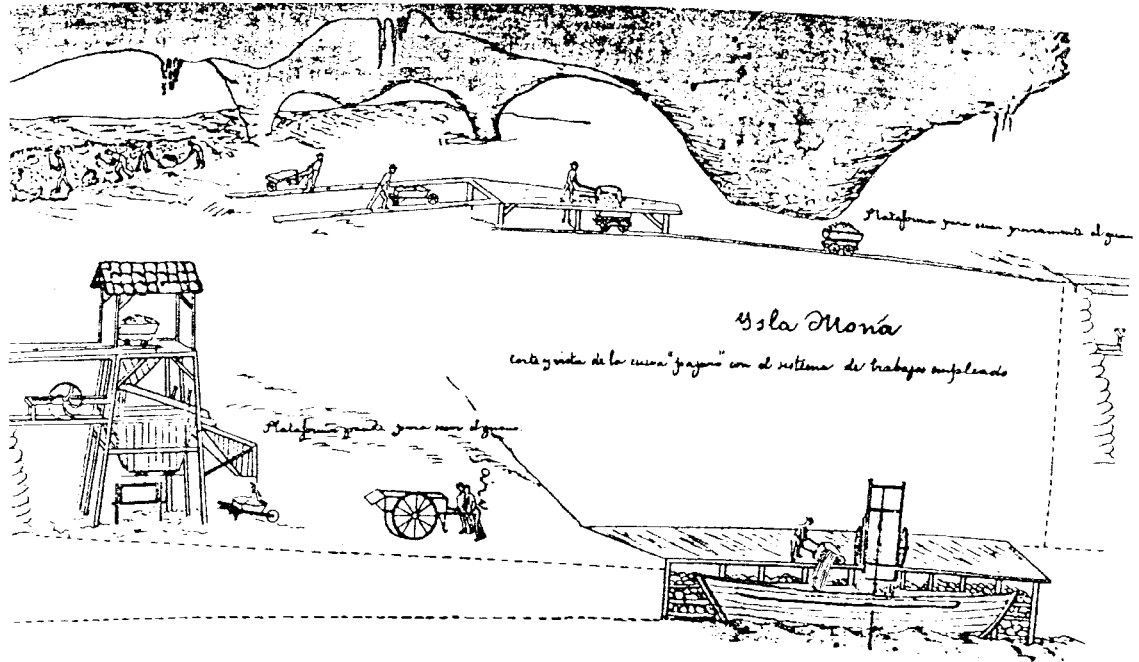


Figure 2. Diagram of the mining operation within Cueva de los Pájaros. The upper side of the figure wraps to the lower left side of the diagram (from Vasconi y Vasconi 1883).



west side of the island. Captain Kuhfal (Kuhfal 1892) of the ship *General Contreras* describes the mining in his log and provides a contemporaneous map of the island (Fig. 3). Briggs (1974: 87-88) translates freely the following passage from that log:

The removal of the guano from the caves is accomplished easily. The entrance to the cave to be exploited is enlarged and where necessary, supported. Gangways or paths are prepared, and frequently tracks are laid down. The guano, which is commonly found in layers thicker than a meter, frequently also must be freed from the underlying rock by blasting. It is then shoveled into pushcarts or tramcars and taken to the cave exit where it is poured through screens into tramcars waiting beneath. These carry the guano to drying ovens. Following drying in the ovens, the guano goes through a mixing mill which produces an homogeneous guano mixture. A small part of the guano is dried in the sun and then mixed. Guano thus prepared for shipping has a very low moisture content. The guano then is put in sacks and loaded onto lighters which are pulled by a small tugboat to ships lying in the roadstead. The lighters hold 5 to 6 tons, and they can deliver as much as 120 tons on board each day. For the working of the guano of the island, aside from large machines and horses, there are 300 to 400 workers busy daily. Supervision is in the hands of Germans stationed there.

Wadsworth (1973: N-10) states, "Loading was a precarious operation. Ships lay anchored or moored to buoys and exposed to the open sea just outside the reef off Playa Pájaros. Using 5 to 8 men from ashore as well as the ship's crews, loading

required up to a month, even in favorable weather." To resolve some of the ship loading problems (Wadsworth 1973: N-12), "The reefs at Playa Pájaros were blasted out to facilitate lightering to ships anchored outside. During the period 1890-92 at least 30 ships were loaded in this way. In rough weather not only was lightering impossible but at times the ships were

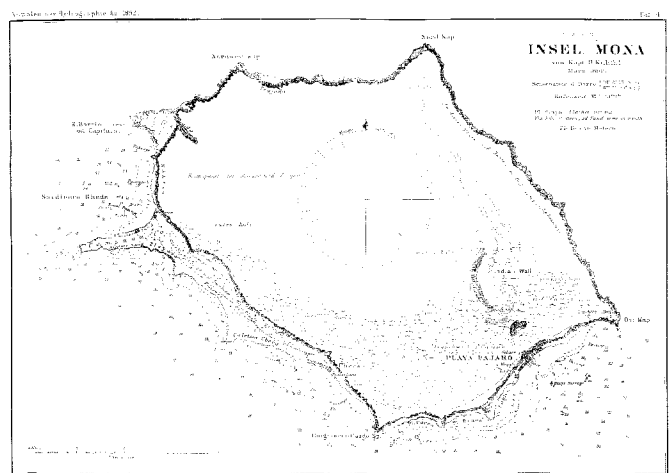


Figure 3. Map of Isla de Mona by Kuhfal (1892). The map is distorted but major topographic features of the island are depicted. The text in the southern portion of the mesa indicates brush, cactus, and good lumber. At Playa Pájaros: the word Schornst refers to a skylight in the cave, while Magazin refers to a storage facility. Also the location marked as Lirio is at the entrance to the cave known today as Cueva de los Pájaros. Cañada marked just north of K. Barrio Nuevo corresponds to the location of Cueva de Esperanza.

forced to put to sea, and both ships and lighters were lost.”

Kaye (1959: 156) provides a less idyllic assessment of the mining operation based upon the nature of the deposits, remains of equipment, and workings still visible in the cave:

The deposits were probably worked by painstaking hand labor. The pockets of phosphorite on the floor of the cave had to be felt out through the dripstone crust, presumably by prodding with picks. The dripstone crust was then stripped and the underlying pockets of ore excavated by hand. Much digging was done in close quarters, where men must have felt their way along bent nearly double beneath the low roof. From the litter of narrow-necked bottles in many caves it is evident that the mining lamps consisted of bottles of kerosene provided with thick wicks.

A single-track line was laid along the main trunk chambers of the cave. Ore was probably hauled from the diggings to the rail line by hand, either in sacks or by drags. The ore was then hauled by rail to the mouth of the caves, where there are signs it was temporarily stockpiled. The ruins of what resembled a small drying plant at Playa Pajaro, and it seems evident that some of the ore was thus treated.

The gathering of the ore from many caves probably presented a particularly difficult problem and apparently was done by various means, depending on the location and setting of the cave. In some places wagons were used, in others rail; and in some caves, such as Cueva del Gato at Cabo Barrionuevo [likely Cueva de Esperanza as located on Briggs & Seiders 1972], ore was loaded directly onto ships precariously tied up against the unprotected sea cliffs. The rusted remains of several rail lines associated with the mining are to be seen today around the island. There were signs of exploration and some mining in all of the caves visited by the writer, and it is probable that most of the caves on the island have been explored to some degree.

The island came under United States sovereignty in 1899. In 1903, all of the island except for the 235-acre lighthouse reservation was transferred to the Government of Puerto Rico. At that time, the Porrata-Doria guano mining concession was terminated and a new 40 year franchise was granted to Percy Saint. This was in turn transferred in 1904 to the Mona Island Phosphate Company, Limited, Louisiana, of which Saint was Vice President and General Manager (U.S. Congress 1906). The last commercial guano extraction took place from 1909 until 1927. The estimated total guano shipped from Isla de Mona was: 1877-1889: ~31,410 metric tons; 1890-1899: ~113,493 metric tons; 1900-1927: ~3,000 metric tons (Wadsworth 1973). Minor amounts of guano were also reported to have been extracted from a cave on Isla Monito, but no

specific figures are available (Wadsworth 1973).

PRESENT STATUS OF GUANO MINING ARTIFACTS

Evidence of the guano mining could be seen on the island from 1992 through 1996. The pervasiveness of the guano mining on the island is a striking characteristic. Every moderate to large cave examined from Cueva del Lirio on the eastern corner of the island around the cliffs clockwise to Cueva de Esperanza on the northwestern corner of the island showed evidence of guano mining. A large percentage of the smaller caves in this area had also been actively mined or contained test pits in the guano deposits.

Trails constructed by the miners to facilitate guano removal are prominent in these caves. Typically, a low gradient rail bed for mine carts extends the length of a cave. A series of side spurs feed into this main pathway. Cuts dug through higher areas of the floor and raised rock rail beds built in low areas maintain a low gradient. These raised rail beds average a meter wide and were carefully constructed with obvious effort to maintain a continuous surface along their length (Fig. 4). Rail impressions are commonly seen in the surface of these beds. Most of the rails have been removed from the caves. The only rail found in place is a segment in Cueva del Lirio. A handful of individual sections of rail, 0.5 m wide and four meters long are in several other caves unattached to the floor (Fig. 5). Badly rusted remains of mine carts can be found in Cueva del Lirio (Fig. 6) and Cueva de los Pájaros. These appear to have deteriorated beyond any hope of preservation.

On the surface near Cueva de Esperanza, a short section of rail leads to the cliff edge where apparently guano was lowered down the cliff face. Several other pieces of mechanical equipment are on a raised stone platform adjacent to this track. This equipment includes several pulleys, metal cable, braking devices, and what may be pieces of a steam driven winch (Fig. 7).



Figure 4. Raised rail beds found in Cueva de Aleman.



Figure 5. A segment of mine track found alongside of the trail in Cueva del Diamante.



Figure 6. Rusting remains of a mine cart found in Cueva del Lirio.

Along the southern coast of the island a surface roadbed runs from Cueva de Playa Brava to Cueva de Pozo Erickson passes several mined caves. This road is ~1.5 to 2 m wide and made of carefully laid local stone (Fig. 8). A similar appearing feature, remains of a rail line used to supply the El Faro lighthouse, is unrelated to guano mining.

There are also several structures in the area below Cueva de Aleman. One is the foundation of a ranch that raised cattle to help feed the miners in the early 1900s. Just east of this foun-



Figure 7. Miscellaneous equipment related to mining found on the mesata surface near Cueva de Esperanza. Items include pulleys, some wire cable, a braking mechanism, and miscellaneous strapping on a rock platform. Guano was lowered down the vertical, 60 m cliff face to ships waiting below.



Figure 8. Rock roadbed running along the southern coast of the island between Punta Ingleses and Cueva de Playa Brava.

ation is a large hollow boulder, a fragment of the cave fallen from the cliff (Fig. 9). Remains of a brick doorframe can be seen around a 1.2 m high entrance into the chamber within the boulder. This chamber may have been used as an explosive storage shed during the mining operation (José Jimenez, verbal communication 1996).

Other items related to the mining operations include a ladder inside one of the entrances to Cueva de los Pájaros and a wooden wheelbarrow inside of Bat Cave (Fig. 10). The guano mining period represents an significant episode in the history of the region. If efforts are not made to preserve historical items and localities representing the mining activities, the arti-



Figure 9. Hollow boulder and remains of a brick doorway on the coastal plain below Cueva de Aleman. This may have been used as an explosive storage facility during the mining operation.

facts will decompose or be removed. At the present time because of funding and personnel limitations, the Puerto Rico Department of Natural and Environmental Resources has only limited resources available to pursue the preservation effort.

ACKNOWLEDGMENTS

I thank the Cave Research Foundation, the University of Minnesota's Department of Geology and Geophysics, and their George and Orpha Gibson Endowment in hydrogeology for financial assistance in conducting field work on Isla de Mona and laboratory processing of samples collected from the island. Individually, I would like to thank John Mylroie, E. Calvin Alexander, Jr., Susan Magdalene, and Robert Frank for their field assistance on Isla de Mona.



Figure 10. Wooden wheelbarrow from the guano mining operations found in Bat Cave.

REFERENCES

- Briggs, R.P. (1974). Economic geology of the Isla de Mona quadrangle, Puerto Rico. *U.S. Geological Survey, Open File Report 74-226*: 116 p.
- Briggs, R.P. & Seiders, V.M. (1972). Geologic map of the Isla de Mona quadrangle, Puerto Rico. *U.S. Geological Survey, Miscellaneous Geological Investigations, Map I-718*.
- Frank, E.F. (1993). *Aspects of karst development and speleogenesis Isla de Mona Puerto Rico: an analogue for Pleistocene speleogenesis in the Bahamas*. MS Thesis, Mississippi State University: 349 p.
- Junta de Calidad Ambiental. (1973). *Las Islas de Mona y Monito: Una evaluacion de sus recursos naturales e historicos*. San Juan, Puerto Rico, Oficina del Gobernador, 2 vol.
- Kaye, C.A. (1959). Geology of Isla Mona, Puerto Rico, and notes on the age of the Mona Passage: *U.S. Geological Survey, Professional Paper 317C*: 141-178.
- Kufal, O. (1892). Mona-Insel, Westindien. *Annalen der Hydrographie und Maritimen Meteorologie* 20: 303-305.
- Mylroie, J.E., Panuska, B.C., Carew, J.L., Frank, E.F., Taggart, B.E., Troester, J.W. & Carrasquillo, R. (1995). Development of flank margin caves on San Salvador Island, Bahamas and Isla de Mona, Puerto Rico. In Boardman, M. (ed.) *Proceedings of the seventh symposium on the geology of the Bahamas, June 16-20, 1994*, Bahamian Field Station, San Salvador, Bahamas: 49-81.
- U.S. Congress (1906). Ordinances of the Executive Council of Porto Rico: January 22, 1906, 59th Congress, 1st Session, *U.S. Senate, Document 159, Serial 4912*: 7-9.
- Vasconi y Vasconi, A. (1883). Resena de las Islas Mona y Monito (June 18). *San Juan, Archivos Generales de Puerto Rico, Obras Publicas, propiedad publica, Mona y Monito*, Legajo No. 84A: 22 p.
- Wadsworth, F.W. (1973). The historical resources of Mona Island, Appendix N. In Junta de Calidad Ambiental, *Las Islas de Mona y Monito: Una evaluacion de sus recursos naturales e historicos, volume 2*: N1-N37.

CAVE SCIENCE NEWS

WORLD'S DEEPEST KARST HYDROLOGIC SYSTEM EXTENDED

A U.S. team led by Bill Stone extended the proven relief of the world's deepest known karst hydrologic system to 2540 m in January 1997. Using standard scuba equipment, the team reached 33 m below the Agua Fria surface level in the Santo Domingo Canyon. Agua Fria is the proven resurgence of Sistema Cheve. The highest entrance to the system is Cueva Escondida at 2798 m msl. The deepest point reached by the divers was 258 m msl. Stone reports that the submerged passage extended at least 8 m deeper but was not explored in order to avoid decompression and, hence, additional use of precious compressed air supplies in the remote region of Oaxaca, Mexico.

Presently, the explored portion of the upper Cheve system is 25.5 km long and -1386 m deep. The physically unconnected but proven lower extension of the hydrologic system, Cueva del Mano, has a surveyed length of 9.5 km and relief of about 120 m. Agua Fria is the resurgence spring physically connected to Cueva del Mano.

SCIENTISTS ESTABLISH AGE OF CARLSBAD CAVERN

For the first time, scientists have established the age of Carlsbad Cavern, a spectacular natural limestone cave that is a national park in eastern New Mexico.

The cave is 3.9 to 4 million years old and was carved out of ancient limestone by the slow drip of water enriched with sulfuric acid, geologist Victor Polyak said. A report on the study was published in the journal *Science*. Polyak said he and his colleagues were able to establish when the Carlsbad Caverns were carved by age-dating alunite, a clay mineral formed as acidic water cuts its way through the limestone.

Formation of Carlsbad and other nearby limestone caves occurred as the Guadalupe Mountains, a spur of the Rocky Mountains in New Mexico and far western Texas, were lifted up. Starting about 12 million years ago, said Polyak, the water table dropped in the limestone formation, possibly due to the mountains rising. The retreating water dissolved away the soluble rock and formed the underground cavities, some of which stretch for miles.

Hydrocarbons, such as oil and gas, probably provided the chemistry needed to dissolve the limestone and make the caves, said Polyak. The oil and gas, he said, migrated from deep beneath the Earth and collected under a cap of stone. Bacteria invaded the reservoir and fed on the oil and gas, he added. A byproduct from this was hydrogen sulfide gas which was chemically changed into sulfuric acid dissolved in the groundwater. As this acid mixture trickled through the limestone, it cut away cavities that grew and grew over millions of years, Polyak said.

ENTRY-LEVEL POSITION FOR A KARST SPECIALIST

The Oak Ridge, Tennessee office of P.E. LaMoreaux & Associates, Inc. (PELA) is seeking a geologist to fill an ENTRY-LEVEL POSITION. PELA's Oak Ridge office specializes in environmental and geotechnical consulting in karst areas. Applicants should have a B.S. in geology or a related subject. The ideal applicant will combine a solid background in karst geology and hydrology, geophysics, caving, and general FIELD WORK with excellent com-

puter and writing skills. Extensive periods of travel will be required, including occasional weekend work. The position will involve field work ranging from physically strenuous labor to the performance of mundane tasks. Office work will consist of computer-based data analysis and assistance with report and proposal preparation. The applicant should be a "team player" with the ability to work independently.

Correspondence should be directed to: Dr. Barry F. Beck, Chief of Operations; P.E. LaMoreaux & Associates, Inc.; 106 Administration Road; Oak Ridge, TN 37830; (423) 483-7483; (423) 483-7639 (fax); pelaor@usit.net.

PELA is an equal-opportunity employer.

SEVENTH MULTIDISCIPLINARY CONFERENCE ON SINKHOLES AND THE ENGINEERING AND ENVIRONMENTAL IMPACTS OF KARST with an INTRODUCTORY COURSE ON THE PRACTICAL ASPECTS OF KARST HYDROGEOLOGY

Announcement and Call for Papers

Harrisburg, Pennsylvania, April 10-14, 1999

Abstracts Due: August 21, 1998

Papers Due: December 11, 1998

Keynote Speech by Dr. William B. White

Short Course on Saturday - April 10, 1999

Field Trip on Sunday - April 11, 1999

Technical Sessions on Monday through Wednesday - April 12-14, 1999.

Papers on all practical aspects of karst geology, hydrogeology and engineering geology are solicited.

For further information contact:

Ms. Gayle Herring, P.E. LaMoreaux and Associates, Inc., 106 Administration Rd., Oak Ridge, Tennessee 37830

T: 423-483-7483 F: 423-483-7639

E-mail: pelaor@usit.net

or see the conference website at:

<http://www.uakron.edu/geology/karstwaters/7th.html>

Sponsors and Cosponsors for coffee breaks and other events are solicited.

1999 CONFERENCE ON THE HYDROLOGY OF THE BLACK HILLS

Announcement and Call for Papers

Rapid City, South Dakota, September 15-16, 1999

Abstracts Due: March 1, 1999

Papers Due: July 15, 1999

The Conference on the Hydrology of the Black Hills will be held in Rapid City, South Dakota; gateway to the Black Hills. The Black Hills area includes Wind Cave National Park, Jewel Cave National Monument, Badlands National Park, Devils Tower National Monument, and Mt. Rushmore National Memorial.

The conference will focus on topics related to the hydrology of the Black Hills area. The Black Hills are an important source of recharge to major regional aquifers, including the Madison,

Minnelusa, and Inyan Kara aquifers. Mining is an important component of the local economy, and large mines, including the Homestake Gold Mine, are located on the Precambrian core of the Black Hills. The majority of the Black Hills are National Forest, and forestry practices affect the Black Hills hydrology. Flooding, such as the 1972 flood which destroyed parts of Rapid City, strongly affects the location and distribution of population growth in the Black Hills. Projected population growth over the next 20 years for the Black Hills, especially in the Rapid City and Spearfish areas, may place significant stresses on water resources. A proceedings will be published and presented to all participants. Persons with accepted abstracts will supply a 10-page (maximum) paper, including figures, by July 15, 1999.

The conference focus is on the Black Hills region, but papers of a general knowledge on related issues, such as karst hydrology, GIS and digital issues, and mining effects on water quality, are welcome.

The conference will cover the topics:

- Abandoned mines, current mines, and water quality
- Forestry related to water quality
- Aquifer vulnerability and contaminants

- Black Hills Hydrology Study (long-term USGS study)
- GIS and digital issues
- Geomorphology and surficial processes
- Coupling of surface water and atmospheric sciences: groundwater and evapotranspiration.
- Streamflow and groundwater recharge to aquifers
- Hydrogeology
- Water supply, resources, and management
- Modeling of groundwater and surface water hazards (flooding, subsidence, slope stability)
- Karst hydrology
- Geochemistry

Conference Organizational Chairs:

Dr. Arden Davis, South Dakota School of Mines and Technology; Mr. J. Foster Sawyer, South Dakota Department of Environment and Natural Resources; Dr. Michael Strobel, U.S. Geological Survey, Water Resources Division

Please send abstracts to Dr. Michael Strobel, USGS, 1608 Mountain View Road, Rapid City, SD 57702

Darrell Armentrout works in shipboard seismic exploration in the Gulf of Mexico and is an avid recreational caver. In his "spare time," Darrell is writing his MS thesis at Mississippi State University.

Dan-Luca Danielopol is a research assistant at the Institute of Limnology, Austrian Academy of Sciences and a professor teaching zoology and groundwater ecology at the University of Vienna, where he also received his PhD in 1976. He worked with the Speleological Institute "E.G. Racovitza, in Romania, and the Laboratoire Souterrain du C.N.R.S. in France. With J. Gibert and J. Stanford, he edited the 1994 book, *Groundwater Ecology* (Academic Press).

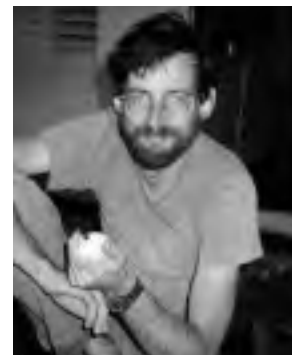


Edward Frank is currently a PhD candidate at the University of Minnesota, Department of Geology and Geophysics. He earned his MS in geology at Mississippi State University in 1993. He has worked in the coal mining industry and as a member of the research faculty at the University of Central Florida's Sinkhole Research Institute.

Myrna Martinez holds a Bachelors degree in Environmental Sciences from the University of Puerto Rico and a Masters Degree in Hydrogeology from Ohio University. Her research on Isla de Mona was for her PhD dissertation at the Pennsylvania State University and was in collaboration with the U.S. Geological Survey.



Donald A. McFarlane is an Associate Professor of Biology at Scripps College, California, and a Research Associate in the Department of Mammalogy, American Museum of Natural History. He has been caving since 1973. For the past 11 years his research has focused on extinct mammals preserved in the caves of the West Indies.



Dr. John Mylroie is Professor of Geology at Mississippi State University. John's primary research interests lie in cave and karst investigations in a variety of geological settings. Additionally, he studies carbonate island geology. Dr. Mylroie has led annual winter field trips to San Salvador Island, Bahamas for some 20 years.



Bruce Panuska is an Associate Professor at Mississippi State University and a geologist specializing in paleomagnetism. His original work was related to tectonic problems in southern Alaska terranes. More recently, he has been using paleomagnetism to investigate stratigraphic problems of Bahamian paleosols and reversal chronology of caves.

Ronald T. Richards is a hydrologic technician with the U. S. Geological Survey and uses geophysics to study ground-water resources. He has a BS in physics from Lewis and Clark College in Portland, Oregon and in August 1998 he began to study for a MS in physics at the University of Puerto Rico in Río Piedras.



Joseph W. Troester is a research hydrologist for the US Geological Survey. He holds a PhD in Geology from the Pennsylvania State University. He studies tropical island hydrogeology and was the project chief of the USGS Isla de Mona project. He now lives in Puerto Rico and has studied water-resources on fifteen islands in the Caribbean.



At 13 Rozemarijn F.A. Tarhule-Lips joined the Dutch Caving Club. She obtained her Licence en Sciences Géographiques (Université de Liège, Belgium, 1990) studying underground meander cut-offs in Belgium. Her PhD research, under supervision of Dr. Ford, looked at causes and timing of speleothem dissolution on Cayman Brac and Isla de Mona.

Carol Wicks is an Assistant Professor at the University of Missouri-Columbia. She has been conducting scientific research in caves and karst areas since 1985. Her PhD and post-doctoral research were on coastal karst systems. Her research is now focused on Missouri's Spring basins.

National Speleological Society
2813 Cave Avenue
Huntsville, Alabama 35810-4431